ASPP-MEDIATED DEPHOSPHORYLATION OF P53 BY PROTEIN PHOSPHATASE 1C

by

Robyn A. Millott

A thesis submitted in partial fulfillment of the requirements for the degree of

Master of Science

Department of Biochemistry
University of Alberta

Abstract

The Apoptotic Stimulating Proteins of p53 (ASPPs) are key regulators of the human tumour suppressor transcription factor, p53. These regulators either activate (ASPP1 and ASPP2) or inhibit (iASPP) p53's function in response to DNA damage. iASPP is overexpressed and attributed to poor survival in several cancers including ovarian, lung, and prostate cancers, while ASPP2 is commonly downregulated in cancer. The molecular mechanisms by which the ASPP proteins mediate their opposing effects on p53 is currently not well understood. Phosphorylation of p53 has been well studied for its importance in p53 stability, localization, and transcriptional activity in response to DNA damage. Previous studies show the catalytic subunit of the Ser/Thr phosphatase, Protein Phosphatase 1 (PP1c), associates with the ASPP proteins, suggesting that ASPP proteins may mediate the post-translational dephosphorylation of p53.

In this work, I have shown that the C-terminal Ankyrin and SH3 domains of iASPP and ASPP2 mediate dephosphorylation of p53Ser15 by PP1c. In addition, iASPP can mediate dephosphorylation of p53Thr18 and DYRK2 phosphorylated p53. Thus, I provide a potential mechanism by which the iASPP may modulate p53 function, and provide some insight into why the N-terminal truncations of ASPP2 may have apparent anti-apoptotic effects. In addition, we used iASPP-mediated dephosphorylation of p53 and mutagenesis of PP1cα and iASPP to provide validation of the newly elucidated iASPP:PP1c structure uncovered in the Glover Lab. In the process, I now hypothesize that the C-terminal tail of PP1c may move to accommodate ASPP-mediated dephosphorylation of p53. A better understanding of how ASPP proteins mediate their opposing functions on p53 may lead to more targeted therapies in cancer treatment.

Acknowledgments

There are countless people I would like to thank for helping me achieve this goal, however with limited space I will only name a few.

Firstly, thank you to my supervisors Dr. Mark Glover and Dr. Charles Holmes. Mark, thank you for the troubleshooting meetings and your calming presence. You helped me out of “the muddiness” of my data on several occasions. Charles, thank you for showing me a side of science research that could be fun, and for teaching me that it’s ok to ask questions and ponder the “what if” scenarios. Thank you to my committee members Dr. Ing-Swie Goping and Dr. Michael Weinfeld for their continued support and advice on the project. Thank you to Dr. Richard Fahlman for agreeing to be an external evaluator for my defense.

Dr. Tamara Skene-Arnold, thank you for getting me on track in the initial stages of the project, and for all the science/ non- science chats that kept me excited to pursue this research. Your enthusiasm for this work and scientific research is a true inspiration. Phuwadet Ply Pasarj, thank you for all the time you spent problem solving with me and your willingness to help a fellow grad student in need. It was recognized and appreciated. Thank you to the wonderful group of graduate students and associates on the third and fourth floors who made coming into the lab every day truly enjoyable: Jennifer Wang, Joe Primeau, Ply Pasarj, Melissa McLellan, Tamara Skene-Arnold, Gareth Armenious, M’lynn Fisher, Jin Kim, Apu Islam, and Ross Edwards.

Thank you to everyone surrounding me and providing me with support through extra-curricular activities and volunteering over the last two years. Regina Sinelnikov, thank you for being my “partner in crime” in running Let’s Talk Science over the past year. Your dedication to science outreach is inspiring. Thank you to my parents for reminding me that there’s a life outside of the lab and keeping me focused on what is truly important. Lastly, thank you to my boyfriend who through five years of living on the other side of the planet has stayed my rock and an ever positive force of optimism.

TABLE OF CONTENTS

LIST OF TABLES

Page

LIST OF FIGURES

Page

List of Abbreviations

β-Me	β-mercaptoethanol
ΔN-ASPP2	ASPP2 (254-1128)
53Bp2	ASPP2 (600-1128)
Amp	Ampicillin
ANOVA	One-way analysis of variance
Apaf1	Apoptotic protease activating factor 1
ASPP	Apoptotic Stimulating Protein of p53
ATM	Protein kinase ataxia-telangiectasia mutated
ATR	ataxia telangiectasia and Rad3-related protein
Bcl-2	B-cell lymphoma 2
Cam	Chloramphenicol
CDK1	Cyclin Dependent Protein Kinase 1
Cdkn1a or p21	Cyclin-dependent kinase inhibitor 1
Chk	Checkpoint kinase
CK1	Casein Kinase 1
CRM1	Chromosomal Maintenance 1
CTDNA	Sonicated calf thymus DNA
DBD	DNA-Binding Domain
DNAPK	DNA-Dependent Protein Kinase
DTT	Dithiothreitol
DYRK2	Dual specificity tyrosine-phosphorylation-regulated kinase 2
E.coli	*Escherichia coli*
EDTA	Ethylenediaminetetraacetic acid
EGTA	Ethylene glycol-bis(β-aminoethyl ether)-N,N,N',N'-tetraacetic acid
Gadd45a	Growth Arrest and DNA Damage Inducible Alpha
Hec1	Kinetochore protein NDC80 homolog
I-2	Inhibitor-2
IPTG	Isopropyl β-D-1-thiogalactopyranoside
Kan	Kanamycin
LB	Luria Bertani
MC	Microcystin
MC-S	Microcystin Sepharose
Mdm2	Mouse double minute 2 human homolog
MYPT1	Myosin phosphatase target subunit 1
NFκB	Nuclear-Factor-κB
Ni-NTA	Ni^{2+}-nitrilotriacetate
Pin1	Peptidyl-prolyl cis-trans isomerase NIMA-interacting 1
PMSF	Phenylmethane sulfonylfluoride
pNPP	para-Nitrophenyl Phosphate
PNUTS	PP1 nuclear targeting subunit

PP1	Protein Phosphatase 1
PP2A	Protein Phosphatase 2A
PP5	Protein Phosphatase 5
PRD	Proline Rich Domain
REG	Regulatory Domain
SB	Laemmli Sample Buffer
SDS	Sodium dodecyl sulphate
SH3	Src homology 3 domain
TAD	Transactivation Domain
TAZ	Tafazzin
TET	Tetramerization Domain
TGFβ	Transforming growth factor beta
VRK	Vaccinia-related kinases

CHAPTER 1

Introduction

CHAPTER ONE: INTRODUCTION

1.1 Governing the Fate of the Cell: An Introduction to p53

Our cells are constantly challenged by innumerable extrinsic and intrinsic stresses such as UV induced DNA damage or metabolic oxidative stress. How our cells respond to this stress impacts not only the health of the cell, but ultimately the organism itself, and impairment in these stress response pathways can result in the development of diseases such as cancer. One of the most comprehensively researched proteins at the hub of stress response pathways is the transcription factor, p53. To date, a search of "p53" within PubMed returns over 150,000 peer-reviewed journal articles. The importance of p53 is underscored by the understanding that it is the most frequently mutated target in cancer and mutations are thought to occur early during cancer progression[1]. In addition, p53-null mice die of spontaneous tumorigenesis at a young age[2].

Labeled a "master regulator", p53 integrates a multitude of diverse signals within the cell (for example DNA damage, oxidative stress, hypoxia, etc.) and affects a large set of responses, including cell-cycle arrest, apoptosis, DNA repair, etc.[3]. p53 is capable of assimilating information from such diverse pathways and affecting so many varied responses largely through its interactions with other proteins in concert with its sequence-specific transcription factor activity[3]. There are an estimated 315 known p53 protein interactions, and over 100 p53 responsive gene targets identified to date[4,5]. These interactions are principally dictated by the structure and post-translational modification state of p53.

1.1.1 p53 Structure

The p53 protein is a 393 amino acid protein that comprises 6 recognized domains: Transactivation Domains 1 and 2 (TAD1, 1-40, and TAD2, 41-83), the Proline Rich Domain (PRD, 63-97), the core DNA Binding Domain (DBD, 102-292), the Tetramerization Domain (TET, 323-356), and the Regulatory Domain (REG, 363-393) (figure 1.1).

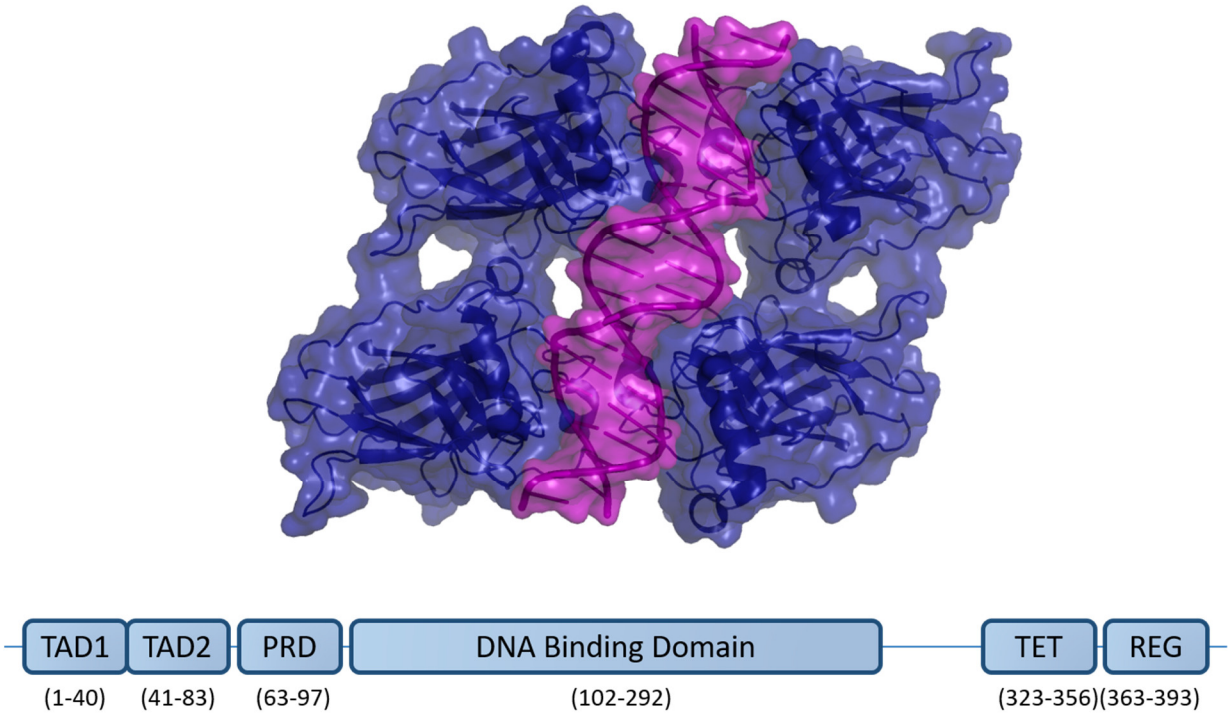

Figure 1.1 p53 structure.
p53 is made up of six domains, the transactivation domains (TAD1 and TAD2), the proline rich domain (PRD), the DNA Binding domain (DBD), the Tetramerization domain (TET), and the Regulatory domain (REG). The crystal structure shows the p53 DBD (blue) bound as a tetramer to the p53 response element of the Bax promoter (purple) (PDB:3KMD)[6].

As a transcription factor, p53 binds to DNA through its DNA binding domain to either promote or inhibit the transcription of a myriad of genes under the control of p53-responsive promoters, such as Apoptotic protease activating factor 1 (Apaf1), Bax, cyclin-dependent kinase inhibitor 1 (Cdkn1a or p21), and Growth Arrest and DNA Damage Inducible Alpha (Gadd45a)[7,8]. p53 forms a tetramer, mediated through the interactions of the TET domains, and binds to two replicates of the DNA target sequence of 5'-RRRC(A/T)(T/A)GYYY-3'[7]. Several of the amino acids that bind to DNA are commonly mutated in cancer, such as Arg248 and Arg 273[9]. In addition to binding DNA, this region can also interact with regulatory proteins, such as the apoptotic stimulating proteins of p53 (ASPPs), which is revisited in section 1.3[10].

The p53 PRD domain contains five PXXP motifs, which are motifs known to bind to Src homology 3 domains (SH3). However, relatively little is understood about the importance of this region. It has been proposed to serve a mostly inert function of acting as a spacer between the DNA binding domain and the transactivation domains, and in support of this, mutations to this region in mouse models have no

substantial effect on tumour suppression[11]. In contrast, Pro82 has been shown to be essential for p53-mediated response to DNA damage[12]. In addition, the non-synonymous nucleotide polymorphism (nsSNP) located within the proline rich domain, R72P, has been associated with increased susceptibility to cancer[13,14].

The transactivation domains of p53 are largely unstructured regions that contribute to the classification of p53 as a partially intrinsically disordered protein[15]. When bound to p53 regulatory proteins, this region generally becomes α-helical[16–18]. Two of the most well documented modulators of p53 are the negative regulator human E3 ubiquitin-protein ligase, Mouse double minute 2 human homolog (Mdm2), and the positive regulator histone/lysine acetyl transferase, p300. Both of these proteins have been found to associate via the TAD domains[18]. When the cell is in an unstressed state, p53 protein levels are kept low by its interaction with Mdm2. Mdm2 binds p53 via the TAD domains, ubiquitinates the C-terminal regulatory domain, which in turn, results in p53 localization to the cytosol and degradation by the proteasome[18]. Many cancer therapies are currently focused on targeting this negative regulation of p53 through development of small molecule inhibitors such as nutlins[19].

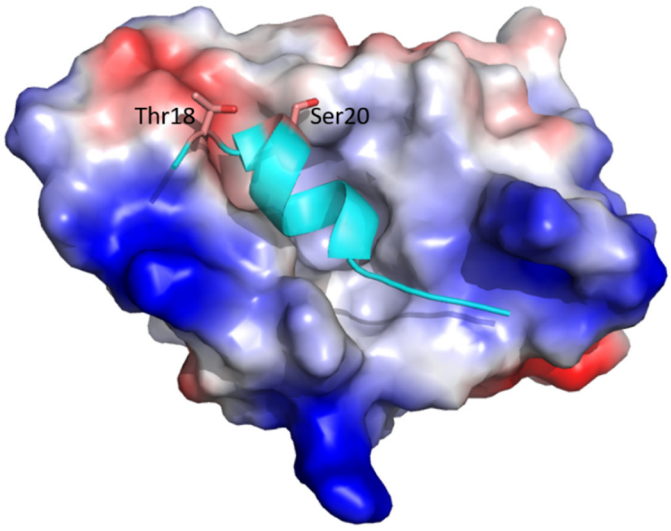

Figure 1.2 p53 TAD1 bound to Mdm2.
The figure depicts p53 TAD1 residues 17-29 (cyan) bound to the E3-ubiquitin ligase Mdm2 (surface representation), PDB:1YCR[20]. Mdm2 acidic residues are coloured in red, and basic residues in blue, as calculated using vacuum electrostatics in PYMOL. The residues of p53 known to be phosphorylated and impair the binding of p53 to Mdm2 are shown in stick representation and coloured in salmon.

As a positive regulator of p53, p300 acetylates p53 C-terminal lysines and prevents the ubiquitination mediated by Mdm2[18]. The interaction of these two regulators is highly dependent on the phosphorylation status of the TAD regions, where phosphorylation of p53Ser15, Thr18, Ser20, Ser33, Ser37, and Ser46 all contribute to increasing the binding with p300, whereas the phosphorylation of p53Thr18 contributes the most to inhibiting the interaction with Mdm2 (figures 1.2 and 1.3)[18].

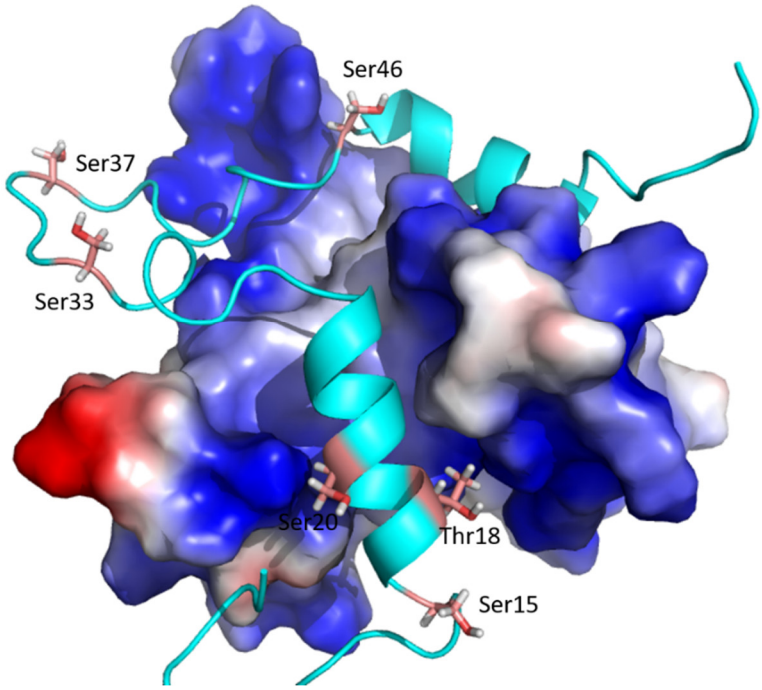

Figure 1.3 p53 TAD1 and TAD2 bound to the TAZ2 domain of p300.
The figure depicts the residues 2-61 of p53 (cyan) bound to the TAZ2 domain of p300 (surface representation), PDB:5HPD[21]. TAZ2 acidic residues are coloured in red, and basic residues are coloured in blue, as calculated using vacuum electrostatics in PYMOL. Residues known to be phosphorylated and contribute to the binding of p53 to TAZ2 are shown in stick representation and coloured in salmon.

1.1.1 Post-translational phosphorylation of p53: a focus on Ser15, Thr18, and Ser46

The complexity of p53 signaling is underlined by the multi-phosphorylation of p53. According to PhosphoSitePlus (www.phosphosite.org), there are 30 Ser/Thr phosphorylation sites currently identified within the p53 protein, which results in over 1 billion (2^{30}) potential phosphorylation states of p53, assuming non-sequential phosphorylation[22]. In response to cellular stresses, p53 can be phosphorylated on one or more Ser/Thr residues, which in turn dictates its interactions with regulatory proteins, and affects its localization, stability, and even its ability to bind specific promoters[18,23]. The majority of these

phosphorylation sites reside within the TAD1 and TAD2 of p53. Due to reagent availability, this thesis focuses on p53Ser15, Thr18, and Ser46[18,23].

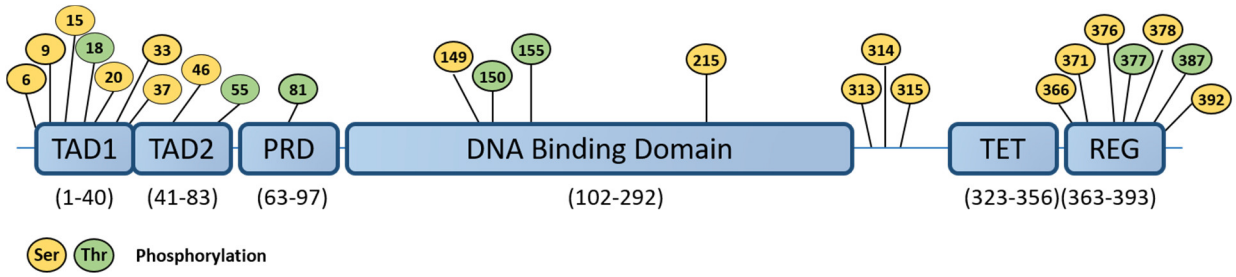

Figure 1.4 p53 is multiply phosphorylated.
p53 contains 30 Ser/Thr phosphorylation sites, with a large proportion residing within the N- and C-termini. The phosphorylations within the TAD1 and TAD2 have been shown to affect binding with positive and negative regulators of p53 function, namely the histone/ lysine acetylase, p300, and the E3-ubiquitin ligase Mdm2.

p53Ser15 phosphorylation has been documented in response to a large variety of stresses including genotoxic stress, hypoxia, microtubule disruption, oncogene activation, replicative senescence, and metabolic stress/ glucose deprivation[24,25]. An array of kinases are capable of phosphorylating this site, including DNA-dependent protein kinase (DNAPK), protein kinase ataxia-telangiectasia mutated (ATM), and ataxia telangiectasia and Rad3-related protein (ATR)[26–28]. As the first site to be phosphorylated in response to stress (seen as early as 30 minutes post-IR) this initial step is thought to be important as a priming site for other phosphorylation sites[29]. For example, Ser15 phosphorylation was shown to be required for the subsequent phosphorylation of Thr18 by setting up a priming site for Casein Kinase 1 (CK1)[30]. Later it was shown that in response to DNA damage, both Thr18 and Ser20 are dependent on the prior phosphorylation of Ser15[29]. In addition, Ser15 phosphorylation contributes to the association with the histone/lysine acetyl transferases p300 and CBP[18,31,32]. The association of p53 and p300/CBP has two effects; 1) the acetylation of lysines within the C-terminus of p53, which protects p53 from ubiquitination and proteasomal degradation, and 2) histone acetylation and chromatin relaxation on p53-responsive promoters[23]. Consequently, this phosphorylation of p53Ser15 is important in the transactivation function of p53, as shown through its necessity in the activation of the p21, BAX, and MDM2 promoters[23,33]. It has also been proposed that Ser15 is important in p53 subcellular localization, as it resides within a potential nuclear exit signal sequence and phosphorylation of this site could be involved in retaining p53 within the nucleus[34].

However, p53Ser15 phosphorylation has also been detected within the mitochondria[35]. It is likely that this site works in combination with other sites and other post-translational modifications for p53 localization, as Thr55 phosphorylation and mono-ubiquitination have also been shown to be important for localization[36,37].

Compared to p53Ser15, relatively less information is available for the conditions under which p53Thr18 is phosphorylated, however its phosphorylation has been primarily documented in response to DNA-damage[18,30]. As with p53Ser15, several kinases are implicated in the phosphorylation of p53Thr18 including; CK1, vaccinia-related kinases 1 and 2 (VRK1 and VRK2), Checkpoint kinases 1 and 2 (Chk1 and Chk2), and DNAPK [30,38–41]. Like p53Ser15, phosphorylation of p53Thr18 contributes to the binding of p53 to p300/CBP proteins, but it is also the main site responsible for the dissociation of p53 from the negative regulator, MDM2[42,43]. Therefore, this site is associated with the stability of cellular p53 levels in response to stress. Phosphorylation of this site (in conjunction with p53Ser20P) is also believed to be key in inducing apoptosis, and in cell cycle arrest through the transactivation of the p21 promoter[33,44].

Like p53Ser15 and p53Thr18, p53Ser46 is phosphorylated in response to several stimuli including DNA damage, hypoxia, and glucose deprivation[45–47] and is phosphorylated by numerous kinases, such as ATM, Homeodomain-interacting protein kinase 2 (HIPK2), and Dual specificity tyrosine-phosphorylation-regulated kinase 2 (DYRK2)[48–50]. While p53Ser15 and p53Thr18 phosphorylation have been documented in several cellular outcomes, p53Ser46 is regarded as a site responsible for guiding p53 towards mediating apoptosis, rather than cell cycle arrest[51]. In a genome-wide study, cells destined for apoptosis had a larger degree of p53 phosphorylated at Ser46 bound to DNA than p53 phosphorylated at Ser15. In addition, in response to DNA damage (via the drug etoposide), Ser46 phosphorylated p53 bound to apoptosis-specific target genes to a greater degree than did p53Ser15P[52]. p53Ser46 phosphorylation is also important for the translocation of cytosolic p53 to the mitochondria and transcription-independent apoptosis through its association to phospho-specific Peptidyl-prolyl cis-trans isomerase NIMA-interacting 1 (Pin1)[53].

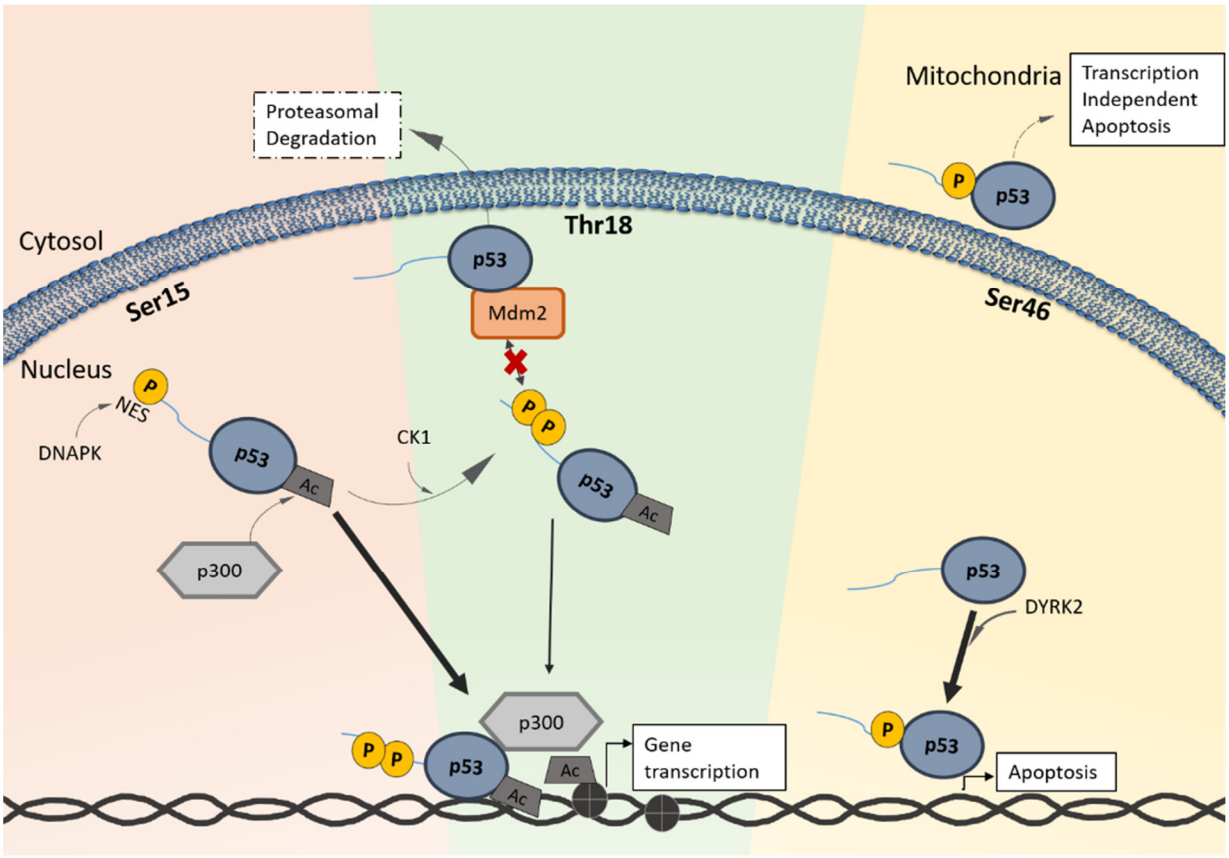

Figure 1.5 p53 Localization, transactivation, and protein stability is modified through post-translational phosphorylation.
Phosphorylation of p53 mediates its response to cellular stress. Phosphorylation of p53Ser15 resides within a nuclear exit signal (NES) that maintains p53 within the nucleus and contributes to the binding of p53 with p300. This results in acetylation of the p53 C-terminus (Ac) as well the histones surrounding p53-response elements, allowing for gene transcription. Ser15 also sets up a priming site for Thr18 phosphorylation, one of the main drivers for the dissociation of p53 from Mdm2 as well as a contributor to p300 binding. p53Ser46 is thought to be important for p53 localization to apoptotic genes, as well as localization of cytosolic p53 to mitochondria for transcription independent apoptosis.

While phosphorylation of p53 has been well-documented, substantially less is known about the regulation of p53 dephosphorylation. Hyperactivation of p53 is associated with degenerative diseases such as multiple sclerosis, Alzheimer's disease, and premature ageing, and thus its activation must be tightly controlled[54–57]. One of the ways p53 activation is controlled is through dephosphorylation, as highlighted by dephosphorylation of p53Ser15 after G2 checkpoint arrest being key for re-initiation of the cell cycle and recovery from the DNA damage response[58]. As a key Ser/Thr phosphatase, Protein phosphatase 1 (PP1) has been associated with the dephosphorylation of p53Ser15, as well as Ser37 and Ser392, and is

generally regarded as inhibitory to p53 transcriptional activation and mediated apoptosis [59–61]. No phosphatase has yet been linked to the dephosphorylation of p53Thr18 or Ser46.

1.2 Who Watches the Watchmen? An Introduction to Protein Phosphatase 1

An estimated 70% of all eukaryotic proteins are regulated by phosphorylation, the majority of which (approximately 96%) occurs on Serine and Threonine residues[62,63]. In humans, there are an estimated 428 Ser/ Thr protein kinases and only 40 Ser/ Thr protein phosphatases to counter their activities[64]. Protein Phosphatase 1 (PP1) is one of two key phosphatases (the other being Protein Phosphatase 2A, PP2A) that dephosphorylates the majority of these Ser/Thr substrates[65]. Unlike the consensus sequences which guide kinase substrate specificity, the PP1 catalytic subunit (PP1c) is highly promiscuous and its specificity and subcellular localization is instead overseen by binding to regulatory subunits[66]. The line "*Who watches the watchmen?*" from the Roman poet Juvenal applies particularly well to the regulation of PP1c dephosphorylation: the PP1c catalytic subunit activity is constantly watched by an overseeing regulatory subunit[67].

1.2.1 The PP1 Catalytic Subunit

PP1 is ubiquitously expressed and is found throughout all tissues, and virtually all subcellular locations[68]. As such, it is implicated in numerous cell signaling pathways, from androgen receptor signaling, to protein synthesis, to cell cycle mediation, to transforming growth factor beta (TGFβ) signaling, among many others[69]. The human PP1 catalytic subunit (PP1c) is highly conserved throughout evolution, sharing greater than 80% sequence identity with PP1c from yeast[70]. The N-terminal 1-300 amino acids make up the catalytic core, while the last 30 amino acids comprise the flexible C-terminal tail. In humans, there are three gene isoforms of PP1c, α, β, and γ, which differ in sequence mostly at their flexible C-termini.

Two metal ions (proposed to be either Fe^{2+}, Zn^{2+}, or Mn^{2+}) ions are coordinated within the PP1c active site that activate a water molecule for nucleophilic attack, and along with Arg96, Arg221, Asp95, His125, catalyze the release of phosphate from a phosphomonoester substrate. Three grooves extend in the shape of a "Y" from the active site (the C-terminal, acidic, and hydrophobic grooves) and are important

for both substrate and inhibitor binding (figure 1.6). These grooves can help in predicting how a substrate might bind, for example a basic polypeptide may be expected to bind to the acidic groove; however, they cannot be used to predict whether a particular phosphorylation site will be dephosphorylated by PP1c[71]. A recently published study elucidated the structure of Protein Phosphatase 5 bound to Cdc37 with a Ser→Glu phosphomimic[72]. This study hypothesized that the - 2 position of a substrate from the phospho-residue may be important in mediating specificity among phosphatases; however, these findings remain to be corroborated experimentally in another phosphatase other than PP5. Regardless, while the substrate specificity of the PP1 catalytic subunit is poorly understood, it is recognized as highly promiscuous[73]. It is generally accepted that PP1c is unlikely to exist as a monomer within the cell and the seemingly unbridled activity of PP1c is kept in check within the cell through association with a regulatory subunit as well as through its own auto-inhibition[73–75].

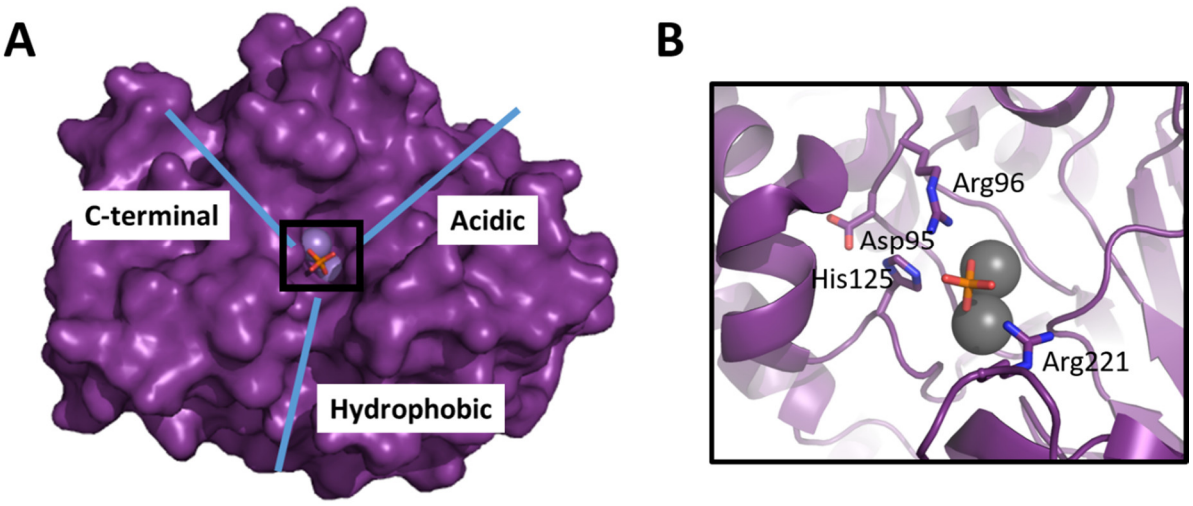

Figure 1.6 Protein Phosphatase 1 Catalytic Subunit.
Panel A depicts residues 7-299 of the catalytic subunit of protein phosphatase 1α (PP1cα), PDB: 4MOV[76]. Three substrate grooves are highlighted in blue; the acidic, hydrophobic, and C-terminal grooves. The active site is at the center of these three grooves with a coordinated Mn^{2+} ion and a substrate phosphate in orange. Panel B shows the residues Arg96, Arg221, Asp95, and His125 that are important for catalyzing dephosphorylation.

1.2.2 Regulating PP1c Activity

Currently, over 200 regulatory subunits of PP1c have been identified[73]. These subunits can bind to the PP1 catalytic subunit using a combination of small binding motifs which associate with respective PP1c surface grooves. Combinations of these motifs span from 5-20% of the surface area of PP1c, resulting in inhibition of substrate binding, increased association with a substrate, or specific cellular localization of the catalytic subunit[66,68,73,77]. Examples include: 1) Inhibitor-2 (I-2) which binds the hydrophobic and acidic grooves of PP1 to occlude the active site (among other sites), 2) Myosin phosphatase target subunit 1 (MYPT1) where its binding lengthens the acidic groove of PP1 and is proposed to promote substrate recruitment, and 3) the PP1 nuclear targeting subunit (PNUTS), which as its name suggests, localizes PP1 to the nucleus (figure 1.7)[71,78,79].

The widely recognized canonical PP1cα regulatory protein binding motif is the RVXF motif, or more precisely [RK]-$X_{0,1}$-[VI]-{P}-[RW] motif [77]. The RVXF sequence aligns along a hydrophobic cleft on the reverse face of PP1cα from the active site, and relies heavily on Van der Waals interactions between this cleft and the valine and phenylalanine residues (at the 2nd and 4th positions respectively) of the regulatory subunit[77]. This sequence occurs in approximately 90% of all identified PP1cα regulatory subunits, and is thought to act as a tether to allow for association of lower-affinity binding sites[80]. The importance of the RVXF motif is underscored by a study that used a peptide fragment to disrupt the RVXF motif in cells, freeing PP1c from regulation resulting in overall cytotoxicity[81].

In addition to the RVXF consensus sequence, several other interactions within the PP1c core have been identified, including the SILK motif, which likely has a similar function as the RVXF motif, and an electrostatic interaction between an acidic patch on the regulatory protein and a basic patch on PP1cα made up of K260 and R261[77,82]. Due to the flexibility of the PP1c C-terminal tail, its interaction with regulatory subunits is poorly characterized. Only one published structure showing the PP1c C-terminal tail with a regulatory subunit exists, that of MYPT1 bound to PP1cβ[71]. This structure shows the PP1c tail interacting with the Ankyrin repeats of MYPT1[71]. In addition, it was recently identified that the PP1c tail has a poly-proline PXXPXR motif, a motif which is known to be important for binding SH3 domains[82].

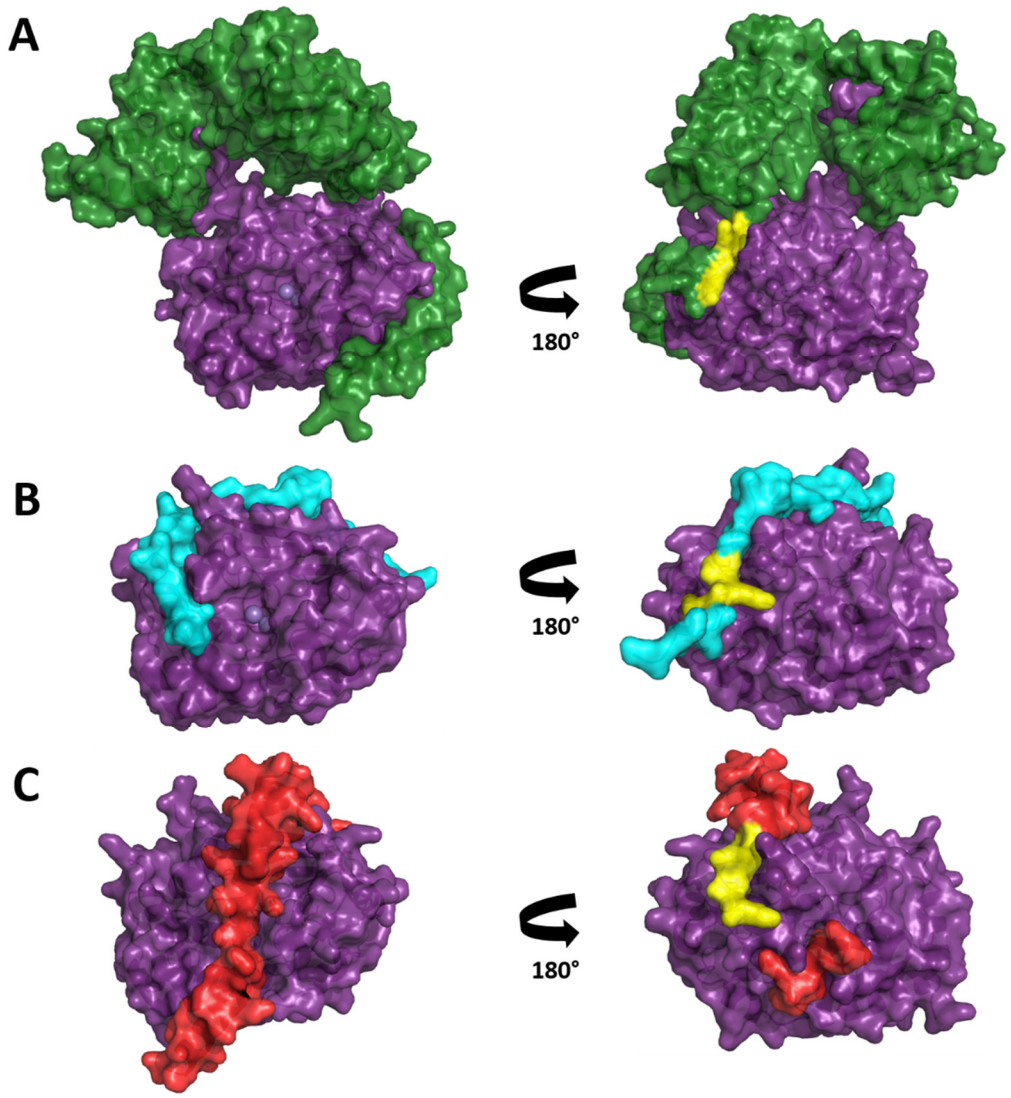

Figure 1.7 Protein Phosphatase 1c crystal structures of MYPT1, PNUTS, and Inhibitor-2.
The figure depicts the crystal structures of three PP1c regulatory subunits, A) MYPT1 PDB:1S70, B) PNUTS PDB:4MOY, and C) Inhibitor-2 PDB:2O8A[71,76,78]. The left hand side shows the front view of PP1c with its active site containing a Mn^{2+}, and the right hand side depicts the 180° rotation of PP1c where the RVXF motif of each regulatory protein is highlighted in yellow binding to a hydrophobic cleft on PP1c.

The study of PP1cα regulatory subunits has been greatly facilitated by the use of a microcystin-linked Sepharose pull down assay. Microcystin (MC) is a small molecule inhibitor of PP1cα, which can be purified from cyanobacteria and linked via an ethanethiol linkage to Sepharose to create microcystin Sepharose (MC-S)[83]. Microcystin binds to the PP1cα active site, leaving the rest of the PP1cα surface open to bind interacting proteins (figure 1.8). This method has been used successfully to study regulatory proteins of PP1cα for over two decades[82].

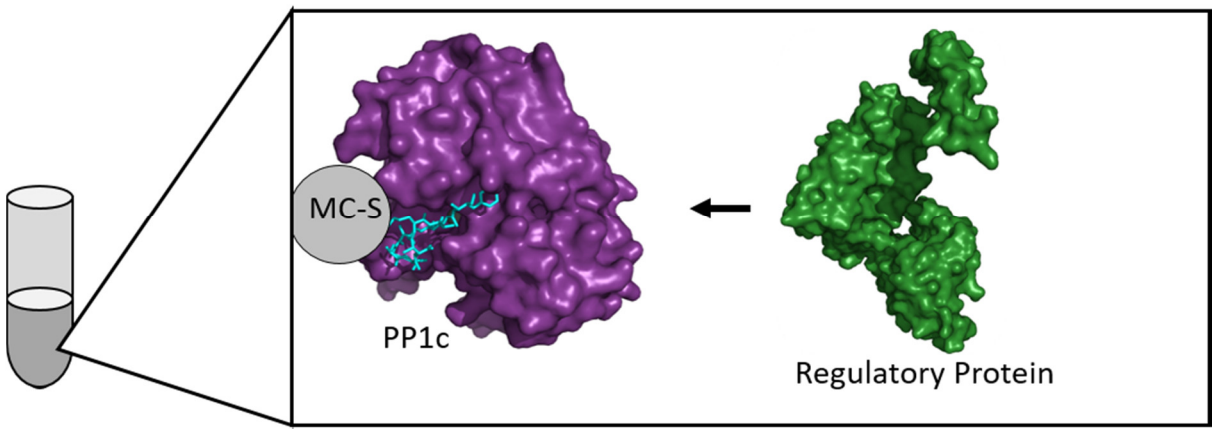

Figure 1.8 Microcystin Sepharose is used to study regulatory subunits of PP1c.
The figure depicts the PP1c small molecule inhibitor microcystin (cyan) linked to Sepharose to create microcystin Sepharose (MC-S). PP1c (purple) can be bound to MC-S to study interactions with regulatory subunits of PP1c (green) through pulldown experiments.

In addition to being mediated by regulatory subunits, the PP1c isoforms are also partially inhibited through phosphorylation of a Thr residue within the third position of the PXXPXR motif on the PP1cα C-terminal tail. In PP1cα, this residue is Thr320. How the phosphorylation of Thr320 inhibits its PP1c is not entirely understood at a mechanistic level, however it is hypothesized that it partially occludes substrate binding to the active site[74,82,84]. However, a T311D mutation in PP1cγ has no effect on the dephosphorylation of phosphorylase *a* and phosphorylation of T311 only shows partial inhibition *in vitro* (although this is thought to be due to auto-dephosphorylation)[82]. Phosphorylation of T320 (and thereby partial inhibition of PP1c) has so far been shown to be important for cell cycle progression as well as differentiation[85–87].

1.3 Opposing ASPPirations: An Introduction to the Apoptotic Stimulating Proteins of p53

The Apoptotic Stimulating Proteins of p53 (or ASPP proteins) comprise a family of three homologous proteins: ASPP1, ASPP2, and iASPP. ASPP1 and ASPP2 were aptly named for their ability to promote p53-mediated apoptosis, whereas iASPP was named for its inhibition of p53-mediated apoptosis[88,89]. All three proteins contain a highly similar C-terminal domain consisting of a proline rich domain, four ankyrin repeats, and an SH3 domain, which are involved in binding and regulating p53 (figure 1.9). iASPP is the most ancient evolutionarily, and ASPP1 and ASPP2 are thought to have evolved later

with their extended N-termini[88]. All three ASPP family members were shown to be regulatory subunits of PP1c, and in particular iASPP and ASPP2 had the most opposing effects on PP1c binding[82].

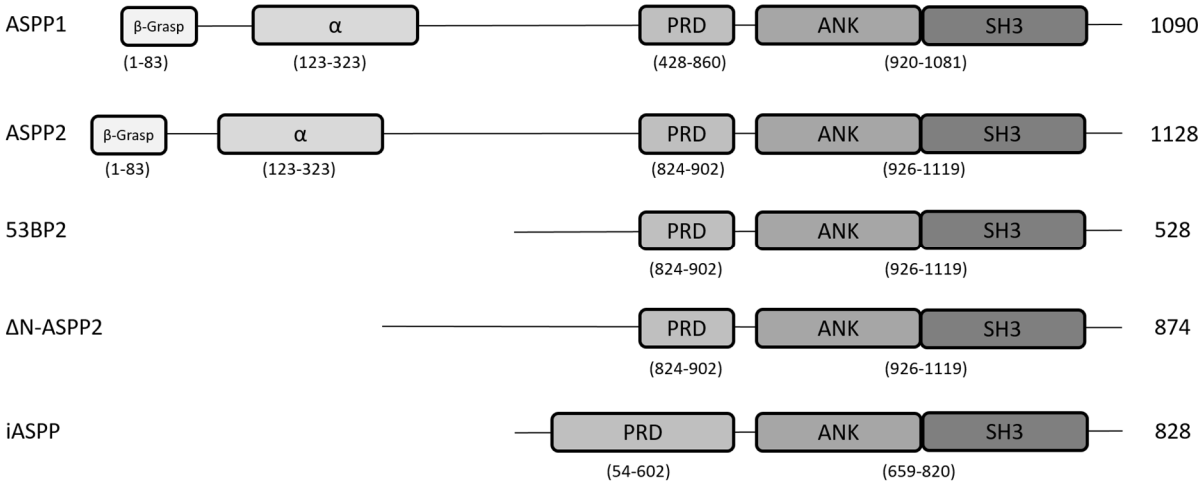

Figure 1.9 The Apoptotic Stimulating Proteins of p53 (ASPPs)
The Apoptotic Stimulating Proteins of p53 (ASPPs) are a homologous family of proteins all containing conserved proline rich (PRD), Ankyrin repeat (ANK), and Src-homology domain 3 (SH3) domains within their C-termini. ASPP1 and ASPP2 are promoters of p-53 dependent apoptosis, while iASPP inhibits p53-dependent apoptosis[88,89]

1.3.1 The Apoptotic Stimulating Protein of p53-2

The first ASPP protein shown to bind to p53 was ASPP2, specifically the C-terminal 600-1128 residues of ASPP2 called 53BP2, through a yeast 2-hybrid screen[90]. 53BP2 was later crystallized with the DNA-binding domain of p53 (figure 1.10). This structure showed that the two most commonly mutated p53 residues in cancer, R248 and R273, were specifically important for the p53:53BP2 interaction[10]. As 53BP2 bound directly to the face of p53 important for binding DNA, and inhibited DNA binding, it was first predicted to be a possible oncogene[91].

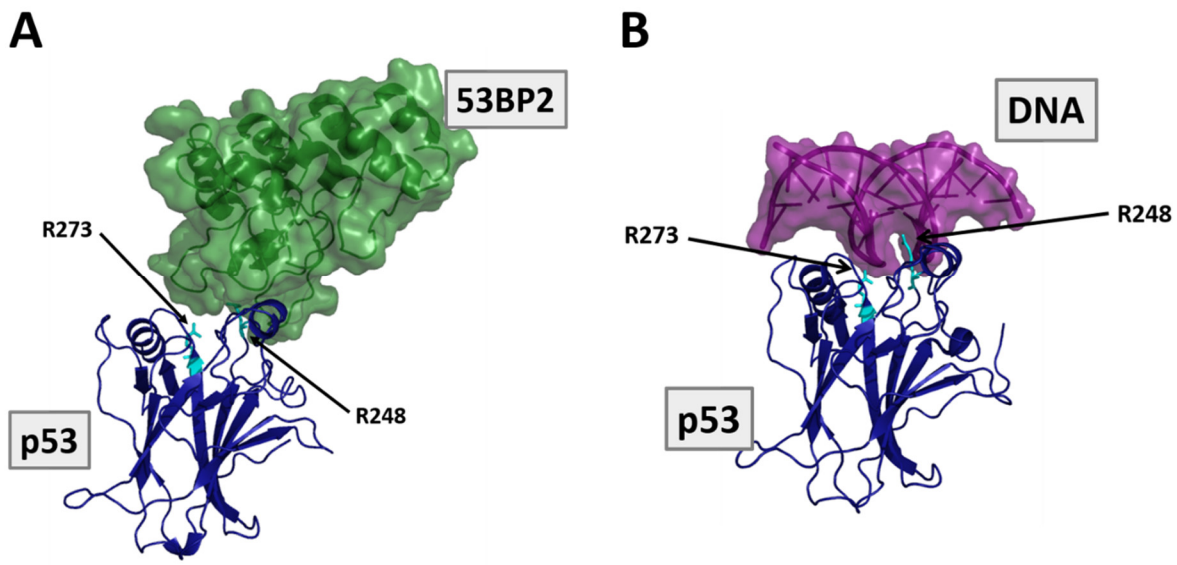

Figure 1.10 53BP2 binds to the DNA interface of p53.
The figure depicts the crystal structures of A) 53BP2 bound to p53-DNA binding domain (PDB:1YCS) and B) DNA bound to p53-DNA binding domain (PDB:4HJE)[10]. The structures highlight that 53BP2 binds to the same face of p53 as DNA, and that the p53 residues most mutated in cancer, R273 and R248 (cyan), are both essential for binding in both complexes.

In initial studies, full-length ASPP2 was shown to enhance p53-DNA binding and specifically stimulate p53 transactivation of genes involved in apoptosis, as opposed to cell cycle arrest, while 53BP2 did not[89]. Instead, when 53BP2 was co-expressed with full-length ASPP2, it reduced the interaction of ASPP2 with p53[89]. More recently, a new ASPP2 isoform (ΔN-ASPP2) that lacks the N-terminal 253 amino acids has been identified[92]. This isoform does not promote apoptosis but rather supports cell survival, and recruitment of p53 to the Bax promoter in response to cisplatin was inhibited by ΔN-ASPP2[92]. This has led to the hypothesis that it is the N-terminus of ASPP2 that is responsible for mediating its pro-apoptotic function. While the N-terminus of ASPP2 is largely unstructured, it contains two structural elements; a β-grasp ubiquitin-like fold Ras-association domain (residues 1-83) and a predicted α-helical region (residues 123-323) (figure 1.9)[93,94]. Although it's not apparent how these elements are directly related to p53-mediated apoptosis, they have been shown to be involved in promoting Ras signaling and senescence[95]. To complicate matters, ASPP2 has also been shown not only to bind the core DNA-binding domain of p53, but also its proline rich domain[14,96]. The significance of these two possible binding sites is not well understood. Thus, the direct mechanism by which ASPP2 enhances p53-mediated apoptosis remains

unclear. ASPP2 knockout mice die shortly after birth, and the haplo-insufficient ASPP2 mice have an increased susceptibility to tumourigenesis[97]. In addition, ASPP2 levels have been found to be downregulated in several cancers expressing wild-type p53, and reduced ASPP2 levels are correlated to poor prognosis[89,98–100]. Therefore, the mechanism for how ASPP2 mediates p53 activity is of importance for further study.

The majority of ASPP2 binding partners interact through the ASPP2 C-terminal Ankyrin and SH3 domains. Examples include the p65 subunit of Nuclear-Factor-κB (NFκB), B-cell lymphoma 2 (Bcl-2), Tafazzin (Taz), and PP1c[93,101–103]. ASPP2 was first identified as a regulatory protein of PP1c through its mediated dephosphorylation of Taz at Ser89, which promotes Taz localization to the nucleus and enhances gene expression of genes involved in cell proliferation[103]. Recently, ASPP2 has also been shown to mediate the dephosphorylation by PP1c of the outer kinetochore protein, Kinetochore protein NDC80 homolog (Hec1), which is thought to be important for mitotic progression[104]. Thus, while ASPP2 is an enhancer of p53-mediated apoptosis (through an unknown mechanism), ASPP2-mediated dephosphorylation by PP1c appears to also promote cellular proliferation. Whether ASPP2 can mediate dephosphorylation of p53 has not yet been explored, and is one of the focuses of this study. Previous studies in the Holmes lab found that the C-terminal of ASPP2 ($ASPP2_{905\text{-}1128}$) cannot complex together with PP1c and p53, and instead preferably associates with PP1c[82]. Given the importance of p53 phosphorylation for its apoptotic function and the finding that ASPP2 does not form a complex with PP1c and p53, I hypothesized that ASPP2 would not enhance the dephosphorylation of p53 by PP1c.

1.3.2 The Inhibitory Apoptotic Stimulating Protein of p53

iASPP was first found to be an inhibitor of apoptosis when its depletion in *C. elegans* significantly increased the number of apoptotic germ cell corpses[88]. It was later shown that iASPP impairs p53-dependent apoptosis, and hypothesized to do so through competition with ASPP2 as both proteins are capable of binding to the p53 DNA binding domain[105]. An overlay of the iASPP C-terminal domain structure and the 53BP2 structure bound to the DNA-binding domain of p53, shows two remarkably similar structures with an RMSD=0.89 as calculated in PYMOL (figure 1.11).

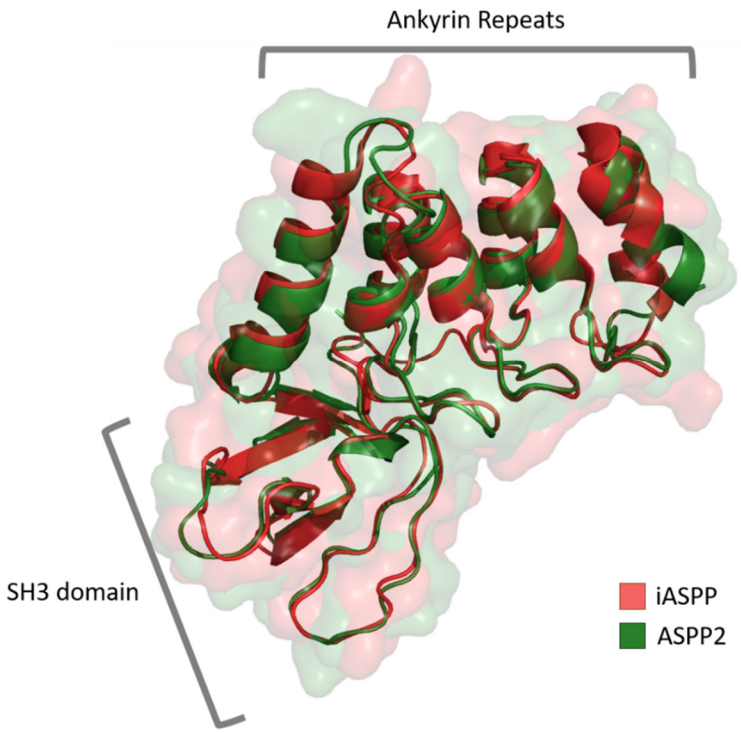

Figure 1.11 Structural alignment of iASPP and ASPP2 reveals strong similarity.
The figure depicts the structural alignment of iASPP (632-823) in red (PDB:2VGE) and ASPP2 (in green (53BP2, PDB:1YCS) using PYMOL. Both structures contain four Ankyrin repeats and an SH3 domain, with an RMSD= 0.89[10,106].

This alone supports the idea that iASPP and ASPP2 would both bind p53 in a similar manner. However, NMR studies show that ASPP2 binding to p53 is approximately 60-fold stronger than the binding of iASPP, therefore the theory that their opposite effects on p53 are through direct competition for binding is unlikely[96]. A combination of cell studies and NMR have shown that iASPP can in fact bind to three regions on p53, the proline rich domain, the DNA-binding domain, and a linker region C-terminal to the DNA-binding domain, with preferential binding for the latter[88,96]. These studies correlate well with unpublished findings in the Glover lab which show iASPP does not impede the p53 DBD from binding to DNA until high μM concentrations (50 μM), while ASPP2 shows a linear competition for p53 starting at lower concentrations (3.2 μM).

As with ASPP2, the mechanism for iASPP-mediated inhibition of p53-dependent apoptosis is unclear. iASPP is an oncogene that inhibits p53 transactivation of apoptotic genes, is upregulated in numerous p53-wildtype cancers correlating to poor prognosis, and is implicated in an increase in tumour

progression and metastasis[107]. Thus, inhibition of iASPP function is a potential target for reactivating wild-type p53 in certain cancers. Recently a small peptide, A34, showed some promise in this respect. The peptide was derived from the p53 linker region and was found to block iASPP inhibition of p53-mediated apoptosis[108].

In addition to binding p53, iASPP was also identified in the Holmes lab as a PP1c regulatory subunit[82]. iASPP holds a non-canonical RVXF motif (RARL), hereinafter referred to as the RVXF-like motif, as the Leu in the fourth position is normally held by a Trp or Phe residue which buries into a hydrophobic cleft on the surface of PP1c[82]. It was later shown that iASPP could mediate the dephosphorylation of desmoplakin by PP1c[109]. The Holmes lab also found that the C-terminal of iASPP ($iASPP_{608-828}$), PP1cα, and $p53_{2-292}$ can form a complex, thus leading to the question of whether iASPP is capable mediating dephosphorylation of p53, thereby inhibiting p53 activation[82]. The effect of iASPP on p53 dephosphorylation has not yet been pursued and is another focus of this thesis.

Given the importance of p53 phosphorylation for its apoptotic function, I hypothesized that iASPP negatively regulates p53 apoptotic function through enhancing the dephosphorylation of p53 by PP1c.

1.3.3 The iASPP:PP1cα crystal structure

Two copies of the $iASPP_{608-828}$ bound to PP1cα structure were recently solved (within the same crystallographic asymmetric unit) (Glover lab, unpublished data) (figure 1.12). These are the first structures of iASPP in complex with another protein, as the only published structure of iASPP is currently that of the C-terminal region alone[106]. In addition this is one of now two structures that shows density of the PP1cα C-terminal tail. Only one other structure of PP1c shows density of its flexible C-terminal tail (the other being the structure of MYPT1 and PP1cβ)[71].

Prior to the determination of the crystal structures, Dr. Tamara Skene-Arnold from the Holmes lab used binding studies to predict areas of importance for the interaction between iASPP to PP1cα[82]. Dr. Skene-Arnold identified three key regions: the RVXF-like motif (RARL), the electrostatic interaction between Arg261 in PP1cα and Asp633 in iASPP (hereinafter referred to as the D633:R261 electrostatic interaction), and finally the PP1cα C-terminal tail interaction with the iASPP Ankyrin and SH3 domains. Of note, mutation to the RVXF-like or PP1cα C-terminal tail completely abolished binding, while the mutation of PP1c R261S

reduced binding by approximately 70% using recombinantly expressed and purified protein in pulldown experiments[82].

These initial binding experiments agree well with the iASPP:PP1cα crystal structures found. The first structure shows $iASPP_{608-828}$ binding at the RVXF-like motif, the D633:R261 electrostatic interface, and the PP1cα C-terminal tail. The second structure showed $iASPP_{608-828}$ binding of the SILK motif, as well as the RVXF-like motif and the D633:R261 electrostatic motif, but no interaction with the PP1cα C-terminal tail. The PXXPXR motif of the PP1cα tail binds within the SH3 domain of iASPP, the same region important for binding p53 (figure 1.12). Given that PP1cα does not bind to p53 in the absence of iASPP, how these three proteins form a complex if the PP1cα tail is bound is unclear. One hypothesis is that the PP1cα tail present in the iASPP:PP1c heterodimer moves to accommodate p53 binding to the iASPP SH3 domain. Investigating the importance of the PP1cα C-terminal tail is another focus of this thesis (figure 1.12)[82].

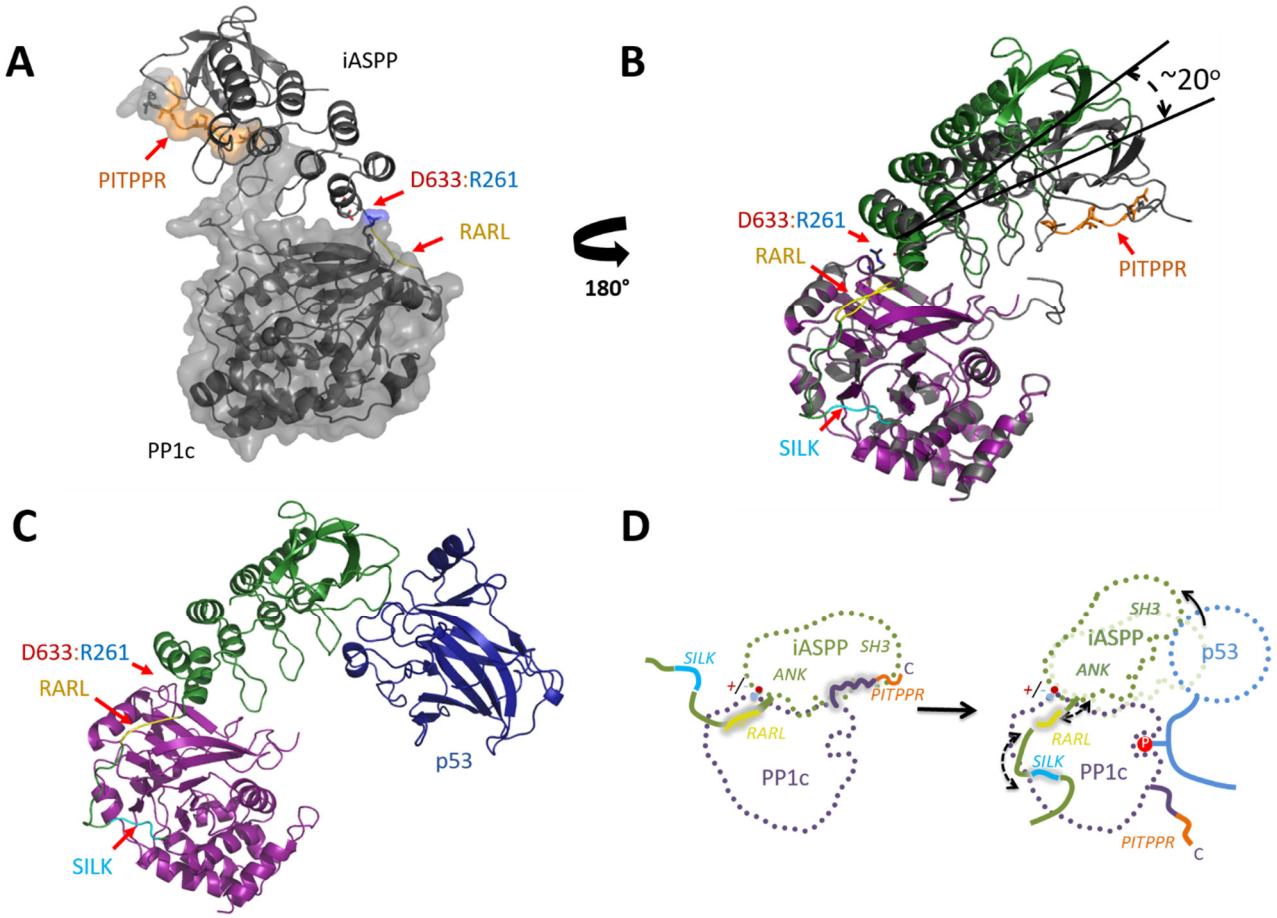

1.12 The Crystal Structure of iASPP:PP1cα

The figure depicts the currently unpublished crystal structures of $iASPP_{608-828}$:PP1cα found within the same unit cell. A) iASPP (cartoon) bound to PP1cα (surface) with three areas of contact known to be important for dimer formation: RVXF-like motif (yellow), D633:R261 electrostatic interaction (Red and Blue), and the PXXPXR:SH3 interaction (orange). B) Comparison of the two iASPP:PP1cα structures, where the complex in A) is overlaid with the second iASPP:PP1cα structure shown in purple (PP1cα) and green (iASPP). The second structure lacks the PXXPXR tail, however binds a SILK motif not present in the first complex. C) A model of the second iASPP:PP1cα complex shown in B) aligned with 53BP2:p53 (PDB:1YCS) where the p53 DNA-binding domain binds to the SH3 domain of iASPP (53BP2 not shown for clarity). D) A representation of how iASPP and PP1cα may accommodate binding of the p53 DNA binding domain. The tail of PP1cα is bound to the SH3 domain of iASPP in the iASPP:PP1cα dimer, however the tail moves to accommodate p53 binding to the iASPP SH3 domain in the trimeric complex. The SILK motif may only bind when the trimer forms. Figure produced in collaboration with Dr. Mark Glover.

1.4 Thesis Aims and Hypothesis

iASPP and ASPP2 both bind to p53 and govern its ability to mediate apoptosis. How the ASPP proteins are capable of mediating their opposing functions on p53 remains unanswered. Both iASPP and ASPP2 were found to interact with PP1c and mediate dephosphorylation of target substrates. Since p53 function is highly dependent on its phosphorylation status, one of the ways ASPP proteins mediate their opposing effects on p53 apoptotic activity may be through mediating site-specific dephosphorylation by PP1c. The ASPP proteins also have differing abilities to form complexes with PP1cα and p53, where $iASPP_{608-828}$ is capable of forming a complex with PP1c and p53, while $ASPP2_{905-1128}$ preferentially associates with PP1cα in a dimeric form. As well, though the PP1cα PXXPXR motif is important for binding to iASPP, its interaction with the iASPP SH3 domain would theoretically occlude iASPP binding to p53. In relation, the $iASPP_{608-828}$:PP1cα structure was recently elucidated and requires functional validation. Thus, the aims of this study were two-fold:

1) Identify Ser/ Thr sites on p53 that are dephosphorylated by PP1cα and test the effect of the C-terminals of iASPP ($iASPP_{608-828}$) and ASPP2 ($ASPP2_{905-1128}$) on mediating dephosphorylation of those sites *in vitro*.

2) If $iASPP_{608-828}$ does mediate dephosphorylation of p53 by PP1c, use site-directed mutagenesis to validate the $iASPP_{608-828}$:PP1cα structure using *in vitro* dephosphorylation of p53, as well as test the functional importance of PP1cα PXXPXR motif in iASPP-PP1cα mediated dephosphorylation of p53.

My hypotheses are that*:*

1) $iASPP_{608-828}$ will mediate the dephosphorylation of p53 by PP1c, while $ASPP2_{905-1128}$ will not,

2) the three interfaces previously identified to be important within the $iASPP_{608-828}$:PP1c crystal structure will be significant for iASPP-mediated dephosphorylation of p53,

3) the PP1cα PXXPXR motif will be least important for iASPP-mediated dephosphorylation given that it would theoretically occlude p53 binding to iASPP.

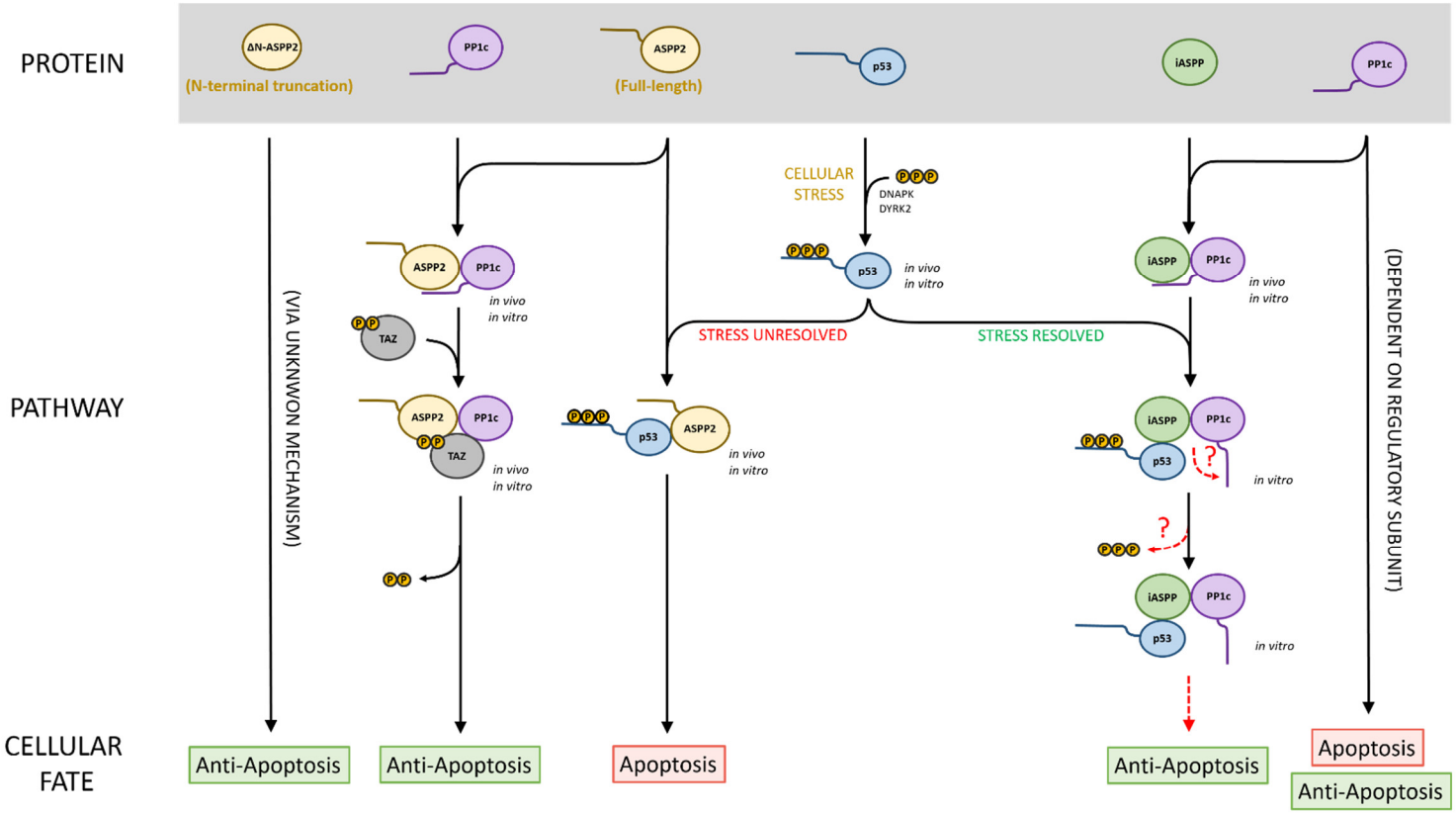

Figure 1.13 Summary of ASPP interactions, pathways, and cellular fates under investigation in this thesis.
The figure represents an outline of some of the ASPP pathways and interactions pertinent to this thesis. p53 is phosphorylated in response to various cellular stresses[23,29]. Apoptosis is one of the end fates of the cell if the stress is unresolved and the apoptotic stimulating protein of p53-2 (ASPP2) is known to associate with p53 and is involved in promoting p53-dependent apoptosis[10,89]. ASPP2 is also known to associate with Protein Phosphatase 1c (PP1c) and mediate dephosphorylation of target substrates such as Tafazzin (Taz) resulting in an overall anti-apoptotic effect[82,103]. In addition, C-terminal truncation of ASPP2, ΔN-ASPP2, was recently found to have anti-apoptotic effects although this mechanism is unclear[92]. Hyperactivation of p53 can contribute to diseases such as Alzheimer's therefore the cell must have a mechanism for turning off the p53 response once stress has been resolved[57]. The inhibitory Apoptotic Stimulating Protein of p53 (iASPP) is known to inhibit p53-dependent apoptosis through an unknown molecular mechanism[88]. PP1c is known to associate with iASPP$_{608-828}$ and together can form a complex with p53[82], leading to the hypothesis that iASPP may inhibit p53-dependent apoptosis through mediating p53 dephosphorylation by PP1c. The iASPP$_{608-828}$:PP1c structure was recently solved and showed two different complexes where one complex showed binding of the PP1c tail to the iASPP SH3 domain, and the second complex did not. To form a p53:PP1c:iASPP complex it is hypothesized that the PP1c tail would have to move to allow binding of p53 to the iASPP SH3 domain.

CHAPTER 2

Materials and Methods

CHAPTER TWO: MATERIALS AND METHODS

2.1 Protein Expression, Purification, and Site-Directed Mutagenesis

2.1.1 Bacterial Strains and Plasmids

All plasmids were stored in DH5α Max Efficiency cells (Invitrogen) at -80°C in equal parts glycerol to Luria Bertani (LB) medium. The sequence for human Wild-Type PP1cα (NM_001008709) was stored in the pKK223.3 expression vector, and was obtained from Dr. Tamara Skene-Arnold [82,110]. This vector contains the tac promoter for the induction of protein expression under the control of Isopropyl β-D-1-thiogalactopyranoside (IPTG), as well as the presence of the Ampicillin (Amp) resistance gene to confer resistance to Amp and allow for selection of only cells containing the pKK223.3 vector. The PP1cα (T320D) and PP1cα (1-300) mutation constructs were also housed in the same vector (for mutagenesis see section 2.1.2). The constructs were transformed into *Escherichia coli* (*E.coli*) C41(DE3) competent cells for expression and purification (see section 2.1.3).

The truncations used within this study for $p53_{2-292}$ (GenBank® accession number NM_000546), $iASPP_{608-828}$ (GenBank® accession number NM_006663), and $ASPP2_{905-1128}$ (GenBank® accession number NM_005426), as well as the $iASPP_{608-828}$ (L625A) mutation, were all generated by Dr. Tamara Skene-Arnold with original cDNA obtained from Dr. Xin Lu (Ludwig Institute for Cancer Research, Oxford, U.K.)[82]. These protein sequences were housed within the pET28a vector, and oriented such that the proteins are N-terminally tagged with six histidine residues to allow for protein purification via Ni^{2+} affinity chromatography. The vectors also contained the IPTG-inducible T7 promoter for regulated protein expression, and the Kanamycin (Kan) resistance gene to allow for selection of only cells containing the pET28a vector. The $iASPP_{608-828}$ (D633R) construct (see section 2.1.2 for site-directed mutagenesis) was also housed in the pET28a vector. These constructs were transformed into Rosetta (DE3)pLysS competent cells (Novagen) for expression and purification (see section 2.1.4). Rosetta (DE3)pLysS cells are derived from BL21(DE3) cells, and contain a chloramphenicol (Cam)-resistant, IPTG-inducible, plasmid with the sequences of tRNAs which would normally limit expression of eukaryotic proteins.

Table 2.1 List of protein constructs and *E.coli* expression strains used in this study. Proteins within the pET28a vector were N-terminally tagged with a His-6 tag, and expressed in Rosetta (DE3)pLysS using Cam and Kan for selection of pET28a vector containing cells. Proteins within the pKK223.3 vector were expressed in C41(DE3) cells using Amp for selection of pKK223.3 vector containing cells.

Protein Construct	Expression Vector	Expression Strain
H_6-p53$_{2-292}$	pET28a	Rosetta (DE3)pLysS
H_6-ASPP2$_{905-1128}$	pET28a	Rosetta (DE3)pLysS
H_6-iASPP$_{608-828}$ (WT)	pET28a	Rosetta (DE3)pLysS
H_6-iASPP$_{608-828}$ (L625A)	pET28a	Rosetta (DE3)pLysS
H_6-iASPP$_{608-828}$ (D633R)	pET28a	Rosetta (DE3)pLysS
PP1cα (WT)	pKK223.3	C41(DE3)
PP1cα (T320D)	pKK223.3	C41(DE3)
PP1cα (1-300)	pKK223.3	C41(DE3)

2.1.2 Site-Directed Mutagenesis and Molecular Cloning

PP1cα (T320D) was engineered using QuikChange® site-directed mutagenesis (Strategene) (see appendix section A for primer sequences). Briefly, forward and reverse primers were designed to create a T320D mutation, as well as introducing a silent restriction enzyme cut site (ClaI). The pKK223.3 vector containing wild-type PP1cα was used as a template, and in conjunction with the designed forward and reverse primers, a polymerase chain reaction (PCR) was used to generate a new plasmid containing the mutation. A thermocycling temperature of 66 °C for elongation was chosen as it was calculated to be approximately 5°C less than the melting temperature (Tm) of the primers. Denaturation, annealing, and elongation were set to 16 cycles.

Table 2.2 Typical PCR Reaction

Reagent	Amount	Source
10X pfu buffer with MgSO4	5 µL	Thermo Scientific
dNTP mix, 2 mM	5 µL	Thermo Scientific
Forward primer (PP1cα (T320D) - Forward)	1.75 µL	Integrated DNA Technologies
Reverse primer (PP1cα (T320D) - Reverse)	1.75 µL	Integrated DNA Technologies
template DNA	2 µL	PP1cα (WT)
dH20	33.5 µL	
pfu polymerase (2.5 units/ul)	1 µL	Thermo Scientific
Final Volume =	50 µL	

Table 2.3 Typical Thermocycling Conditions

Temp (°C)	Time (min:sec)	Description
95	5:00	Initial denaturation
95	0:30	*Denaturation*
66	1:00	*Annealing*
68	5:30	*Elongation*
68	3:00	*Final elongation*
4	infinite	

DpnI (Invitrogen) is a restriction enzyme which digests only methylated DNA, thus was used to enzymatically digest the original plasmid at 37°C overnight, leaving only the nascent mutant-containing plasmid. Plasmids were transformed into DH5α Max Efficiency cells (Invitrogen), and selected for Amp resistance by growing on agar plates containing 200 µg/mL Amp. Plasmids were isolated using the Thermo Scientific GeneJet Plasmid Miniprep Kit, and were screened by restriction enzyme digest of the newly introduced ClaI (Thermo Scientific) restriction enzyme cut site using the Thermo Scientific recommended protocol. These digests were run on a 1% agarose gel for separation and visualization of digested potential clones. Potential clones were verified by Sanger sequencing (The Applied Genomics Core-TAGC). Positive clones were transformed into C41(DE3) competent cells for expression and purification, and cell stocks were stored at -80°C.

The same overall process was used to generate iASPP$_{608-828}$ (D633R) from the pET28A vector containing iASPP$_{608-828}$. However, primers were used to introduce the D633R mutation and a silent restriction enzyme cut site (SacI) approximately 18 nucleic acids 3' to the mutation site (see appendix section A for primers). Dr. Tamara Skene-Arnold generated this clone using a thermocycling elongation temperature of 5°C less than the Tm of the designed primers. Positive clones were selected by plating on LB agar plates containing 30 µg/mL of Kan, and screening for potential clones with the SacI restriction enzyme. The sequences of potential clones were verified by Sanger sequencing. Positive clones were transformed into Rosetta (DE3)pLysS competent cells for expression and purification, and cell stocks were stored at -80°C.

The PP1cα (1-300) truncation was generated by first engineering a reverse primer that integrated a HindIII cut site after the 300th codon and a forward primer containing an EcoRI site isolated PP1cα (1-300). These primers were used to PCR amplify the PP1cα (1-300) truncation from the wild-type PP1cα

template. The amplified sequence was then cut with EcoRI and HindIII, and ligated into the pKK223.3 vector also cut with the same restriction enzymes. Ligated vectors were transformed into DH5α, and selected for on Amp containing plates as with PP1cα (T320D). Potential clones were screened using the EcoRI and HindIII enzymes to digest the vector and assess for the appearance of a band representing the truncated PP1cα (1-300). Positive clones were verified by DNA sequencing. Plasmids were stored in E.coli DH5α cell stocks at -80°C, and transformed into C41 (DE3) for expression and purification as described in section 2.1.3 and 2.1.4.

2.1.3 PP1cα Wild-Type and Mutant Protein Expression and Purification

PP1cα (T320D) and PP1cα (1-300) mutants were engineered using QuikChange® site-directed mutagenesis (as described in section 2.1.2). PP1cα (WT), PP1cα (T320D), and PP1cα (1-300) were recombinantly expressed and purified from C41(DE3) under the control of the tac promoter using the pKK223.3 vector as outlined in Skene-Arnold, *et al* [82]. A glycerol cell stock was plated onto LB agar plates containing 200 µg/mL Amp. A single colony was used to inoculate 400 mL LB containing 200 µg/mL Amp and 1 mM $MnCl_2$. The culture was incubated with shaking overnight (16-18 hours) at 37°C. The overnight culture was used to subculture 4 L of LB containing 200 µg/mL Amp, 1 mM $MnCl_2$, and 0.001% Vitamin B (w/v), and allowed to grow at 37°C with shaking for 2-3 hours, until an optical density of 0.5 at 600nm was reached. Protein expression was induced by the addition of 0.5 mM IPTG for 18 hours at 26°C with shaking. Cells were pelleted at 6000 x g and stored at -80°C until lysis.

The cell pellet was thawed and then resuspended in PP1cα lysis buffer (50 mM imidazole pH 7.5, 0.5 mM ethylenediaminetetraacetic acid (EDTA), 0.5 mM ethylene glycol-bis(β-aminoethyl ether)-N,N,N',N'-tetraacetic acid (EGTA), 2.0 mM $MnCl_2$, 100mM NaCl) containing 0.5 mM phenylmethane sulfonylfluoride (PMSF), 2.0 mM benzamidine, 3.0 mM dithiothreitol (DTT), 10% glycerol (v/v), 2 µg/ µL DNase A, and one sigmaFAST™ protease inhibitor tablet per 100 mL lysis buffer. Resuspended cells were passed three times through an Emulsiflex-C3 high-pressure homogenizer (Avestin) and centrifuged at 13,000 x g for 45 minutes at 4°C to isolate the cytosolic protein supernatant. The supernatant was loaded onto a 75 mL Heparin-Sepharose CL-6B column (GE Healthcare), washed with PP1cα lysis buffer, and eluted by gradient elution over 400 mL using PP1cα lysis buffer containing 100-400 mM NaCl. Fractions of 5 mL were collected and

analyzed by sodium dodecyl sulfate polyacrylamide gel electrophoresis (SDS-PAGE) for purity, and by pNPP assay (see section 2.1.5) for phosphatase activity. Those fractions containing the highest purity and activity were pooled and diluted with Inhibitor-2 buffer (50 mM imidazole pH 7.5, 0.5 mM EGTA, 2.0 mM $MnCl_2$, 0.5 mM PMSF, 3.0 mM DTT, 20% glycerol (v/v)) such that the final concentration of NaCl was 80 mM. The pools were loaded onto a human Inhibitor-2 affinity column (generated by Phuwadet Pasarj in the Holmes lab using NHS-activated Sepharose from GE Healthcare), and PP1cα was eluted with Inhibitor-2 buffer containing either 200 mM or 1 M NaCl. Fractions were pooled based on purity and phosphatase activity, as above, and concentrated to 0.5-2 mg/ mL.

The protein concentration was determined by loading a known volume of protein onto a 10% SDS-PAGE with a 0.25-2µg bovine serum albumin (BSA) standard curve. After staining and visualization using coomassie stain, the signal intensities of each protein band was measured by ImageJ. The protein concentration was determined using the BSA standard curve as reference. PP1cα (WT), PP1cα (T320D), and PP1cα (1-300) were purified to >95% homogeneity as assessed by SDS-PAGE (Figure 2.1). The protein was stored at -20°C in Inhibitor-2 buffer containing 50% (v/v) glycerol.

2.1.4 p53 and ASPP Protein Expression and Purification

N-terminally His-tagged human Wild-Type $iASPP_{608-828}$, $ASPP2_{905-1128}$, $iASPP_{608-828}$ (L625A) mutant, and $p53_{2-292}$ were originally genetically engineered as outlined in Skene-Arnold, *et al* [82]. $iASPP_{608-828}$ (D633R) mutant was engineered using QuikChange® site-directed mutagenesis (section 2.1.2). All constructs were recombinantly expressed and purified from *E.coli* Rosetta pLys cells under the control of the T7 promoter using the pET28A vector. Glycerol cell stock was plated onto LB Agar plates containing 34 µg/mL Cam and 30 µg/mL of Kan. A single colony was used to inoculate 400 mL LB containing 34 µg/mL Cam and 30 µg/mL Kan. The culture was incubated with shaking overnight (16-18 hours) at 37°C. The overnight culture was used to subculture 4 L of LB containing 34 µg/mL Cam and 30 µg/mL Kan, and grown at 37°C with shaking for 2-3 hours, until an optical density of 0.5 at 600nm was reached. Protein expression was induced by the addition of 0.3 mM IPTG for 18 hours at 26°C with shaking. Cells were pelleted at 6000 x g and stored at -80°C until lysis.

The cell pellet was resuspended in ASPP lysis buffer (25 mM sodium phosphate pH 8.0,125 mM

NaCl, and 1% Tween-20 (v/v)), containing 15 mM imidazole, 0.5 M NaCl, 2.7 mM KCl, 1.0 mM PMSF, 5 mM β-mercaptoethanol (β-Me), 2 µg/ µL DNase A, and one sigmaFAST™ protease inhibitor EDTA-free tablet per 100 mL lysis buffer. Resuspended cells were passed three times through an Emulsiflex-C3 high-pressure homogenizer (Avestin) and centrifuged at 13,000 x g for 45 minutes at 4°C to isolate the cytosolic fraction. The supernatant was loaded onto a Ni-NTA (Ni^{2+}-nitrilotriacetate) affinity His-prep FF 16/10 column (GE Healthcare), washed with ASPP lysis buffer, and eluted by step-wise gradient elution using lysis buffer containing 150 mM, 250 mM, or 500 mM imidazole. Fractions of 5 mL were collected and analyzed by SDS-PAGE for purity. Those fractions containing the highest purity (250 mM imidazole elutions) were pooled, loaded, and finally separated on a Superdex 75 26/60 size exclusion column (GE Healthcare) using ASPP elution buffer (25 mM Tris-HCl pH 8.0, 300 mM NaCl, 1 mM DTT). Fractions were pooled based on purity and concentrated to 0.1-4 mg/ mL. The concentration was determined by SDS-PAGE as described in section 2.1.3. $p53_{2-292}$, $iASPP_{608-828}$ (WT), $iASPP_{608-828}$ (L625A), $iASPP_{608-828}$ (D633R), and $ASPP2_{905-1128}$ constructs were purified to > 80% homogeneity as assessed by SDS-PAGE (Figure 2.1). The protein was stored at -20°C in ASPP elution buffer with 50% (v/v) glycerol.

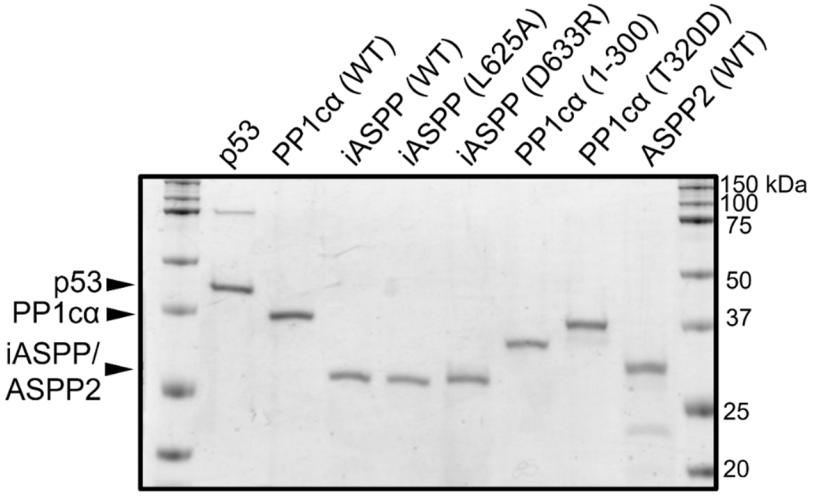

Figure 2.1 Proteins expressed and purified for use within this thesis.
The figure depicts approximately 0.5 µg of each protein recombinantly expressed and purified for use in this study run on an 8% SDS-PAGE gel and stained with coomassie. $p53_{2-292}$, $iASPP_{608-828}$ (WT), $iASPP_{608-828}$ (L625A), $iASPP_{608-828}$ (D633R), and $ASPP2_{905-1128}$ contructs were purified to >80%homogeneity using Ni^{2+} NTA affinity column followed by size exclusion gel filtration. PP1cα (WT), PP1cα (T320D), and PP1cα (1-300) were purified to >95% homogeneity using an inhibitor-2 ligand affinity column, followed by separation with a heparin column.

2.1.5 Para-Nitrophenyl Phosphate Assay for Phosphatase Activity

To assess the activity of PP1cα, PP1cα (T320D), PP1cα (1-300) during protein purification, a para-Nitrophenyl Phosphate (pNPP) colourimetric assay was used. Each fraction (10 µL) was diluted in pNPP buffer (50 mM Tris-HCl, pH 8.3, 1.0 mM EGTA, 30 mM $MgCl_2$, 1 mg/ mL bovine serum albumin (BSA), 0.5 mM $MnCl_2$, and 0.2% β-Me) and 5 mM pNPP in a total reaction volume of 60 µL in a 96-well plate. Reactions were incubated for 10 minutes at 37°C until the absorbance at 405 nm was approximately 0.2-0.8 in peak fractions. Those fractions containing the highest activity were pooled as described in section 2.1.3.

2.2 *In vitro* Dephosphorylation of p53

The initial method for evaluating the dephosphorylation of p53 by PP1cα as mediated by the ASPP proteins was designed by Dr. Tamara Skene-Arnold in the Holmes Laboratory, as is outlined in her PhD thesis[110]. Preliminary data in Dr. Skene-Arnold's PhD thesis showed promising results for iASPP-mediated dephosphorylation of p53Ser15 by PP1cα. Briefly, 100 ng of DNAPK (obtained from Dr. Susan-Lees Miller, University of Calgary) was used to phosphorylate 1 µg of p53 in Buffer P (50 mM Tris-HCl pH 8.0, 10 mM $MgCl_2$, 1 mM DTT, 0.2 mM EGTA, 0.5 mM $MnCl_2$,75 mM KCl, 0.5 mM ATP, 10 µg/ml sonicated calf thymus DNA) for 30 minutes at 30°C. Phosphorylation was stopped using the ATP competitive inhibitor of DNAPK, LY294002. Phosphorylated p53, PP1cα, and iASPP, were added in equal amounts (to emulate the conditions under which the p53:PP1cα:iASPP complex was found through gel filtration) and dephosphorylated for 45 minutes at 30°C in Buffer P. The results were analyzed using phospho-specific antibodies and western blotting.

This initial method was further developed and modified for the purposes of this thesis as outlined in the following methods.

2.2.1 DNAPK and DYRK2 Phosphorylation Time Courses

Phosphorylation time courses of p53Ser15, Thr18, and Ser37 were conducted as follows. p53 (0.5 µg, 944mM final concentration) was phosphorylated by 75 U of DNA-dependent Protein Kinase (DNAPK) (Promega) in a reaction volume of 20 µL using DNAPK Kinase Buffer (50 mM Tris-HCl, pH 8.0, 10 mM

$MgCl_2$, 0.2 mM EGTA) containing 75 mM KCl, 1.0 mM DTT, 0.5 mM ATP, 10 µg/ mL sonicated calf thymus DNA, and 0.5 mM $MnCl_2$, for 15-360 minutes at 30°C. Reaction was stopped by the addition of 2 x Laemmli Sample Buffer (SB). Phosphorylation was assessed using western blotting and site-specific phospho-antibodies as described in 2.2.5.

The phosphorylation time course of p53Ser46 was conducted as above with the following modifications. p53 (0.5 µg, 944mM final concentration) was phosphorylated by 75 U of DYRK2 (Sigma-Aldrich) in a reaction volume of 20 µL using DYRK2 Kinase Buffer (50 mM Tris-HCl, pH 7.5, 10 mM $MgCl_2$, 0.2 mM EGTA) containing 75 mM KCl, 1.0 mM DTT, 0.5 mM ATP, and 0.5 mM $MnCl_2$, for 15-360 minutes at 30°C. Reaction was stopped with 2 x SB and phosphorylation over time was assessed by western blotting using phospho-specific antibodies as described in section 2.2.5.

2.2.2 PP1cα Dephosphorylation Time Courses of p53Ser15, Thr18, Ser37, Ser46, and DYRK2-phosphorylated p53

For assessing the dephosphorylation of over time of p53Ser15, Thr18, and Ser37, p53 (0.5 µg, 944mM final concentration) was phosphorylated by 75 U of DNA-dependent Protein Kinase (DNAPK) (Promega) in a reaction volume of 20 µL using DNAPK Kinase Buffer (50 mM Tris-HCl, pH 8.0, 10 mM $MgCl_2$, 0.2 mM EGTA) containing 75 mM KCl, 1.0 mM DTT, 0.5 mM Adenosine Triphosphate (ATP), 10 µg/ mL sonicated calf thymus DNA (ctDNA), and 0.5 mM $MnCl_2$, for 90 minutes at 30°C. The phosphorylation reaction was stopped by the addition of 1 mM of the specific inhibitor, LY294002, and incubated at room temperature for 10 minutes. PP1cα (0.125 µg, 333 mM final concentration) was subsequently incubated with phosphorylated p53 (0.125 µg, 472 mM final concentration) in a total reaction volume of 10 µL diluted in DNAPK Kinase Buffer containing 1.0 mM DTT and 0.5 $MnCl_2$, for 1-62 minutes at 30°C. Accounting for contributing species from all proteins added, the final dephosphorylation reaction conditions were: 50 mM Tris HCl, pH 8.0, 20 mM NaCl, 40 mM KCl, 1 mM Imidazole, 5% glycerol, 0.8 mM $MnCl_2$, 1.6 mM DTT, 10 mM $MgCl_2$, 0.2 mM EGTA, 0.3 mM ATP, 5.5 µg/mL CTDNA, and 0.01 mM PMSF. Dephosphorylation was stopped by the addition of 2 x SB, and phosphorylation was assessed by western blotting as described in section 2.2.5.

The dephosphorylation time course of p53Ser46 was similar to p53Ser15, Thr18, and Ser37 with the following modifications. p53 (0.5 µg, 944mM final concentration) was phosphorylated by 75 U of Dual Specificity Tyrosine-Regulated Kinase-2 (DYRK2) (Sigma-Aldrich) in a reaction volume of 20 µL DYRK2 Kinase Buffer (50 mM Tris-HCl, pH 7.5, 10 mM $MgCl_2$, 0.2 mM EGTA) containing 75 mM KCl, 1.0 mM DTT, 0.5 mM ATP, and 0.5 mM $MnCl_2$, for 90 minutes at 30°C. The phosphorylation reaction was stopped by the addition of 1 mM of the specific inhibitor, INDY, and incubated at room temperature for 10 minutes. PP1cα (0.125 µg, 333 mM final concentration) was subsequently incubated with phosphorylated p53 (0.125µg, 472 mM final concentration) in a total reaction volume of 10 µL in DYRK2 Kinase Buffer containing 1.0 mM DTT and 0.5 $MnCl_2$, for 0-120 minutes at 30°C. Accounting for contributing species from all proteins added, the final reaction conditions were the same as those for Ser15, Thr18, and Ser37, however the pH was changed to 7.5 and no sonicated calf thymus DNA was added. Dephosphorylation was stopped by the addition of 2 x SB, and phosphorylation was assessed by western blotting and gel shift analysis as described in section 2.2.5.

2.2.3 ASPP-mediated Dephosphorylation of p53

ASPP-mediated dephosphorylation of p53Ser15 and p53Thr18 were assessed in a similar manner as section 2.2.2 with the following modifications. p53 (0.5 µg, 944mM final concentration) was phosphorylated by 75 U of DNAPK in a final reaction volume of 20 µL using DNAPK Kinase Buffer containing 75 mM KCl, 2.0 mM DTT, 0.5 mM ATP, 10 µg/ mL sonicated calf thymus DNA, 1.0 mM $MnCl_2$, 10mM NaCl, and 0.025% Tween-20, for 90 minutes at 30°C. p53Ser46 (or DYRK2 phosphorylated p53) was phosphorylated in the same manner with DYRK2, however the pH was 7.5 (instead of pH 8) and no calf thymus DNA was added.

PP1cα, either alone or combined with ASPP, was pre-incubated at 30°C for 15 minutes in either DNAPK or DYRK2 Kinase Buffer containing 2.0 mM DTT and 1.0 mM $MnCl_2$. The pre-incubation was then incubated together with phosphorylated p53 (0.125 µg, 472 mM final concentration) at 30°C for 30 minutes in the same buffer and a total reaction volume of 10 µL (0.125 µg of PP1cα, iASPP, and ASPP2, with final concentrations of 333 mM, 517 mM, and 492 mM respectively) . Assessment of PP1cα or ASPP mutations

were assessed in the same manner. Dephosphorylation was stopped by the addition of 2 x SB, and phosphorylation was assessed by western blotting as described in section 2.2.5.

Accounting for contributing species from all proteins added, the final dephosphorylation reaction conditions for Ser15 and Thr18 were: 48 mM Tris HCl, pH 8.0, 40 mM NaCl, 40 mM KCl, 1 mM Imidazole, 8% glycerol, 1 mM $MnCl_2$, 2 mM DTT, 8 mM $MgCl_2$, 0.2 mM EGTA, 0.3 mM ATP, 5.5 µg/mL sonicated calf thymus DNA, and 0.01 mM PMSF. The final dephosphorylation reaction conditions for Ser46/ DYRK2 phosphorylated p53 were the same however the pH was 7.5 and no calf thymus DNA was added. These final conditions differ slightly from the PP1cα time courses alone (see section 2.2.2). For all further experiments with the ASPP proteins, these modified buffer conditions were used to allow for an environment that further stabilized the ASPP and PP1cα proteins in solution (see appendix section B1 for the difference in solubility).

The effect of the ASPP proteins on p53Ser15 dephosphorylation by PP1cα was further analyzed using a time course to show that the ASPP proteins do indeed increase the rate of dephosphorylation. The same procedure was used as above, with PP1cα alone, or in the presence of either iASPP or ASPP2. However, the dephosphorylation was measured from 0 - 45 minutes, instead of using a single time point (30 minutes).

The effects of the ASPP proteins on dephosphorylation of DYRK-phosphorylated p53 by PP1cα were assessed similarly to p53Ser15, however the dephosphorylation reaction was carried out over 20 minutes, and phosphorylation was assessed by analyzing the mobility shift from phosphorylated to dephosphorylated state of p53 without the use of phosphospecific antibodies (see section 2.2.5)

2.2.4 PP1cα (T320D), and PP1cα (1-300) Dephosphorylation Time Courses

Dephosphorylation time courses were used to assess the effects of the PP1cα (T320D) and PP1cα (1-300) mutations on the ability of PP1cα to dephosphorylate p53Ser15. p53 was phosphorylated by DNAPK as indicated in section 2.2.3. PP1cα (T320D) or PP1cα (1-300) were pre-incubated at 30°C for 15 minutes in DNAPK Kinase Buffer containing 2.0 mM DTT and 1.0 $MnCl_2$. The pre-incubated PP1cα (1-300) and PP1cα (T320D) with final concentrations of 364 mM or 333 mM, respectively were then incubated together with phosphorylated p53 (472 mM final concentration) at 30°C for 0 - 90 minutes in a final reaction

volume of 10 µL, and the final dephosphorylation reaction conditions were the same as section 2.2.3. Dephosphorylation was stopped by the addition of 2 x SB, and phosphorylation was assessed by western blotting as described in section 2.2.5.

2.2.5 Western Blotting and Detection of $p53_{2-292}$ Phosphorylation

Phosphorylation and dephosphorylation reactions were evaluated by Western Blot. Samples were loaded onto a 12% SDS-PAGE gel and transferred 0.4 µm nitrocellulose membrane (GE Healthsciences) using a modified Towbin's transfer buffer (25 mM Tris-HCl, 190 mM glycine, 20% methanol, 0.1% sodium dodecyl sulphate (SDS)) and a Mini Trans-Blot® Cell wet transfer apparatus (BIO-RAD). Nitrocellulose was stained with a Pierce™ Reversible Protein Stain Kit, and visualized for total protein, before being blocked by 5% (w/v) skim milk powder in TBST (50 mM Tris-HCl, pH7.5, 150 mM NaCl, 0.1% Tween-20) for 1 hour at room temperature. Phospho-specific antibodies (Cell Signalling Technologies) were incubated either overnight at 4°C, or 1 hour at room temperature in 5% skim milk powder/TBST. p53Ser15 (#16GB) was diluted 1:15000, p53Thr18 (#2529) was diluted 1:4000, and p53Ser46 (#2521) was diluted 1:8000. The nitrocellulose was washed in TBST and then incubated with the appropriate secondary antibody conjugated to the horse radish peroxidase enzyme (HRP) for 1 hour at room temperature. The western blot was developed by Chemiluminescence using Clarity™ Western ECL Substrate (BIO-RAD). Band intensities of total p53 (using the reversible stain) and phospho-p53 (western blotting) were quantified using Image Studio Light Software or ImageJ. The phospho-p53 signal was normalized to the total p53 stain, then normalized to either the phosphorylated-p53 alone lane or PP1cα alone as indicated.

For the determination of the effect of ASPPs on dephosphorylation of DYRK2-phosphorylated p53 by PP1cα, samples were run on an 8% SDS-PAGE to obtain separation of the phopho-p53 (upper band) from the dephospho-p53 (lower band). Samples were transferred to nitrocellulose and the Pierce™ Reversible Protein Stain Kit was used to image the band shifts. Band intensities were quantified using ImageJ software. Phospho-p53 signal was divided by the signals of the phospho-p53 and dephospho-p53 combined to obtain % total phosphorylation. % total phosphorylation was then normalized to the PP1cα alone lane.

The phospho-specific signal was divided by the total p53 signal obtained from the nitrocellulose Pierce™ Reversible Protein Stain.

2.2.6 Statistical Analysis

Normalized data was evaluated for outliers by calculating the first and third quartiles to obtain the interquartile range using Excel. A data point was deemed an outlier if it was 1.5 times the interquartile range from either the first or third quartile.

The data was entered into Graphpad Prism, and analyzed using a one-way analysis of variance (ANOVA), followed by the Tukey's test for individual multiple comparison tests ($p<0.05$). For the Graphpad Prism ANOVA and multiple comparison test read outs, see section C of the appendix.

2.3 Binding Experiments of p53, PP1cα, and ASPP proteins

2.3.1 Microcystin-Sepharose Pulldown Experiments

Microcystin-LR (MC) was originally isolated from *Microcystis aeruginosa* (collected from Little Beaver Lake, Alberta) using solvent extraction followed by C18 reverse phase high performance liquid chromatography (HPLC)[83,111]. It was then linked to N-Hydroxysuccinimidyl-Sepharose (NHS-Sepharose) by Phuwadet Pasarj and Melissa McLellan in the Holmes lab to create microcystin Sepharose (MC-S)[83,111]. The Sepharose was used in a modified pull-down experiment to assess the interaction of potential interactors of PP1cα, following a similar method to Skene-Arnold, *et al.* [82].

To assess whether BSA would be a valid control as a protein that does not bind to PP1cα, 5 µg of PP1cα was bound to MC-S in MC Binding Buffer (50 mM Tris-HCl, pH 7.4, 0.1 mM EDTA, 0.5 mM $MnCl_2$, 0.2% β-Me) at a final volume of 600 µL (222 mM final concentration) for 2 hours, end-over-end, at 4°C. Sepharose was washed with binding buffer and 5 µg of BSA (250 mM final concentration) was incubated in 300 µL Binding Buffer containing 150 mM NaCl and 0.1% Tween-20, overnight, end-over-end. The Sepharose was then washed with binding buffer, and PP1cα and BSA were eluted from the beads with 2 x

SB and heat. Samples were loaded onto 12 % SDS-PAGE gels and bands were visualized with coomassie stain as shown in the appendix section B.3.

To evaluate whether iASPP$_{608-828}$, p53$_{2-292}$, and PP1cα, as well as ASPP2$_{905-1128}$, p53$_{2-292}$, and PP1cα, could form trimeric complexes, MC-seph pulldown experiments were performed as above with the following modifications. Equimolar (0.25nmol) amounts of p53 (8.0 µg), PP1cα (9.3 µg), and either iASPP (6 µg) or ASPP2 (6.4 µg) were incubated together at 30°C for 45 minutes in 300 µL Trimeric Binding Buffer ((50 mM Tris-HCl, pH 7.5, 0.1 mM EDTA, 1.0 mM $MnCl_2$, 50 mM NaCl, 75 mM KCl, and 0.2% β-Me), similar to Skene-Arnold *et al.*[82]. The incubated protein complexes were added to MC-seph for 3 hours, 4°C, end-over-end, then washed with Trimeric Binding Buffer. PP1cα, p53, and iASPP$_{608-828}$ or ASPP2$_{905-1128}$ were eluted from the beads using 2 x SB and heat, loaded onto a 12% SDS-PAGE gel, and visualized with coomassie stain.

MC-S pulldown experiments were also used evaluate the effects of PP1cα (T320D), PP1cα (1-300), iASPP$_{608-828}$ (L625A), and iASPP$_{608-828}$ (D633R), on the binding of PP1cα (WT) to iASPP$_{608-828}$. 2 µg of PP1cα (WT), PP1cα (T320D), or PP1cα (1-300) (89 mM, 89mM, and 97 mM final concentration respectively) in 600 µL were incubated with resin for 2 hours, 4°C, end-over-end in Trimeric Binding Buffer. Resin was washed and subsequently, 2 µg of iASPP$_{608-828}$, iASPP$_{608-828}$ (L625A), or iASPP$_{608-828}$ (D633R), (275mM final concentration) in 300 µL was incubated with resin in Trimeric Binding Buffer for 2 hours, 4°C, end-over-end. The resin was washed, and elution and visualization were the same as above.

2.3.2 Nickel-NTA Affinity Pulldown Experiments

To assess whether BSA would be a valid control as a protein that does not bind to p53$_{2-292}$, 5 µg of p53 (314 mM final concentration) was bound to His-Pur Ni^{2+} NTA resin (Thermo Fischer Scientific) in 600 µL Ni^{2+} NTA Binding Buffer (50 mM Tris-HCl, pH 7.5, 150 mM NaCl, 10 mM imidazole, and 0.5 mM $MnCl_2$) for 2 hours, end-over-end, at 4°C. Resin was washed with Ni^{2+} NTA Wash Buffer (Ni^{2+} NTA Binding Buffer containing 0.1% Tween-20, and 30 mM imidazole). 5 µg of BSA (250 mM final concentration) was added and incubated with p53 bound to the beads in 600 µL Bind Buffer overnight, end-over-end. The resin was washed, and p53 and BSA were eluted from the beads with 2 x SB and heat. Samples were loaded onto 12 % SDS-PAGE gels and bands were visualized with coomassie stain.

Ni^{2+} NTA pulldown experiments were also used to evaluate the effects of PP1cα (T320D), PP1cα (1-300), $iASPP_{608-828}$ (L625A), and $iASPP_{608-828}$ (D633R), on the binding of PP1cα (WT) to $iASPP_{608-828}$. 2 µg of $iASPP_{608-828}$, $iASPP_{608-828}$ (L625A), or $iASPP_{608-828}$ (D633R), (138 mM final concentration) were incubated with resin for 2 hours, 4°C, end-over-end in 600 µL of the appropriate buffer. Resin was washed and subsequently, 2 µg of PP1cα (WT), PP1cα (T320D), or PP1cα (1-300) (178 mM, 178 mM, and 194 mM respectively) was incubated with resin in 300 µL bind buffer for 2 hours, 4°C, end-over-end. The resin was washed, and elution and visualization were the same as above. This experiment was conducted three times with buffers of differing ionic strength (1 replicate each). One experiment used the Trimeric Complex Buffer, however there was a significant amount of unspecific binding from the PP1cα (WT) as well as the PP1cα mutants (figure 4.1). A second experiment was run using Ni^{2+} NTA Binding Buffer containing 150 mM NaCl (as used with BSA experiments above), however a significant amount of unspecific binding of PP1cα WT was still observed. A third experiment was run using the Ni^{2+} NTA Binding Buffer containing 500 mM NaCl, which minimized the amount of PP1cα unspecific binding. The first experiment (using the Trimeric Binding Buffer) is included in section 4.2.1.

The intensities of the iASPP and PP1cα bands were quantified using ImageJ software, and the intensities measured for PP1cα unspecific binding were subtracted from the PP1cα intensities measured in the PP1cα: iASPP samples. The intensities of the PP1cα proteins were divided by those of the iASPP proteins to obtain a PP1cα: iASPP ratio. The ratios of the PP1cα and iASPP mutations were then normalized to the PP1cα (WT): iASPP (WT) ratio and represented as a normalized percentage.

CHAPTER 3

ASPP Proteins Mediate the Dephosphorylation of p53 by PP1cα

CHAPTER THREE: ASPP PROTEINS MEDIATE THE DEPHOSPHORYLATION OF P53 BY PP1cα

p53Ser15, Thr18, and Ser46 phosphorylation are all signs of p53 activation in response to cellular stress. While PP1cα has been shown to dephosphorylate p53Ser15, the dephosphorylation of p53Thr18 or Ser46 by PP1cα has not yet been assessed. The ASPP proteins were previously found to associate with both p53 and PP1cα *in vitro* [82]. Given their opposing functions on p53, and the differential abilities of their C-termini to form a complex with PP1c and p53, I hypothesized that the C-terminal of iASPP would mediate the dephosphorylation of all three p53 phosphorylation sites while the C-terminal of ASPP2 would not.

3.1 Results

3.1.1 DNAPK phosphorylates p53Ser15, Thr18, and Ser37, and DYRK2 phosphorylates p53Ser46 *in vitro.*

Before assessing which sites are dephosphorylated by PP1cα, DNAPK and DYRK2 phosphorylation time courses were conducted. This allowed us to ensure there was sufficient phosphorylation under the conditions used prior to dephosphorylation, as well as test the relative specificity of the phospho-antibodies for discerning phosphorylated p53 versus dephosphorylated p53. As shown in figure 3.1 A, the phosphorylation as assessed by p53Ser15, Thr18, and Ser37 antibodies increases in intensity over time of incubation with DNAPK. In figure 3.1 B, there is no apparent phosphorylation in the reaction containing the DNAPK inhibitor, LY294002.

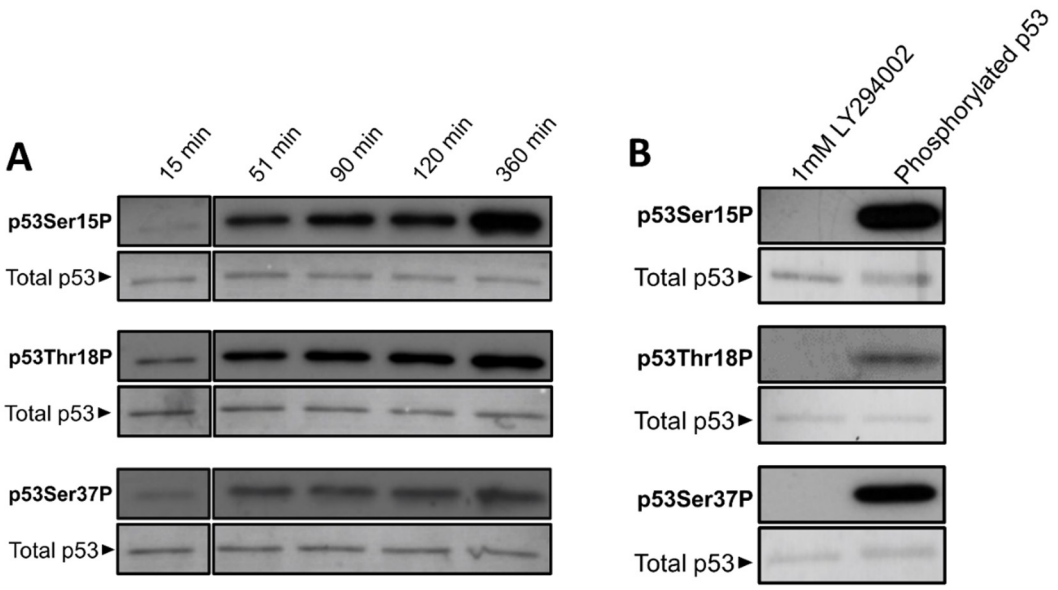

Figure 3.1 DNAPK phosphorylates p53Ser15, Thr18, and Ser37 *in vitro*, and phosphorylation is inhibited by specific inhibitor, LY294002.
Panel A depicts the phosphorylation of p53Ser15, Thr18, and Ser37 by DNAPK *in vitro* over 360 minutes as measured by western blot using phosphospecific antibodies. p53 was phosphorylated by DNAPK at 30 °C for 15-360 minutes. The samples were run on 12% SDS-PAGE, and transferred onto a 0.4µm nitrocellulose membrane. The membrane was stained with Pierce™ Reversible Protein Stain for detection of total p53 protein amount (bottom panels). Phospho-p53 antibodies specific for phosphorylated Ser15, Ser37, or Thr18 were then used to detect respective levels of phosphorylation (upper panels). Panel B depicts the specificity of the phospho-antibodies was tested using 1 mM LY294002 DNAPK inhibitor run in parallel to phosphorylated p53. n=1

To assess whether p53Ser46 was also phosphorylated under similar conditions, a phosphorylation time course of p53Ser46 by DYRK2 was conducted similar to those conducted with DNAPK. As expected, the p53Ser46 signal increases over time of incubation with DYRK2, and when the DYRK2 inhibitor, INDY, is added no phosphorylation is apparent.

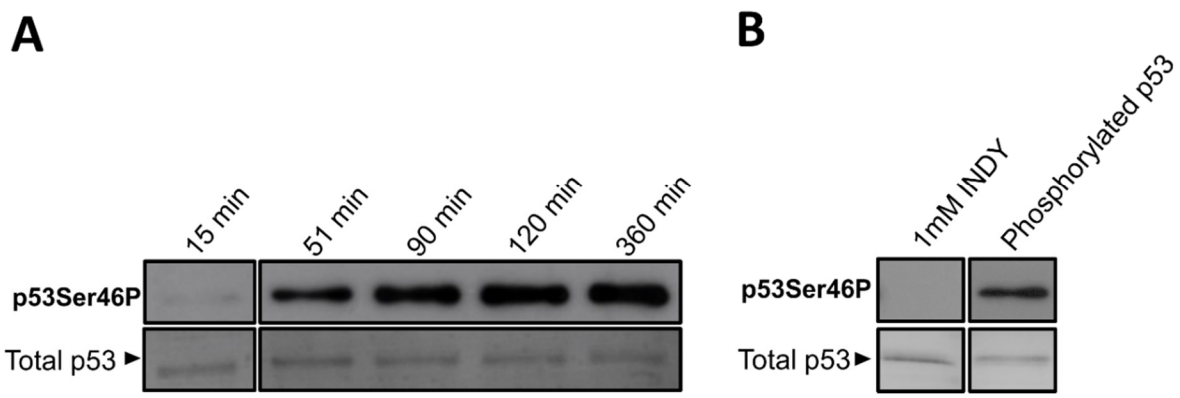

Figure 3.2 DYRK2 phosphorylates p53Ser46 *in vitro* and phosphorylation is inhibited by specific inhibitor, INDY.
A) The figure depicts the phosphorylation of p53SerSer46 *in vitro* over 360 minutes as measured by western blot using a phosphospecific antibody. p53 was phosphorylated by DYRK2 at 30 °C for 15-360 minutes. The samples were run on 12% SDS-PAGE, and transferred onto a 0.4µm nitrocellulose membrane. The membrane was stained with Pierce™ Reversible Protein Stain for detection of total p53 protein amount (bottom panels). Phospho-p53 antibody specific for phosphorylated p53Ser46 was then used to detect respective levels of phosphorylation (upper panels). B) The specificity of the phospho-antibody was tested using 1 mM INDY DYRK2 inhibitor run in parallel to phosphorylated p53. n=1

3.1.2 p53Ser15, Thr18, and Ser37 are dephosphorylated by PP1cα *in vitro.*

p53Ser15 and p53Ser37 have previously been shown to be dephosphorylated by PP1cα both in cells and in *in vitro* dephosphorylation experiments [61]. The results presented here replicate those findings using a dephosphorylation time course (Figure 3.3). Furthermore, given its importance in p53 stability by mediating the dissociation of Mdm2, the dephosphorylation of p53Thr18 by PP1cα was also assessed using this method. p53Ser15, Thr18, and Ser37 were phosphorylated by DNAPK and phosphorylation was subsequently inhibited with 1 mM LY294002. Phospho-p53 was then dephosphorylated by PP1cα from 0-62 minutes, as outlined in the methods (section 2.2.2). The results show that in addition to p53Ser15 and Ser37, p53Thr18 is also capable of being dephosphorylated by PP1cα. Although the exact rate of dephosphorylation cannot be obtained due to the fact that these experiments were not conducted under Michaelis Menten conditions (the substrate concentration is not in excess) it is apparent that p53Thr18 and Ser37 are dephosphorylated at comparatively similar rates, while p53Ser15 is considerably slower (figure 3.3). While Thr18 and Ser37 both reach 0% phosphorylation by 62 minutes, Ser15 is still 50% phosphorylated by 62 minutes relative to the start of the time course.

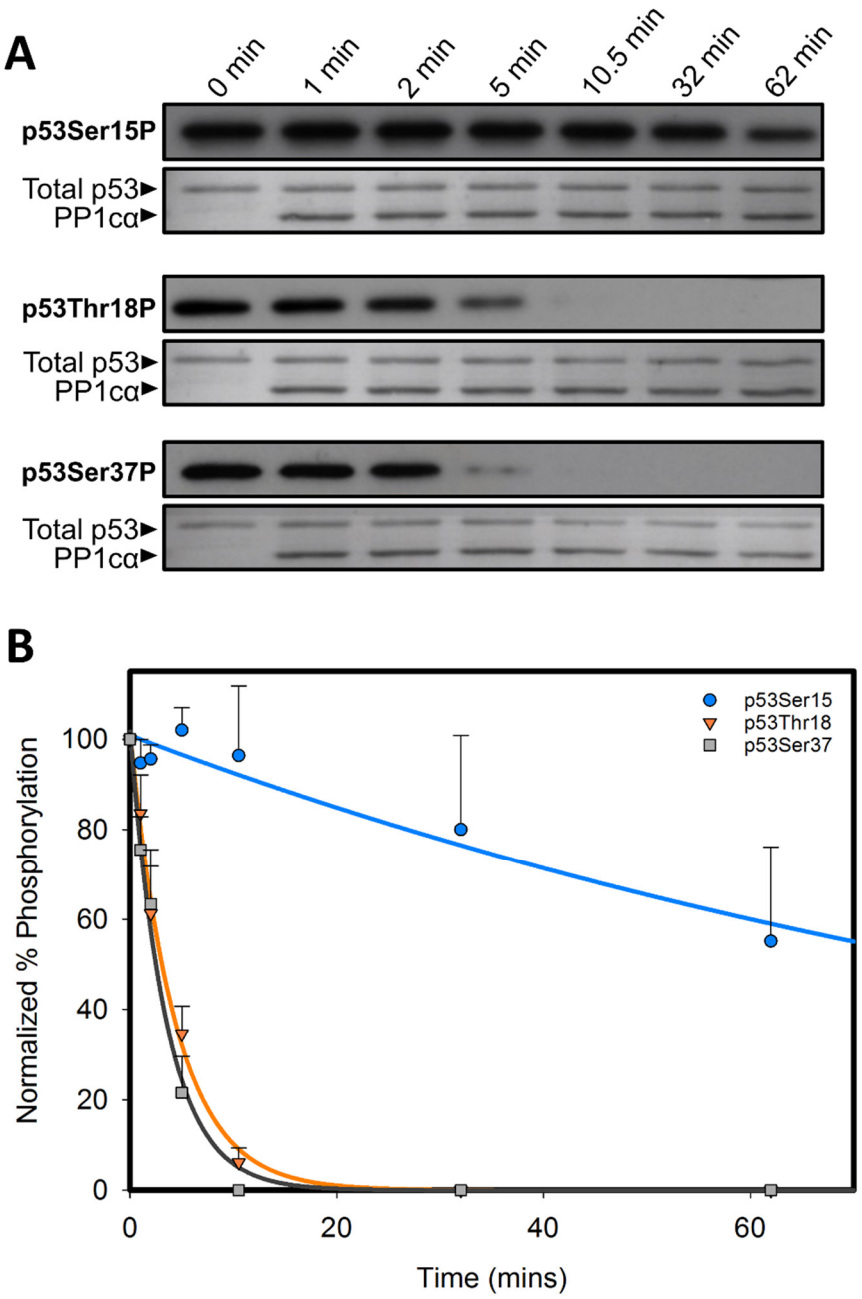

Figure 3.3 p53Ser15, Thr18, and Ser37 are dephosphorylated by Protein Phosphatase-1cα at different rates *in vitro*.
The figure depicts the dephosphorylation of p53Ser15, Thr18, and Ser37 by PP1cα over 62 minutes as measured by western blot using phospho-specific antibodies. p53 was phosphorylated by DNAPK for 90 minutes at 30°C. The phosphorylation reaction was stopped by the addition 1 mM DNAPK inhibitor LY249002. PP1cα was subsequently incubated with phosphorylated p53 (333 mM and 472 mM, respectively) from 0 to 62 mins at 30°C. Samples were run on a 12% SDS-PAGE, and transferred to a 0.4µm nitrocellulose membrane. A) The membrane was stained with Pierce™ Reversible Protein Stain for detection of total p53 protein amount (bottom panels). Phospho-p53 antibodies specific for phosphorylated p53Ser15, Thr18, and Ser37 was used to detect respective levels of phosphorylation (upper panels). B) The band intensities were quantified using ImageJ and the phosphorylated signal was normalized to total p53 stain. The graph represents the % phosphorylation normalized to 0 minutes. n=3

3.1.3 DYRK2 Phosphorylated-p53 is dephosphorylated by PP1cα *in vitro*

DYRK2 was used to phosphorylate p53 and the phosphorylation was stopped by using the DYRK2 inhibitor, INDY. After the addition of INDY, PP1cα was added for 0-62 minutes, and the phosphorylation status of p53 was evaluated using a phospho-specific antibody against p53Ser46. Using the phospho-specific antibody, no apparent dephosphorylation of Ser46 was detected (figure 3.4). Upon closer evaluation, the signal of the phospho-p53Ser46 appears to *increase* with the addition of PP1cα over time. However, the Pierce™ Reversible Protein Stain used for detecting total p53 levels clearly shows a band shift upon addition of PP1cα. In order to separate the prominent band shifts, a second set of time courses was conducted using an 8% SDS-PAGE instead of a 12% SDS-PAGE (figure 3.5). Using this method there are at least 3 bands present over the dephosphorylation time course: 1) The upper-most band in the positive control, 2) at 2 minutes dephosphorylation, the most prominent band is slightly below the positive control band, but still higher than the dephospho-p53, 3) at 60 minutes dephosphorylation, the most prominent band is the lowest, dephospho-p53.

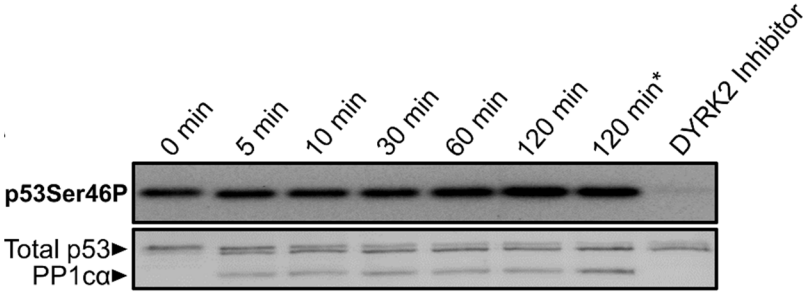

Figure 3.4 p53Ser46 dephosphorylation cannot be assessed using western blotting.
The figure depicts the dephosphorylation of DYRK2 phosphorylated p53 by PP1cα over time using p53Ser46 antibody and western blotting. p53 was phosphorylated by DYRK2 for 90 minutes at 30°C. The phosphorylation reaction was stopped by the addition 1 mM DYRK2 inhibitor, INDY. PP1cα was subsequently incubated with phosphorylated p53 (333 mM and 472 mM, respectively) at 30°C for 0-120 minutes. Samples were run on a 12% SDS-PAGE, and transferred to a 0.4µm nitrocellulose membrane. The membrane was stained with Pierce™ Reversible Protein Stain for detection of total p53 protein amount (bottom panel). Phospho-p53 antibody specific for phosphorylated p53Ser46 was used to detect levels of phosphorylation (upper panel). * The amount of PP1c was doubled in this sample. n=2

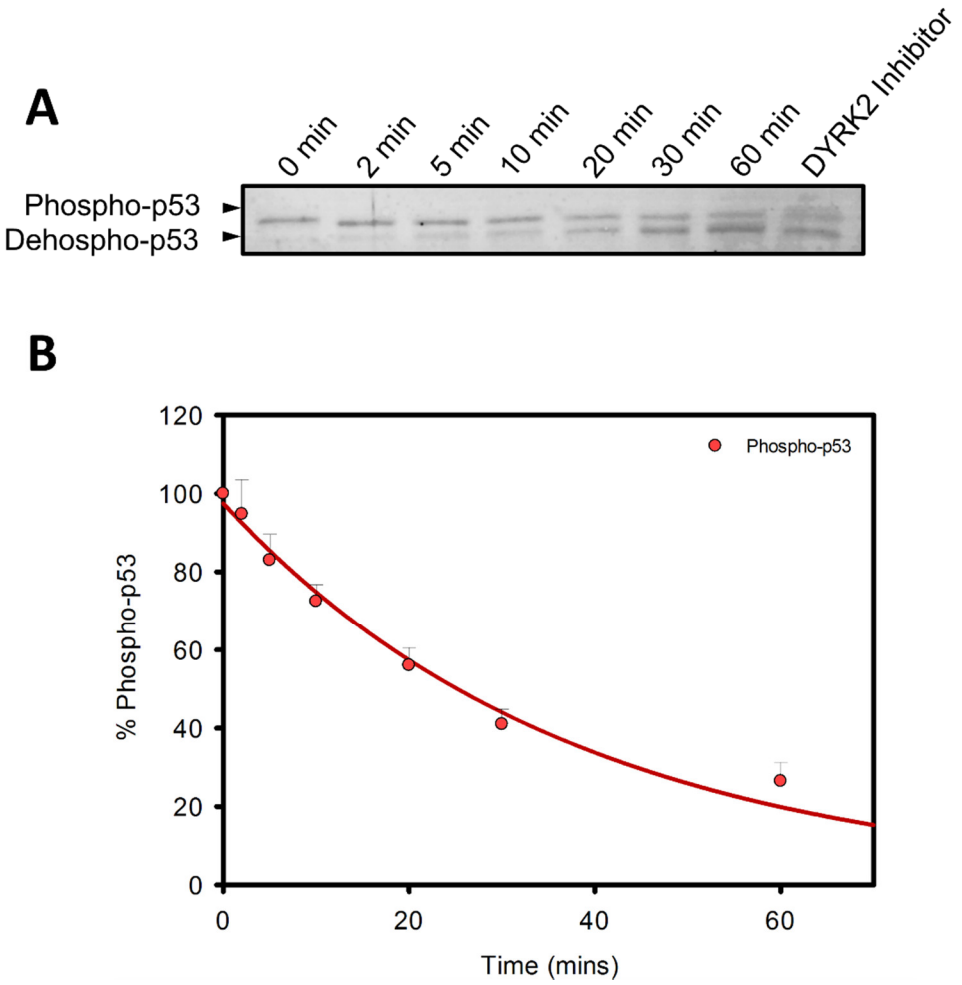

Figure 3.5 PP1cα dephosphorylates DYRK2-phosphorylated p53 *in vitro*.
The figure depicts the dephosphorylation of DYRK2-phosphorylated p53 by PP1cα over time using band shift analysis. p53 was phosphorylated by DYRK2 for 90 minutes at 30°C. The phosphorylation reaction was stopped by the addition 1 mM DYRK2 inhibitor, INDY. PP1cα was subsequently incubated with p53 (333 mM and 472 mM, respectively) at 30°C for 0-60 minutes. Samples were run on an 8% SDS-PAGE, and transferred to a 0.4µm nitrocellulose membrane. A) The membrane was stained with Pierce™ Reversible Protein Stain for detection of phospho-p53 (upper band) and dephospho-p53 (lower band). B) The band intensities were quantified using ImageJ and the phospho-p53 signal was divided by the sum of the phospho-p53 signal and the dephospho-p53 signal to obtain %phospho-p53. Data is represented as % phospho-p53 relative to the 2 minute time point. n=3

3.1.4 The iASPP and ASPP2 C-terminal domains mediate dephosphorylation of p53Ser15 by PP1cα *in vitro*

To assess whether the ASPP proteins mediate dephosphorylation of p53Ser15, DNAPK was used to phosphorylate p53, as described in section 3.2.2, and the reaction was stopped by the addition of LY294002. PP1cα alone or in the presence of the C-terminal domains of iASPP or ASPP2, was incubated with phospho-p53 for 30 minutes at 30°C. The µg amounts of p53, PP1cα, and ASPP protein were kept at a 1:1:1 ratio. This was to facilitate the formation of the "trimeric complex" found in previous studies[82]. Given their differing molecular weights, this amounted to a molar ratio of 1.4:1:1.6 for p53:PP1cα:iASPP, and 1.4:1:1.5 for p53:PP1cα:ASPP2. A similar experiment using a 1:1 ratio of substrate:PP1cα has been used previously to assess the dephosphorylation of lipin-1 by PP1cα[112]. The reaction buffer for these experiments differs from that of the initial phosphorylation and dephosphorylation time courses (section 3.2.2) by the addition of 1 mM $MnCl_2$, 2 mM DTT, 10 mM NaCl, and 0.025% Tween-20, to stabilize the ASPP proteins and further stabilize PP1cα (see appendix figure B.1). The 30 minute time point was chosen for the following experiments to allow for approximately 50% dephosphorylation of p53 with PP1cα alone, relative to the positive control. This allowed for the detection of a positive or negative effect of the ASPP proteins on PP1cα dephosphorylation of p53, relative to PP1cα alone. BSA was included as a control since it does not interact with either PP1cα or p53 (as shown in appendix figure B.3).

The addition of iASPP results in a decrease of the levels of phosphorylated p53Ser15 (that is to say, iASPP increases the dephosphorylation of phosphorylated p53Ser15) by PP1cα as shown in figure 3.6A. In the presence of iASPP, the level of phosphorylated p53Ser15 decreased by 81% relative to PP1cα alone. This difference was deemed statistically significant following an ANOVA, and a subsequent multiple comparisons test, where $p<0.05$ (see appendix section C). ASPP2 had a similar effect on the dephosphorylation of p53, where the presence of ASPP2 decreased p53Ser15 phosphorylation by almost 80% relative to PP1cα alone. The BSA control had no effect on PP1cα dephosphorylation, with 106% phosphorylated p53Ser15 relative to PP1cα alone. A dephosphorylation time course from 0-45 minutes (figure 3.6C and D) with either PP1cα alone, or in the presence of iASPP or ASPP2, shows the same overall effect: the ASPP proteins increase the rate of dephosphorylation of p53Ser15 by PP1cα.

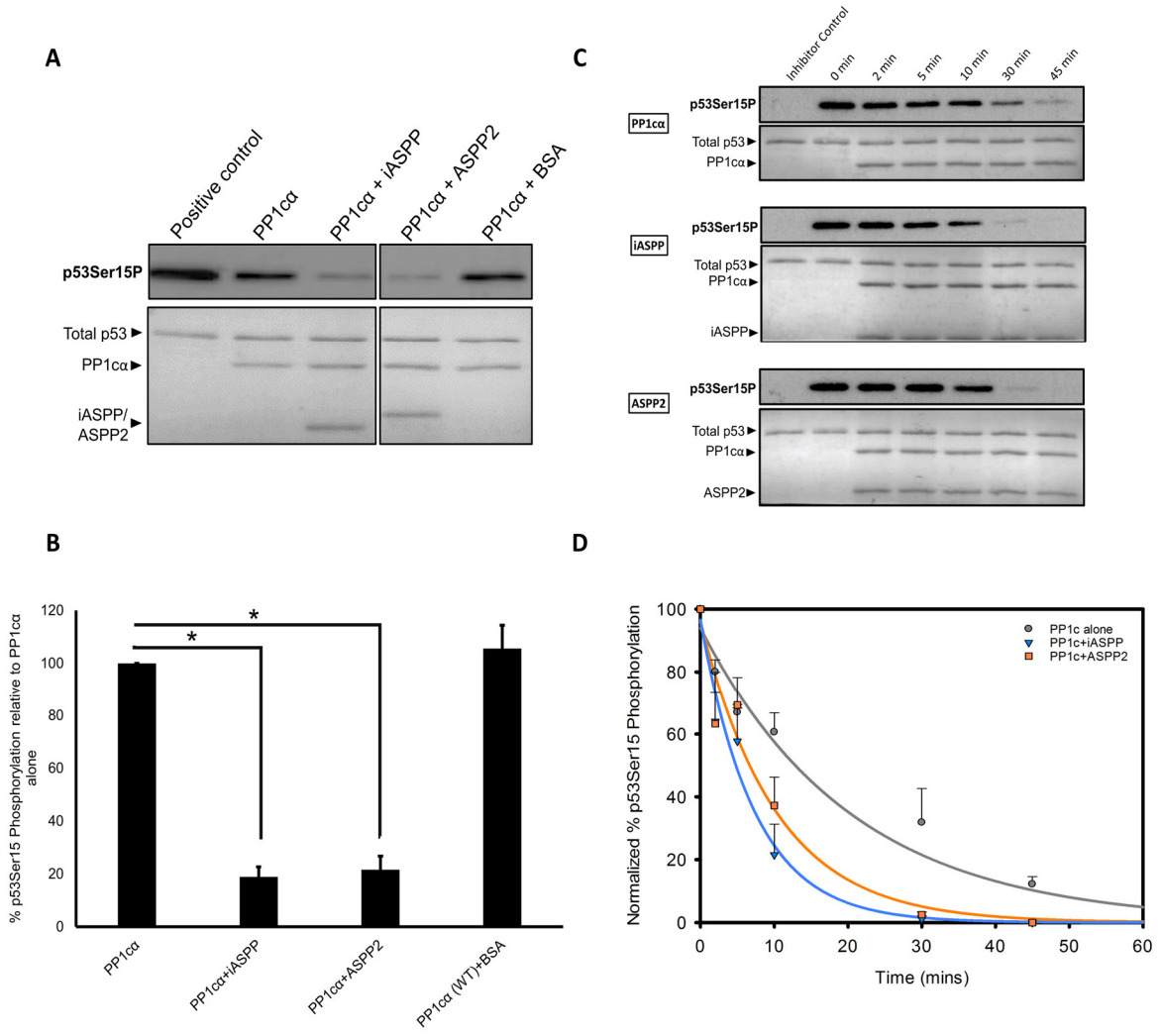

Figure 3.6 iASPP and ASPP2 C-terminal domains mediate dephosphorylation p53Ser15 by PP1cα. The figure depicts the *in vitro* dephosphorylation of p53Ser15 by PP1cα in the presence or absence of iASPP or ASPP2 C-terminal domains. p53 was phosphorylated by DNAPK for 90 minutes at 30°C. The phosphorylation reaction was stopped by the addition 1 mM DNAPK inhibitor LY249002. PP1cα in the presence or absence iASPP or ASPP2 (472 mM, 333 mM, and 517 mM, or 492 mM, respectively) was subsequently incubated with p53 for 30 minutes (A and B) or from 0 to 45 minutes (C and D) at 30°C. Samples were run on a 12% SDS-PAGE, and transferred to a 0.4µm nitrocellulose membrane. The membrane was stained with Pierce™ Reversible Protein Stain for detection of total p53 protein amount (bottom panels, A and C). Phospho-p53 antibody specific for phosphorylated p53Ser15 was used to detect respective levels of phosphorylation (upper panels, A and C). The band intensities were quantified using ImageJ and the phosphorylated signal was normalized to total p53 signal. B) Signals are represented as % phosphorylation compared to PP1cα alone. D) Signals are represented as % phosphorylation relative to the phosphorylation signal at 0 minutes. A,B) n=5, C,D) n=3.

3.1.5 iASPP C-terminal domain mediates dephosphorylation of p53Thr18 by PP1cα *in vitro*

Because the rate of Thr18 dephosphorylation by PP1cα was faster compared with that of Ser15 (figure 3.3), a titration curve of PP1cα was used to assess the amount of PP1cα that was needed to dephosphorylate p53Thr18 by approximately 50% at 30 minutes. At a ratio of 1 µg of PP1cα: 8 µg p53 (472 mM: 42 mM, respectively) the Thr18 residue was approximately 50% dephosphorylated at 30 mins (compared to 1 µg PP1cα: 1 µg p53, or 472 mM: 333 mM respectively, for Ser15) as shown in appendix figure B.4.

PP1cα was incubated with DNAPK-phosphorylated p53, in the presence or absence of ASPP protein to assess the effect of the ASPP proteins on p53Thr18 dephosphorylation by PP1cα. Upon addition of iASPP, a statistically significant decrease in phosphorylation by approximately 30% relative to PP1cα alone was observed (figure 3.7). The addition of ASPP2 resulted in a decrease of 6% phosphorylation relative to PP1cα alone, which was deemed a non-statistically significant change (see appendix section C for statistics). However, the difference between the effect of iASPP compared to ASPP2 was not statistically significant. The BSA control had no statistically different result from PP1cα alone or ASPP2 with PP1cα.

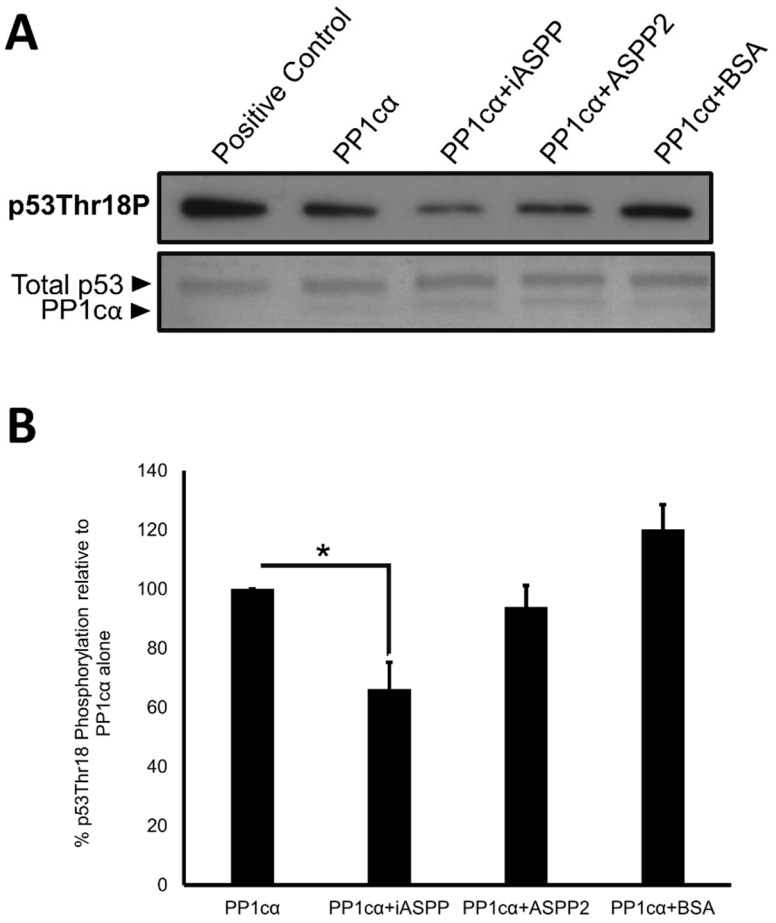

Figure 3.7 iASPP C-terminal domain mediates dephosphorylation of p53Thr18 by PP1cα.
The figure depicts the *in vitro* dephosphorylation of p53Thr18 by PP1cα in the presence or absence of iASPP or ASPP2 C-terminal domains. p53 was phosphorylated by DNAPK for 90 minutes at 30°C. The phosphorylation reaction was stopped by the addition 1 mM DNAPK inhibitor LY249002. Phosphorylated p53 was incubated with PP1cα in the presence or absence iASPP or ASPP2 (472 mM, 42 mM, and 65 mM or 62 mM, respectively) for 30 minutes at 30°C. Samples were run on a 12% SDS-PAGE, and transferred to a 0.4μm nitrocellulose membrane. A) The membrane was stained with Pierce™ Reversible Protein Stain for detection of total p53 protein amount (bottom panel, A). Phospho-p53 antibody specific for phosphorylated p53Ser15 was used to detect respective levels of phosphorylation (upper panel, A). B) The band intensities were quantified using ImageJ and the phosphorylated signal was normalized to total p53 signal. Signals are represented as % phosphorylation compared to PP1cα alone. n=3

3.1.6 iASPP C-terminal mediates dephosphorylation of DYRK2 Phosphorylated-p53 *in vitro*

Given that iASPP can mediate dephosphorylation of both p53Ser15 and Thr18, while ASPP2 can mediate dephosphorylation of p53Ser15 (section 3.2.4 and 3.2.5), I wanted to examine whether the ASPP

proteins are involved in mediating the dephosphorylation of p53Ser46. During the dephosphorylation time course experiments (section 3.2.3) the signal from the p53Ser46 phospho-specific antibody was found to increase over time, therefore western blot analysis could not be used to test the effect of the ASPP proteins on this site. However, there was a band shift that could be detected when DYRK2-phosphorylated p53 was dephosphorylated by PP1cα. This property was used to assess the effect of the ASPP proteins on the overall dephosphorylation of one or more sites on p53 that are phosphorylated by DYRK2.

The dephosphorylation experiments in section 3.2.3 revealed that at 20 minutes dephosphorylation by PP1cα at 30°C, the two most prominent bands (phospho-p53 and dephospho-p53) are in approximately 1:1 ratio. Thus 20 minutes was used to evaluate the effect of the ASPP proteins on the overall dephosphorylation of DYRK2-phosphorylated p53 by using the change in band shift. An increased amount of the lower band relative to the upper band indicates an increase in the dephosphorylated-p53.

DYRK2-phosphorylated p53 was incubated with PP1cα alone, or in the presence of the ASPP proteins. The samples were run on an 8% SDS-PAGE to allow for quantification of the separation of the upper band from the lower band on nitrocellulose using the Pierce™ Reversible Protein Stain. Using this method, iASPP decreased the total phosphorylation of p53 relative to PP1cα alone by 32%, a statistically significant difference (figure 3.8). On the other hand, ASPP2 was not deemed statistically different compared to PP1cα alone or the BSA control, but of note was not statistically different from iASPP.

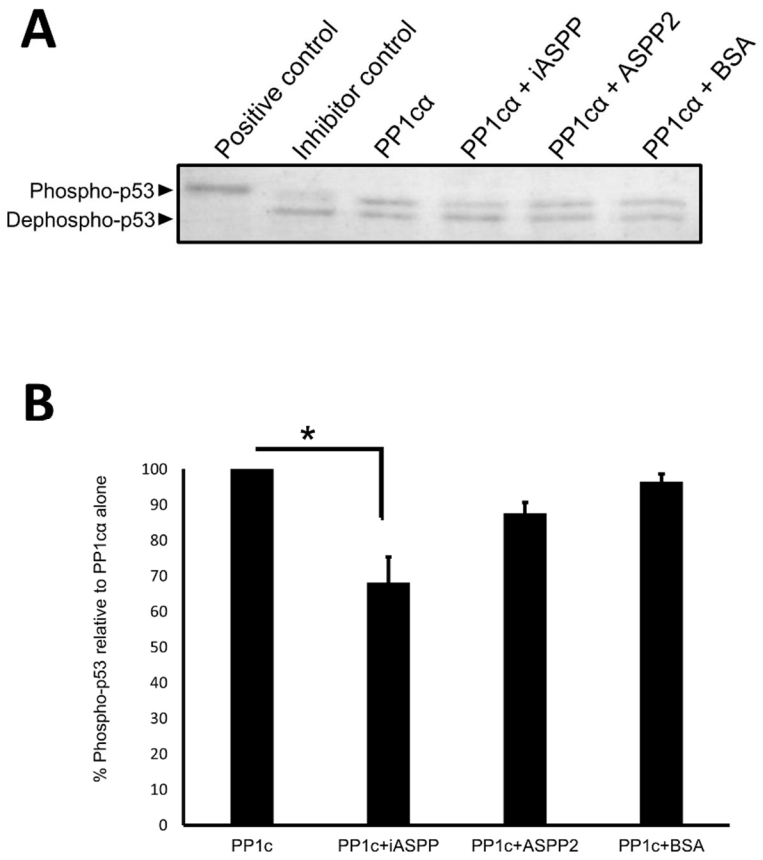

Figure 3.8 iASPP C-terminal domain mediates dephosphorylation of DYRK2 phosphorylated-p53. The figure depicts the *in vitro* dephosphorylation of DYRK2 phosphorylated p53 by PP1cα in the presence or absence of iASPP or ASPP2. p53 was phosphorylated by DYRK2 for 90 minutes at 30°C. The phosphorylation reaction was stopped by the addition 1 mM DYRK2 inhibitor INDY. Phosphorylated p53 was incubated with PP1cα in the presence or absence of iASPP or ASPP2 (472 mM, 333 mM, and 517 mM, or 492 mM, respectively) for 20 minutes at 30°C. Samples were run on a 12% SDS-PAGE, and transferred to a 0.4µm nitrocellulose membrane. A) The membrane was stained with Pierce™ Reversible Protein Stain for detection of phospho-p53 (upper band) and dephospho-p53 (lower band). B) The band intensities were quantified using ImageJ and the phospho-p53 signal was divided by the phospho-p53 signal plus the dephospho-p53 signal to obtain % phospho-p53. Data was represented as % phospho-p53 relative to PP1cα alone. n=3

3.1.7 iASPP and ASPP2 C-terminal domains form complexes with PP1cα and $p53_{2-292}$

Previous experiments using gel filtration showed iASPP C-terminal domain could form a complex with PP1cα and p53, whereas the C-terminal domain of ASPP2 could not[82]. Given this previous study, the effects obtained showing that both ASPP proteins mediate p53Ser15 dephosphorylation *in vitro* were somewhat unexpected. To reassess the binding of the ASPP proteins to PP1cα and p53 under the

conditions used in the *in vitro* dephosphorylation experiments, a MC-S experiment was used to pulldown p53, ASPP, and PP1cα complexes (outlined in methods section 2.3).

p53, ASPP, and PP1cα were incubated together at 30°C for 45 minutes at a 1:1:1 molar ratio, similar to the method used for the gel filtration experiments (see methods section 2.3). Incubations of ASPP protein and p53 (without PP1cα) were included as controls for non-specific binding to MC-S. The buffer used for the pulldown experiments was Trimeric Binding Buffer (50 mM Tris-HCl, pH 7.5, 50 mM NaCl, 75 mM KCl, 1.0 mM $MnCl_2$, 0.1 mM EDTA, and 0.2% β-Me) which was modeled after the buffer used in the dephosphorylation experiments (50 mM Tris-HCl, pH 8.0, 0.2 mM EGTA, 1.0 mM $MnCl_2$, 10mM NaCl, 40 mM KCl, 2.0 mM DTT, 10 mM $MgCl_2$ 0.3 mM ATP, 6 µg/ mL sonicated calf thymus DNA, 0.025% Tween-20). The buffer used for the previous gel filtration experiments was 50 mM imidazole, pH 7.8, 300 mM NaCl, 2 mM $MnCl_2$, 0.5 mM EDTA, 0.5 mM EGTA, 2.0 mM DTT and 10% glycerol.

The results in figure 3.9 show the presence of p53 in both the iASPP, p53, PP1cα condition and the ASPP2, p53, PP1cα condition, which is indicative of both ASPPs being capable of forming a complex with PP1cα and p53.

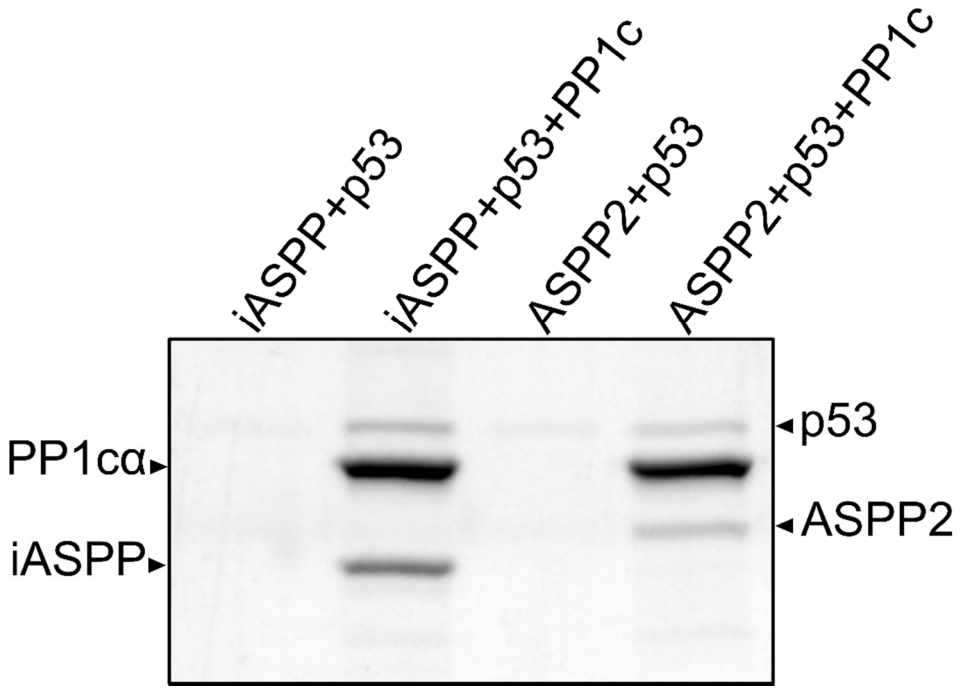

Figure 3.9 iASPP and ASPP2 form complexes with p53 and PP1cα.
The figure depicts the results of a MC-S binding experiment between PP1cα, p53, iASPP or ASPP2, where PP1cα is capable of pulling down iASPP or ASPP2 with p53. Equimolar amounts (0.25 nmol) of p53, PP1cα, and either iASPP or ASPP2 were incubated together at 30°C for 45 minutes in Trimeric Binding Buffer ((50 mM Tris-HCl, pH 7.5, 0.1 mM EDTA, 1.0 mM $MnCl_2$, 50 mM NaCl, 75 mM KCl, and 0.2% β-Me). The incubated protein complexes were added to MC-S for 3 hours, 4°C, end-over-end, then washed with Trimeric Binding Buffer. PP1cα, p53, and iASPP or ASPP2 were eluted from the beads using 2 x Laemmli Buffer and heat, loaded onto a 12% SDS-PAGE gel, and visualized with coomassie stain. n=2

3.2 Discussion

The goal of these experiments was to determine if the C-terminal domains of iASPP and ASPP2 could mediate the dephosphorylation of p53 by PP1cα *in vitro.* The work presented in this section showed that: 1) both iASPP and ASPP2 are capable of mediating dephosphorylation of p53Ser15, 2) iASPP is also capable of mediating dephosphorylation of p53Thr18 and DYRK2 phosphorylated p53, and 3) both iASPP and ASPP2 can form complexes with PP1cα and p53.

3.2.1 Phosphorylation of p53 *in vitro* and using phospho-specific antibodies

Initially, when choosing which phosphorylation sites of p53 to assess, two main considerations were taken into account. Firstly, which sites had the most information available for their known effects on p53, that is to say, if I did see ASPP-mediated site-specific dephosphorylation of p53 by PP1cα, could I relate these findings back to the function of those sites in cells. Based on this criteria, of the 30 recognized Ser/Thr phosphorylation sites on p53, the most well studied sites are Ser15, Thr18, Ser20, Ser37, Ser46, and Thr55. Secondly, the practicality of studying these sites *in vitro*: is there a kinase known to phosphorylate one of more sites *in vitro* and is there a documented kinase inhibitor available to inhibit the phosphorylation reaction before continuing with the dephosphorylation reaction. Given these criteria, Ser15, Thr18, Ser37, and Ser46 were initially screened for dephosphorylation by PP1cα alone, before evaluating the effects of the ASPP proteins on mediating dephosphorylation. Before dephosphorylation could be evaluated, phosphorylation of these sites was first assessed. Figure 3.1A shows an increase in the phosphorylation of p53Ser15, Thr18, and Ser37 over time. This result confirmed that DNAPK could indeed phosphorylate all three sites *in vitro*, as expected given previous literature[40,113]. These three sites are the only documented sites for DNAPK phosphorylation of p53 *in vitro*[40,113]. Figure 3.2A shows an increase in phosphorylation over time with DYRK2, confirming that p53 is phosphorylated by DYRK2 *in vitro*. p53Ser46 is the only documented site of phosphorylation by DYRK2[50].

Because of the difficulty of expressing and purifying recombinant p53 (due to its intrinsically disordered properties, p53 has a tendency to aggregate), designing and purifying phospho site-specific p53 mutations to verify the validity of each phospho-antibody was beyond the scope of this thesis, however alanine mutations should be used to confirm site-specificity in future. The site specificities for the p53Ser15 and p53Ser46 antibodies (purchased from Cell Signalling) have been tested using S15A and S46A p53 mutations, where these mutants were no longer detected using their respective phospho-antibodies in cells, although there may still be batch lot differences[114,115]. In addition, according to CiteAb, the p53Ser15 antibody has been used in 187 papers, p53Thr18 in five, p53Ser37 in 137, and p53Ser46 in 152 papers. Even so, I tested the relative specificity of the phospho-specific antibodies using the DNAPK ATP-competitive inhibitor, LY294002, and the DYRK2 inhibitor, INDY, as shown in Figure 3.1B and 3.2B. The absence of an antibody signal in the presence of LY294002 or INDY (combined with the increasing signal

over time of incubation with the respective kinase) verified that these antibodies do indeed detect phosphorylated p53.

3.2.2 Dephosphorylation of p53Ser15 versus p53Thr18 and p53Ser37

Dephosphorylation time courses with PP1cα alone were conducted to assess if p53Ser15, Thr18, Ser37, and Ser46 were all capable of being dephosphorylated by PP1cα alone. Figure 3.3, clearly shows that PP1cα dephosphorylates p53Ser15, Thr18, and Ser37. Dephosphorylation of p53Ser15 and Ser37 was expected given prior work by Dr. Tamara Skene-Arnold in the Holmes lab, however p53Thr18 is a newly identified substrate site for PP1cα.

It is not entirely surprising that PP1cα was capable of dephosphorylating all three sites. Unlike protein kinases, where the specificity towards a substrate can be predicted based on the amino acids in the surrounding sequence, there is no identified substrate sequence specificity for PP1cα[66]. In fact, recombinant PP1cα can even dephosphorylate pNPP which is a substrate modelled after a tyrosine residue. That is to say, without the regulation afforded by a regulatory protein, the recombinant PP1cα catalytic subunit has a broad range of substrates[66]. However, the difference in the rates of dephosphorylation was unexpected. While p53Thr18 and Ser37 are dephosphorylated at comparable rates, p53Ser15 is dephosphorylated at a much slower rate.

From a cellular perspective, p53Ser15 is one of the first sites to become phosphorylated in response to cellular stress[29]. In a comprehensive study evaluating multi-site phosphorylation of p53 in response to DNA damage over time, the phosphorylation of p53Thr18 was found to be dependent on the prior phosphorylation of p53Ser15[29]. Therefore, given this chain of events, it might follow that the first site to be phosphorylated would be one of the last sites to be dephosphorylated when turning off the stress signal. The timing of this “off” signal and site-interdependency for dephosphorylation has not been assessed in cells.

Without any information about the orientation or structure of the p53 N-terminus bound to the PP1cα active site, it is difficult to explain why the dephosphorylation of one site might be favoured over another. Evaluating the sequence, there are two adjacent proline residues (Pro13 and Pro12) N-terminal to p53Ser15 that may sterically hinder its access to the active site, making it slower to dephosphorylate than

the other two sites. In addition, p53Ser15 dephosphorylation may depend on the prior dephosphorylation of Thr18 or Ser37, either through the alleviation of negative charge within the vicinity, or through a change in secondary structure of p53 upon dephosphorylation. The N-terminus of p53 is considered to be intrinsically disordered with some regions of helicity in its free state[15]. There are currently eight structures of the p53 N-terminus bound to a regulatory protein in its dephosphorylated form, which shows it binds as an amphipathic α-helix to most interaction partners (figures 1.2 and 1.3). Yet, the one structure of p53 phosphorylated at Ser46 and Thr55, shows that it binds in an extended "acidic string" conformation to the p62-PH subunit of TFIIH (figure 3.6)[17].

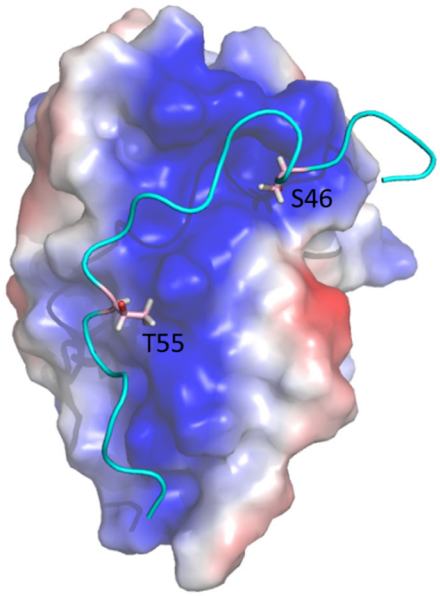

Figure 3.10 Phosphorylated p53 TAD domain binds as an acidic string.
The figure depicts residues 41-61 of p53 (cyan) bound to the p62-PH subunit of TFIIH (surface vacuum electrostatic representation) (PDB: 2RUK). The phosphorylated residues of Ser46 and Thr55 are coloured in pink. This structure is the only current structure of phosphorylated TAD bound to a regulatory domain, and it shows binding in an "acidic string" conformation. Other structures of the dephosphorylated TAD domain of p53 show it binding in a helical conformation (for example MDM2 and p300)[116].

In addition, computational studies predict that the mono-phosphorylation of Thr18 can disrupt helicity, while double-phosphorylation of Thr18 and Ser20 maintains helicity[117]. It could be hypothesized that dephosphorylation of Thr18 could change the secondary structure of the N-terminus and allow subsequent access of phosphorylated p53Ser15 to the active site. There still remains no structure of a peptide substrate bound to PP1cα for a comparable example. A recent study used a phosphomimetic of

Cdc37 to assess its binding to the active site of PP5[72]. It would be interesting to generate similar phosphomimetics of p53Ser15, Thr18, or Ser37 to gain an idea of how these sites access the active site.

3.2.3 Analyzing the Dephosphorylation of DYRK2 phosphorylated-p53

The substrate specificity of PP1c is relatively broad; therefore, it was predicted that p53Ser46 would be dephosphorylated by PP1cα alone. Following western blotting using the p53Ser46 antibody, the signal does not decrease over time of incubation with PP1cα (figure 3.4 A). A total protein stain shows a clearly visible band mobility shift from higher molecular weight to lower molecular weight over time with PP1cα, which in itself is indicative of a change in phosphorylation status to a more dephosphorylated state (figure 3.4, lower panel, and figure 3.5)[118]. In addition, the p53Ser46 signal only increases in conditions where PP1cα is added (see appendix section B2). Given the ambiguity of results using this antibody and no assurance that another antibody would not have the same issues, the choice was made to use the band mobility shift from phospho-p53 to dephospho-p53 to assess the PP1cα dephosphorylation on DYRK2 phosphorylated-p53.

Although it is not possible to discern the specific sites that are dephosphorylated by PP1cα using this method, the band mobility shift for the dephosphorylation time course indicates there are at least three bands, which points to at least two phospho-species of p53 (figure 3.5). The identity of these sites remains to be elucidated. Phosphorylation-dependent mobility shift (PDMS) depends on both the introduction or removal of negatively charged phosphate as well as the location of said phosphate site with respect to other negatively charged amino acids[118]. A study which used the EIIA protein as a model showed that a gap of 1-3 amino acids (either N-terminal, C- terminal, or both) between the phospho-site and another negatively charged amino acid resulted in a detectable mobility shift, while a gap of 0 or 4 had no effect on mobility[118]. They also found that the shift increased as the gap increased up to 4. The authors relate this finding back to the amount of SDS that is bound in each of these situations, where a decreased amount of SDS binding resulted in a slower band migration.

The only known site of phosphorylation for p53 by DYRK2 is Ser46, however using the DYRK2 consensus sequence (RXS/TP) seven other sites on $p53_{2\text{-}292}$ are predicted to be phosphorylated by DYRK2: Ser9, Ser33, Ser46, Thr81, Ser94, Ser99, Ser127, and Thr230.

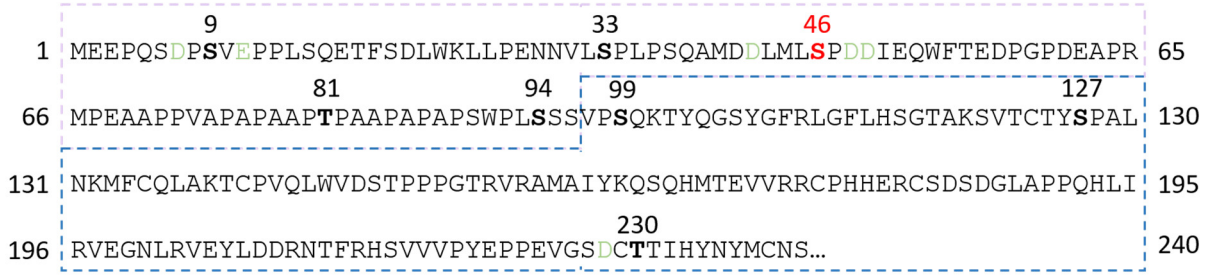

Figure 3.11 Potential sites of p53$_{2\text{-}292}$ phosphorylation by DYRK2
The figure depicts the first 240 amino acids of p53 with the predicted sites of DYRK2 phosphorylation bolded with the residue number above, as predicted using the DYRK2 substrate recognition motif RXS/TP. The only verified phosphorylation site, Ser46, is bolded and red. The dotted lines represent the boundaries of the TAD domains (purple) and the DNA-Binding domain (blue). Acidic Glu or Asp residues within 1-4 amino acids of potential DYRK2 phosphorylation sites are labelled in green. Due to the presence of Glu or Asp residues within close proximity, the dephosphorylation of Ser9, Ser46, and Thr230 might be predicted to produce a gel mobility shift[118].

Using the PDMS logic outlined above, the eight potential sites that could give rise to PDMS are narrowed down to only three possibilities: Ser9, Ser46, and Thr230. Given that Thr230 is relatively enclosed within the structure of the p53 DNA-binding domain, it's more likely that the two sites would be Ser9 and Ser46. The small shift between 0-2 minutes would correlate to the dephosphorylation of Ser9 as this site has gaps of only 1 from the next aspartic acid or glutamic acid residue, and the larger shift between the middle species and the lower species over 2-60 minutes would correlate to the dephosphorylation of Ser46 as there are aspartic acid residues 1, 2, and 3 gaps away (figure 3.11). Although this interpretation relies on the hypothesis generated in a single paper[118], if it is indeed correct, p53Ser46 is dephosphorylated by PP1cα. However, given the uncertainty in the identity of these three bands, the remainder of this thesis compares the middle band, "phospho-p53", with the lower band, "dephospho-p53".

3.2.4 iASPP$_{608\text{-}828}$-mediated dephosphorylation of p53Ser15, Thr18, and DYRK2-phosphorylated p53

Prior to this study, it was shown that PP1cα was an overall inhibitor of p53-mediated apoptosis, and was implicated in the dephosphorylation of p53Ser392[119]. Further, PP1cα was found to dephosphorylate p53Ser15 and Ser37 both *in vitro* and *in vivo*, however the PP1cα regulatory subunit responsible for mediating this dephosphorylation was unknown[61]. I now show that iASPP is capable of

mediating the dephosphorylation of not only p53Ser15, but also p53Thr18 and DYRK2-phosphorylated p53 (Figures 3.6, 3.7, and 3.8). As outlined in the introduction, p53Ser15 phosphorylation is one of the first signs of p53 activation in response to cellular stress and is important for p53-dependent transcription, and p53Thr18 is regarded as important for the stabilization of p53 levels in response to stress through dissociation from MDM2. p53Ser46 (phosphorylated by DYRK2) guides p53-dependent transcription towards the promoters of pro-apoptotic genes versus cell cycle arrest, as well as being important for p53 translocation to the mitochondria for transcription independent apoptosis[18,23,52].

Documented *in vivo* functions of iASPP align well with the predicted effects of mediating the dephosphorylation of these sites. For p53Ser15, if iASPP mediates the dephosphorylation *in vivo*, it could be predicted to cause a decrease in overall p53-dependent transcription. Confirming this prediction, iASPP knockdown increases recruitment of p53 to Bax and p21 promoters, whereas overexpression decreased recruitment in cervical cancer cells[120]. In addition, overexpression of iASPP results in decreased p53Ser15 phosphorylation in retinal ganglion cells following axotomy[121]. For p53Thr18, the predicted outcome of dephosphorylation would mainly be a decrease in the levels of p53 protein. The effect of iASPP on p53 protein levels is currently unclear, while some studies show no effect on p53 levels, others show that overexpression of iASPP results in p53 degradation via MDM2[122,123]. However, in support of iASPP-mediated dephosphorylation of p53Thr18, preliminary experiments in the Glover lab using U2OS cells show that the knockdown of iASPP results in a significant increase in p53 levels (data not shown). Lastly, although this study cannot definitively implicate iASPP in p53Ser46 dephosphorylation, our data do suggest that iASPP mediates the dephosphorylation of DYRK2-phosphorylated p53, one site of which is p53Ser46. If iASPP did indeed mediate the dephosphorylation of p53Ser46, it could be expected for iASPP to have an inhibitory effect on p53-transactivation of pro-apoptotic genes, which of course, is its namesake and what has been documented previously [88].

The molecular mechanism by which iASPP inhibits p53-dependent transcription of apoptotic programming is unclear. Our current results may, in part, provide one explanation, however *in vivo* experiments are needed to confirm the applicability of these results. This could be tested by blocking the interaction of iASPP with p53, or PP1cα, and assessing if there is an increase in phosphorylation of the aforementioned sites. Initially, one way to assess this could be to use targeted mutations, synthetic peptides

such as A34 which target the iASPP:p53 interaction[108], or marine compounds such as those that target the p53:PP1c interaction (under development in the Holmes lab), and evaluate overall p53 phosphorylation *in vivo* using phospho-specific antibodies. These studies have not yet been conducted.

It would also be of interest to know the location of iASPP-mediated dephosphorylation of p53 in order to better understand its role in regulating p53. iASPP is predominantly nuclear however it is known to shuttle between the nucleus and the cytoplasm[124]. In the cytoplasm, iASPP is thought to be "locked" in a dimer until phosphorylated at iASPP Ser84 and S113 by Cyclin B1/CDK1, or cleaved by caspases, which then allows it to enter the nucleus. Therefore it might be predicted that in the cytoplasm, iASPP could not interact with cytoplasmic PP1cα in this "locked" dimeric form, as the SH3 and Ankyrin binding sites would be predicted to be bound within the dimer and not open for binding PP1cα[125,126]. However, as far as comparable situations, the only other known example of iASPP-mediated dephosphorylation by PP1cα of a substrate is that of desmoplakin, which is a cytoplasmic substrate[109]. p53 phosphorylated at p53Ser15, as well as p53Ser46, have both been found within the mitochondria, and a small fraction of iASPP has been found to localize to the mitochondria[35,53,127]. Therefore, the localization of iASPP-mediated dephosphorylation is theoretically possible within the nucleus, cytoplasm, or mitochondria.

The results from our study strongly parallel those found with the Ser/Thr Protein Phosphatase 2A (PP2A), its regulatory protein, B56γ, and p53Thr55 dephosphorylation[128]. p53Thr55 is phosphorylated under normal cellular conditions, which allows for its association with the nuclear export protein, Chromosomal Maintenance 1 (CRM1) leading to localization to the cytoplasm and association with MDM2[114]. In response to DNA damage, p53Thr55 is dephosphorylated by PP2A bound with B56γ and translocates to the nucleus to coordinate the DNA damage response. Remarkably, the dephosphorylation of p53Thr55 is dependent on the presence of phosphorylated p53Ser15[114]. This site-interdependence has been explored in depth with respect to phosphorylation, however much less is known about site-interdependency in dephosphorylation[29]. Given the site-interdependency found for PP2A, it would be interesting to test whether p53Thr55 phosphorylation is important for iASPP-mediated dephosphorylation of p53 by PP1cα.

3.2.5 ASPP2$_{905-1128}$-mediated dephosphorylation of p53Ser15

As a positive regulator of p53-apoptotic function, it might be expected that ASPP2 would not mediate the dephosphorylation of p53. In addition, previous studies in the Holmes lab found that ASPP2$_{905-1128}$ could not complex together with p53 and PP1cα, whereas iASPP$_{608-828}$ did[82]. However, as mentioned in the introduction, the ASPP2 N-terminal truncation, ΔN-ASPP2, has anti-apoptotic effects on p53, specifically the impairment of p53 recruitment to apoptotic response-elements[92]. Thus it might be predicted that p53 dephosphorylation may be affected by the ASPP2$_{905-1128}$ C-terminal construct used for these experiments. In our study, ASPP2$_{905-1128}$ was found to mediate the dephosphorylation of p53Ser15 (see figure 3.6 and statistical significance in appendix section C). That is to say, that in the absence of the ASPP2 N-terminus, ASPP2$_{905-1128}$ mediates p53Ser15 dephosphorylation. An overlay of the Ankyrin-Rich and SH3 domains of iASPP$_{608-828}$ (bound to PP1cα- unpublished) and ASPP2$_{892-1128}$ (bound to the p53 DNA binding domain-PDB: 1YCS) shows remarkable structure similarity, with an RMSD=0.89 as computed in PYMOL (figure 1.10). Therefore, from a structural standpoint, it is not surprising that both iASPP$_{608-828}$ and ASPP2$_{905-1128}$ mediate dephosphorylation of p53 by PP1cα. This also provides one explanation for the anti-apoptotic results seen with ΔN-ASPP2, but also reinforces that it is likely the N-terminal portion of ASPP2 that is required for its pro-apoptotic functions. From an evolutionary perspective, iASPP is thought to be the first of the homologous ASPP proteins to have evolved as it is the only member found within *C.elegans*[129,130]. The ASPP1 and 2 proteins are thought to have evolved later with the extended N-terminus responsible for their apoptotic function[129].

It seems counterintuitive that the full-length ASPP2 protein would retain the ability to mediate dephosphorylation of p53Ser15, yet, this would not be the first time the interaction of ASPP2 and PP1cα has had an apparent anti-apoptotic effect. Despite its name, ASPP2, in conjunction with PP1cα, has been shown to have anti-apoptotic effects through mediating the dephosphorylation of the TAZ protein *in vivo*, resulting in its transcription of genes involved in cell proliferation, among others[103]. Though, with the overwhelming evidence that ASPP2 is a pro-apoptotic enhancer of p53, it may be that the full-length ASPP2 protein does not mediate dephosphorylation of p53. In addition, whether or not ASPP2-promoted apoptosis requires p53Ser15 phosphorylation is yet to be determined. Some studies propose that p53Ser15 may not

have to be phosphorylated to promote apoptosis. For example one study using nutlins caused an increase in the protein levels of p53 that was void of p53Ser15 phosphorylation, compared with etoposide treated cells which had an increase in phosphorylated p53Ser15[131]. They went on to show that the nutlin treated cells were capable of inducing apoptosis just as well as etoposide treated cells.

Nonetheless, ASPP2-mediated dephosphorylation of p53 under certain circumstances may have a pro-apoptotic function. Some studies suggest it may in fact be disadvantageous for p53 to be phosphorylated at p53Ser15 and associate with p300, as paradoxically p300 functions as a cytoplasmic E4 polyubiquitin ligase[132]. Unlike iASPP, a similar "locked dimer" formation for ASPP2 has not been found within the cytosol and rather several interactions with ASPP2 occur in a seemingly monomeric interaction[95]. In addition, although ASPP2 is known to localize with p53 at the site of transcription of pro-apoptotic genes, the localization of ASPP2 is primarily cytoplasmic rather than nucleic[124]. Therefore, ASPP2 may be promoting p53 pro-apoptotic activity by protecting p53 from cytosolic association with p300. In addition, some studies suggest that p53Ser15 phosphorylation is required for the binding of Mdm2 and Nuclear matrix-associated protein (SMAR1), resulting in deacetylation of p53 and negative regulation of p53-dependent transcription[133]. Whilst *in vivo* studies are required to assess the full role of ASPP2-mediated dephosphorylation of p53Ser15, one can now say with certainty that the C-terminal Ankyrin and SH3 domains of ASPP2 are capable of mediating dephosphorylation of p53Ser15.

At a molecular level, how the ASPP proteins combine with PP1cα and p53 to mediate dephosphorylation is intriguing. Despite the overlay of the iASPP (PDB:2VGE) and ASPP2 (bound to p53-PDB:1YCS) crystal structures being highly similar, a study published by Ahn, J. *et al* (2009) used NMR to highlight the differences in $iASPP_{623-828}$ and $ASPP2_{925-1128}$ binding to $p53_{56-289}$. They identified that ASPP2 binds with greater affinity to p53 than iASPP does, by approximately 60-fold, and that their interaction surfaces had some distinctions[96]. Specifically, binding of p53 to ASPP2 caused perturbations within the SH3 and the last three Ankyrin repeats, whereas for iASPP, perturbations were smaller and localized to the SH3 domain and the last two Ankyrin repeats[96]. It is known that iASPP can bind to three regions on p53; the proline rich domain, the DNA-binding domain, and the C-terminal linker domain (between the DBD and the TET domains), while ASPP2 only binds to the proline rich domain and the DNA-binding domain[14,107]. Within our dephosphorylation experiments, $p53_{2-292}$ contains the proline rich domain and DNA-binding

domain. Which of the two p53 regions is important for mediating dephosphorylation, and how PP1cα affects this interaction is of interest for further study and may provide insight into the function of the p53 PRD, as well as whether the ASPP proteins and PP1cα could bind together with p53 to DNA.

Although experiments were conducted to assess the difference between iASPP and ASPP2 mediated dephosphorylation on p53Thr18, the variability of the assay did not allow us to make any clear conclusions regarding these sites with respect to ASPP2. While it is clear that iASPP can mediate dephosphorylation of p53Thr18, whether ASPP2 does the same is unclear given our data. The statistics indicate that ASPP2 is no different than PP1c alone, or BSA, which would suggest that there is indeed a difference between iASPP and ASPP2 mediated dephosphorylation of this site. However, when directly comparing the effect of iASPP to the effect of ASPP2 there is no statistically significant difference between the two proteins. A similar issue is apparent with the DYRK2 phosphorylated p53, where the effect of ASPP2 is not statistically different from BSA, while iASPP is, however when directly comparing the difference between iASPP and ASPP2 there is no statistically significant difference.

When considering the ASPP-mediated dephosphorylation results, a potential confounding variable is that the PP1cα level (as determined by the Pierce™ Reversible Protein Stain) in the ASPP versus the PP1cα alone lanes is consistently 20% higher in the ASPP lanes (figures 3.6, 3.7, and 3.8). This could be due to the ASPP proteins stabilizing PP1cα in solution. However, a stability test of PP1cα in the presence or absence of iASPP and ASPP2 was performed and showed PP1cα was stable on its own in the buffer conditions used (appendix section B.1). It's unknown why there consistently appears to be more PP1cα in the ASPP lanes. PP1cα is in relative excess for an enzyme at a 1:1 ratio to p53 substrate for measuring p53Ser15, and the rate of p53Ser15 dephosphorylation is relatively slow, therefore I would predict that this does not substantially affect the results. Regardless, a titration curve of PP1cα levels to relative phosphorylation amount could be used to normalize our data to PP1cα levels and assure that the 20% difference between the PP1cα alone lane and the ASPP lanes does not substantially affect the results.

3.2.6 Both iASPP and ASPP2 C-terminal domains form complexes with PP1cα and p53

Both iASPP and ASPP2 C-terminal domains were capable of mediating the dephosphorylation of p53Ser15 by PP1cα *in vitro* (figure 3.6). In addition, gel filtration experiments have shown that iASPP forms

a complex with p53 and PP1cα, whereas ASPP2 does not and instead preferentially binds to PP1cα[82]. To further verify this binding profile under the buffer conditions used within our dephosphorylation experiments, a MC-S pull-down experiment was performed and showed that in fact, both iASPP and ASPP2 can form a complex with PP1cα and p53 using this method (figure 3.9). Although I cannot directly compare our results to the gel filtration results due to the difference in method used, an explanation for the difference is that the complex might not form at higher salt concentrations. 50 mM NaCl and 75mM KCl was used in our pull-down versus 300 mM NaCl used in the gel filtration experiments. Whether these trimeric complexes exist *in vivo* requires further study, however the ability of both ASPP proteins to form a complex with PP1cα and p53 is certainly consistent with the ability of both ASPP proteins to mediate *in vitro* dephosphorylation of p53Ser15.

Overall, the work described in this chapter shows that both iASPP and ASPP2 can form complexes with PP1cα and p53, and can mediate dephosphorylation of p53 by PP1cα, which provides insight into their functions within the cell.

CHAPTER 4

Probing the iASPP-PP1cα structure using iASPP-mediated dephosphorylation of p53 by PP1cα

CHAPTER FOUR: PROBING THE iASPP-PP1cα STRUCTURE USING iASPP-MEDIATED DEPHOSPHORYLATION OF P53 BY PP1cα

The work in the previous chapter (Chapter 3) found that $iASPP_{608-828}$ could mediate the dephosphorylation of p53Ser15. The $iASPP_{608-828}$:PP1cα crystal structure, as well as previous work within the Holmes Lab, identified three key interaction sites between iASPP and PP1cα: the RVXF-like motif, D633: R261 electrostatic interaction, and the PP1cα C-terminal tail interactions with iASPP Ankyrin/SH3 domains (figure 1.12). In this chapter, to validate the iASPP:PP1cα structure, as well as gain insight into which interactions were integral for iASPP-mediated dephosphorylation of p53, site-directed mutagenesis was performed for the three identified iASPP:PP1cα interaction sites. The iASPP (L625A) mutation was used to abolish the RVXF-like motif, the iASPP (D633R) mutation was created to eliminate the D633:R261 electrostatic interaction, and the PP1cα 1-300 truncation was created to remove the interaction of the iASPP Ankyrin/ SH3 domains and the PP1cα C-terminal tail. The PP1cα (T320D) mutation was also created to analyze the importance of the PP1c PXXPXR and iASPP SH3 domain interaction specifically, as this mutation lies within the third position of the motif and was shown to obliterate binding between iASPP:PP1cα in previous work[82]. It was predicted that because the PXXPXR-SH3 interaction could theoretically occlude binding of p53 to the SH3 domain, the PP1cα (T320D) mutation would have the least effect on mediated dephosphorylation of p53.

4.1 Results

4.1.1 iASPP:PP1cα binding is dependent on at least three interfaces

The effects on iASPP:PP1cα binding due to iASPP (L625A), iASPP (D633R), PP1cα (T320D), and PP1cα (1-300) were assessed using a Ni^{2+} NTA pulldown experiment and a corollary MC-S pulldown experiment. For the Ni^{2+} NTA pulldown, His-tagged iASPP (WT) or an iASPP mutation, was used as bait protein against PP1cα (WT) or a PP1cα mutation. For the MC-S pulldown, PP1cα (WT), or a PP1cα mutation was used as bait protein to pulldown iASPP (WT) or an iASPP mutation.

The Ni^{2+} NTA pulldown was performed under three conditions of increasing ionic strength. All three experiments (1 replicate each) showed the same general findings overall. For the binding experiment conducted under buffer conditions similar to the dephosphorylation experiments that follow (section 4.2.3), iASPP (L625A) and iASPP (D633R) mutations decreased the PP1cα: iASPP binding by approximately 22% and 24%, respectively (figure 4.1). The PP1cα (T320D) mutation decreased binding by approximately 84%, while the PP1cα (1-300) truncation completely abolished binding.

The MC-S experiment showed the same effects on binding as the Ni^{2+} NTA experiments, where iASPP (L625A) and iASPP (D633R) mutations decreased the iASPP: PP1cα binding by approximately 24% and 20%, respectively. The PP1cα (T320D) mutation decreased binding by approximately 93% while PP1cα (1-300) truncation again completely abolished binding. Of note, the PP1cα (T320D) mutation showed inhibited binding to the MC-S itself (figure 4.1). A second experiment replicated these results showing that the PP1cα (T320D) mutation decreases binding to MC-S by 60% compared to PP1cα (WT) (data not shown).

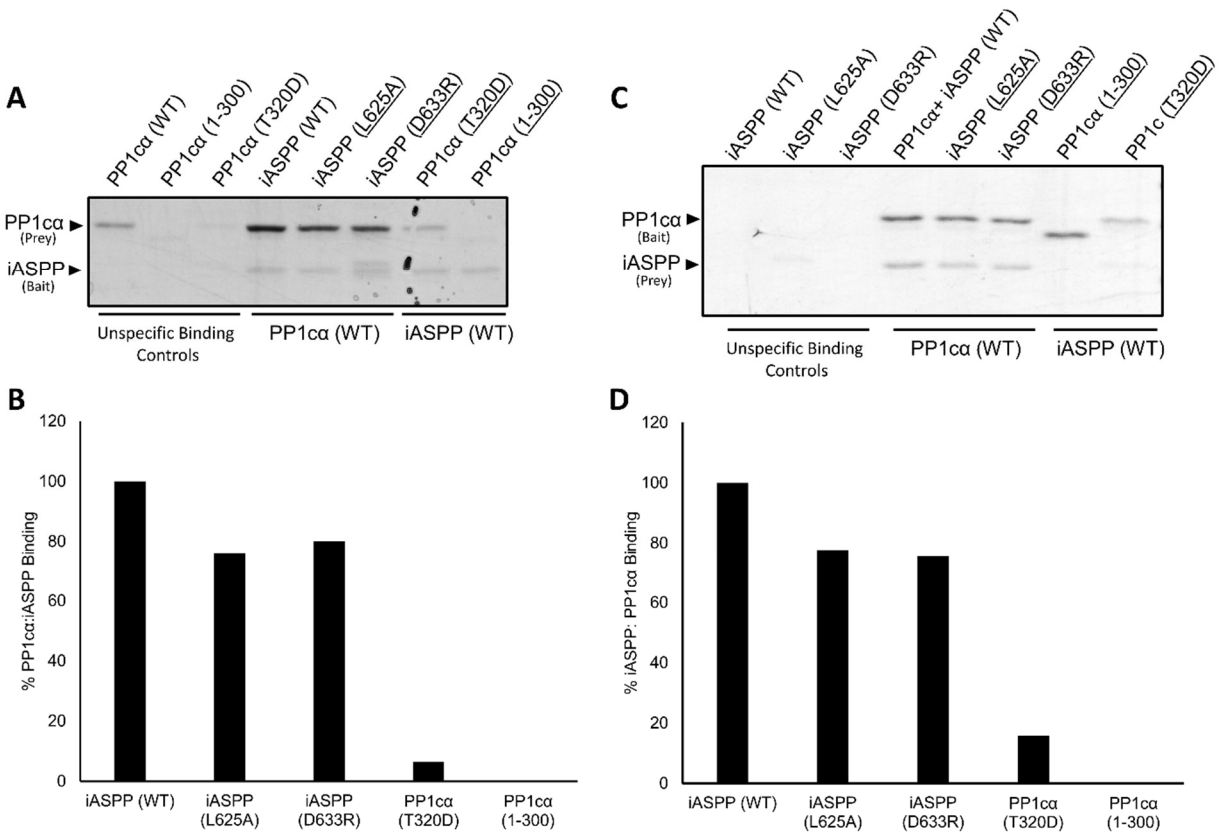

Figure 4.1 The iASPP:PP1cα interaction depends on at least three binding interfaces.
The figure depicts the results of a Ni^{2+} NTA and a MC-S binding experiment between PP1cα and iASPP and visualized by SDS-PAGE and coomassie staining. A,B) iASPP (WT) or mutant were bound to Ni^{2+} NTA for 2 hours, 4°C in Trimeric Complex Buffer. The resin was washed and PP1cα (WT) or mutation was incubated for 2 hours, 4°C in Trimeric Complex Buffer. Bound iASPP:PP1cα was eluted using 2 x Laemmli buffer and heat. C,D) PP1cα (WT) or mutant were bound to MC-S for 2 hours, 4°C in Trimeric Complex Buffer. The resin was washed and iASPP (WT) or mutation was incubated for 2 hours, 4°C in Trimeric Complex Buffer. Bound PP1cα: iASPP was eluted using 2 x Laemmli buffer and heat. B,D) Band intensities were measured using ImageJ, and the amount of prey protein was divided by the amount of bait protein, then plotted as a percentage of the PP1cα: iASPP control. A,B) n=1 (2 other replicates done under different salt conditions with similar results), C,D) n=2.

4.1.2 iASPP-mediated dephosphorylation of p53Ser15 by PP1cα is dependent on the interaction of at least three interfaces

To provide functional validation of the PP1cα:iASPP crystal structure, as well as gain insight into which sites are integral for iASPP-mediated dephosphorylation of p53, the mutations tested in section 4.2.1 were tested for their importance in the functional *in vitro* dephosphorylation of p53Ser15 assay in the following sections.

4.1.2.1 PP1cα (WT), PP1cα (T320D), PP1cα (1-300) exhibit similar rates of dephosphorylation of p53Ser15

Before the PP1cα (T320D) and PP1cα (1-300) mutations could be tested and compared to PP1cα (WT), the activity of each enzyme was assessed using a dephosphorylation time course. p53Ser15 was phosphorylated by DNAPK as outlined in the methods section 2.2, and the same µg amount of either PP1cα (T320D) or PP1cα (1-300) was incubated over 0-45 minutes at 30°C (figure 4.2). The time courses were plotted against the PP1cα (WT) time course conducted for the ASPP time course experiments in section 3.3.4 (Figure 3.6). The change over time of p53Ser15 phosphorylation for PP1cα (WT), PP1cα (T320D), or PP1cα (1-300), were not deemed significantly different from each other overall (see appendix section C).

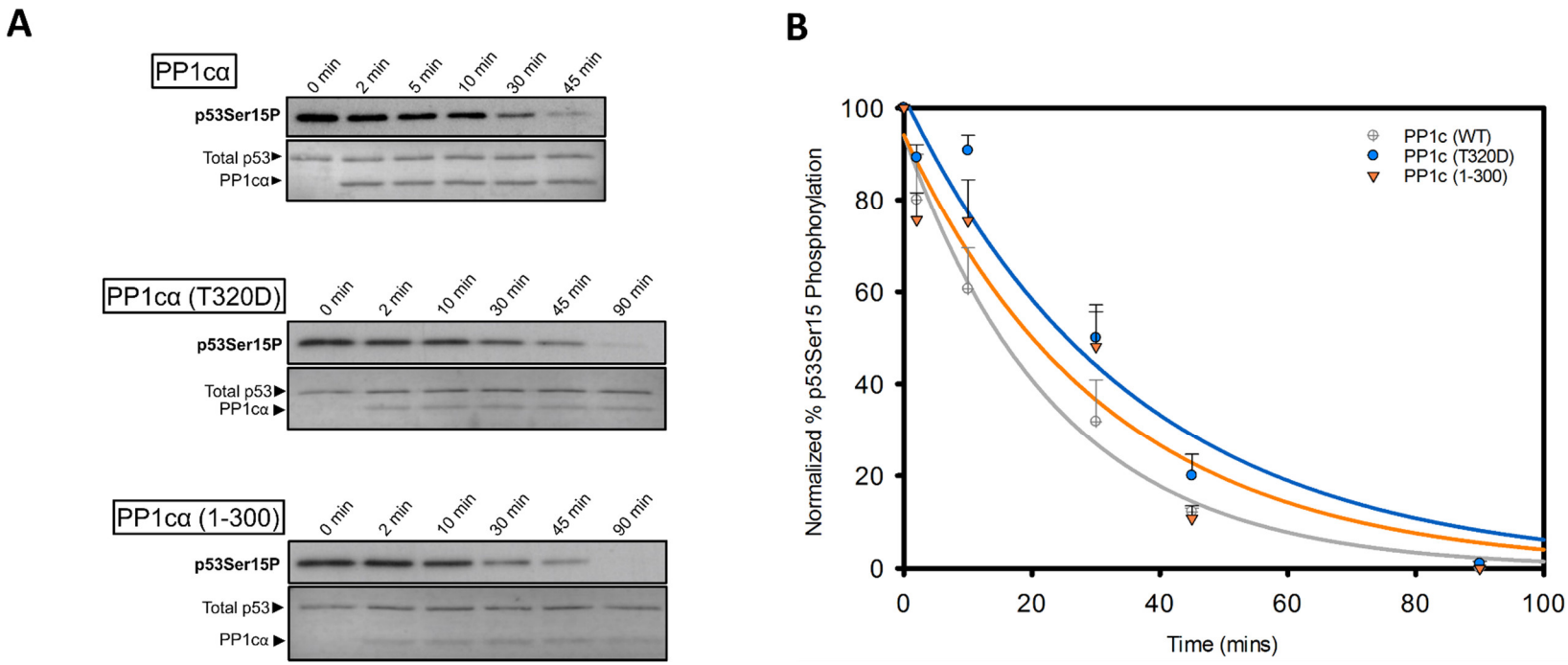

Figure 4.2 PP1cα (T320D) and PP1cα (1-300) have similar rates of dephosphorylation as PP1cα (WT).
The figure depicts a dephosphorylation time course over 90 minutes of PP1cα (T320D) and PP1cα (1-300) as compared to PP1cα (WT) from figure 3.6 measured by western blot using p53Ser15 phospho-specific antibody. p53 was phosphorylated by DNAPK for 90 minutes at 30°C. The phosphorylation reaction was stopped by the addition 1 mM DNAPK inhibitor LY249002. PP1cα (WT), PP1cα (T320D), or PP1cα (1-300) was subsequently incubated with p53 from 0 to 90 mins at 30°C (333 mM, 333 mM, or 364 mM, and 472 mM final concentration respectively). Samples were run on a 12% SDS-PAGE, and transferred to a 0.4µm nitrocellulose membrane. A) The membrane was stained with Pierce™ Reversible Protein Stain for detection of total p53 protein amount (bottom panels). Phospho-p53 antibody specific for phosphorylated p53Ser15 was used to detect respective levels of phosphorylation (upper panels). B) The band intensities were quantified using ImageJ and the phosphorylated signal was normalized to total p53 stain. The graph represents the % phosphorylation normalized to 0 minutes. n=3

4.1.2.2 Evaluating the effects of single mutations of iASPP or PP1cα

Initially, the iASPP mutations targeting the RVXF-like interaction and the D633:R261 electrostatic interaction, iASPP (L625A) and iASPP (D633R) respectively, were added to the ASPP dephosphorylation experiments in the presence of PP1cα (WT) and compared to iASPP (WT). As shown in Figure 4.3, both mutations had similarly deleterious effects on iASPP-mediated dephosphorylation of p53Ser15 by PP1cα (WT), where iASPP (L625A) and iASPP (D633R) increased the phosphorylation relative to iASPP (WT) by almost double (iASPP (WT) = 19%, iASPP (L625A) = 41%, and iASPP (D633R) = 45%). These differences were found to be statistically significant from iASPP (WT).

To determine the importance of the PP1cα C-terminal tail interaction in ASPP-mediated dephosphorylation of p53Ser15, separate experiments were conducted with PP1cα (T320D) and PP1cα (1-300) in the presence of iASPP (WT). In each experiment, the effect of iASPP (WT) + PP1cα mutant was normalized to the effect of their respective PP1cα mutants alone. These percentages were plotted against each other in figure 4.3. PP1cα (T320D) no significant effect on iASPP- mediated dephosphorylation of p53Ser15 compared to that of PP1cα (WT), where PP1cα (WT) in the presence of iASPP (WT) was 19% phosphorylation, and PP1cα (T320D) in the presence of iASPP (WT) resulted in 19% phosphorylation. In addition, the mutation to PP1cα (1-300) did not abolish iASPP-mediated dephosphorylation.

Taken together, iASPP (L625A) and iASPP (D633R) in the presence of PP1cα (WT) were important for iASPP-mediated dephosphorylation. The PP1cα mutations were not as significant as could be expected based on binding experiments. In particular, PP1cα (T320D) had no effect compared to PP1cα (WT).

4.1.2.3 Evaluating the effects of double iASPP and PP1cα mutations

The same experiment was conducted using both PP1cα mutations and iASPP mutations to look at the effect of “double mutants” on iASPP-mediated dephosphorylation of p53Ser15. Figure 4.3 shows that, when paired with PP1cα (1-300), the iASPP (L625A) and iASPP (D633R) mutations are still capable of mediating dephosphorylation. The differences between iASPP (L625A) and iASPP (D633R) paired with

PP1cα (1-300) were not statistically significant from each other, similar to what was found with these single iASPP mutants paired with PP1cα (WT).

For PP1cα (T320D), there was no additional effect on iASPP-mediated dephosphorylation of p53 compared to PP1cα (WT) unless it was paired with the iASPP (L625A) mutation: phosphorylation for iASPP (L625A) and PP1cα (WT) was 41%, which increased to 75% with iASPP (L625A) and PP1cα (T320D). In comparison, phosphorylation for iASPP (D633R) paired with PP1cα (WT) was 45%, and was 47% when iASPP (D633R) was paired with PP1cα (T320D).

Overall, three interaction interfaces were identified as being important for iASPP-mediated dephosphorylation of p53Ser15; the RVXF-like motif, D633:R261 electrostatic interaction, and the PP1cα full-length tail. Of note the PP1cα (T320D) had no significant effect unless paired with iASPP (L625A). In addition, no combination of two mutations was capable of completely abolishing the iASPP-mediated effect.

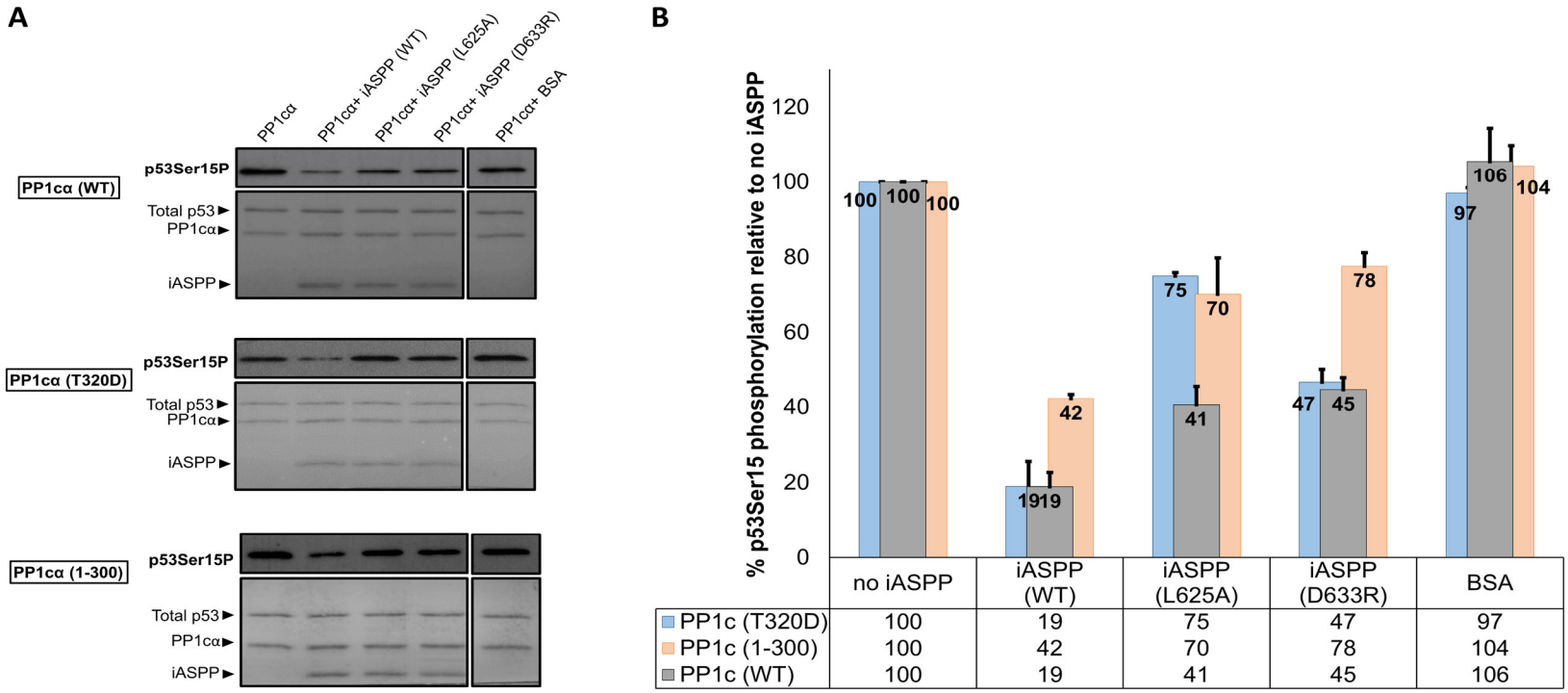

Figure 4.3 iASPP-mediated dephosphorylation is dependent on at least three iASPP:PP1cα binding interfaces.
The figure depicts the *in vitro* dephosphorylation of p53Ser15 by PP1cα (WT), PP1cα (T320D), or PP1cα (1-300) in the presence or absence of iASPP (WT), iASPP (L625A), or iASPP (D633R). p53 was phosphorylated by DNAPK for 90 minutes at 30°C. The phosphorylation reaction was stopped by the addition 1 mM DNAPK inhibitor LY249002. PP1cα in the presence or absence iASPP was subsequently incubated with p53 for 30 minutes at 30°C (333 mM, 517 mM, and 472 mM final concentrations respectively). Samples were run on a 12% SDS-PAGE, and transferred to a 0.4µm nitrocellulose membrane. A) The membrane was stained with Pierce™ Reversible Protein Stain for detection of total p53 protein amount (bottom panel). Phospho-p53 antibody specific for phosphorylated p53Ser15 was used to detect respective levels of phosphorylation (upper panel). B) The band intensities were quantified using image studio light and the phosphorylated signal was normalized to total p53 signal. Signals are represented as % phosphorylation compared to respective PP1cα alone.

4.2 Discussion

The work presented in this section showed that: 1) The RVXF-like, D633:R261 electrostatic, and C-terminal tail interactions are important for mediating dephosphorylation, which in turn provides functional validation of those sites being important for the iASPP:PP1cα structure, and 2) unlike what may be predicted based on PP1c:iASPP dimeric binding experiments, the PP1cα (T320D) mutation has no effect on iASPP-mediated dephosphorylation of p53Ser15, which suggests that the C-terminal tail of PP1cα may move to allow p53 to interact with iASPP.

4.2.1 iASPP:PP1cα binding relies on the RVXF-like, D633:R261 electrostatic, and PP1cα C-terminal tail interactions

In previous work, three sites of interaction between iASPP and PP1c were identified as important for binding using pull-down experiments: the RVXF-like motif, the electrostatic interaction between an acidic patch on iASPP and the residues K260 and R261 on PP1cα, and finally the iASPP-SH3/Ankyrin: PP1cγ C-terminal tail[82]. Since these preliminary studies, the iASPP:PP1cα crystal structure was solved showing that all three of these sites interact (figure 4.4).

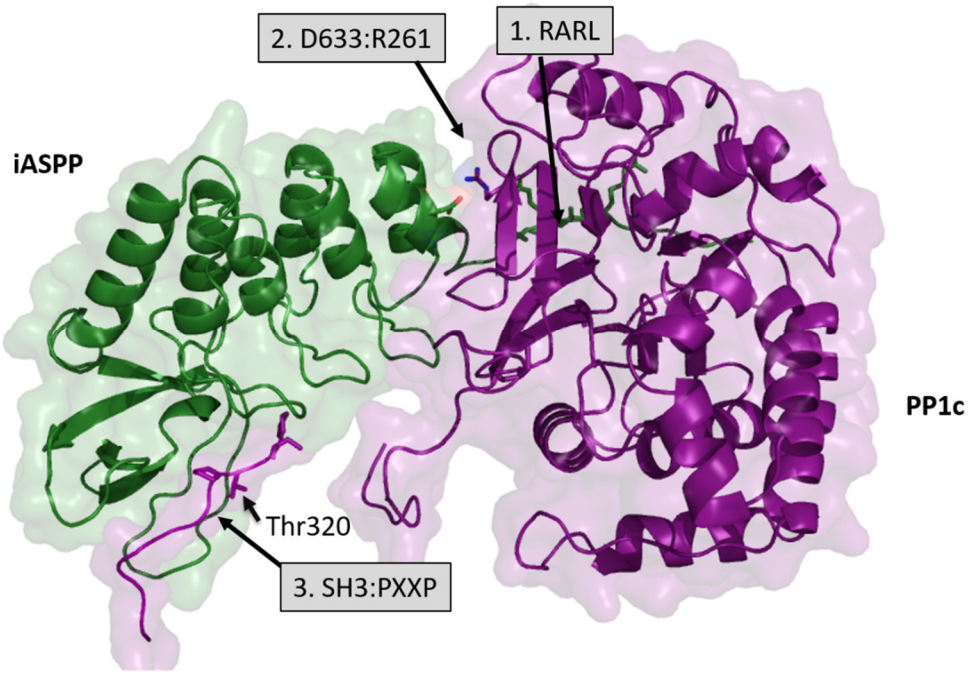

Figure 4.4 iASPP:PP1cα crystal structure identifies the RVXF-like, D633:R261 electrostatic, and SH3:PXXPXR interactions as important for binding.
The figure depicts the unpublished iASPP (green) and PP1cα (purple) where three regions are identified as being important for binding: RVXF-like motif, D633:R261 electrostatic, and the PP1cα PXXPXR motif interaction with iASPP SH3 domain. Thr320Asp mutation has been shown to abolish binding to iASPP.

To provide functional validation of these three interaction sites, site-directed mutagenesis of iASPP and PP1cα were performed. The T320D mutant and 1-300 truncation were introduced into the PP1cα isoform to target the importance of the iASPP-SH3/Ankyrin: PP1cα C-terminal tail interactions. In addition, the structure identified the acidic residue on iASPP, D633, within the acidic patch on iASPP which could be important for binding to the basic R261 on PP1cα. This acidic aspartic acid residue was exchanged for a basic Arg residue, to create $iASPP_{608-828}$ (D633R). The final mutation used was $iASPP_{608-828}$ (L625A), which was previously generated to mutate the RVXF-like motif of iASPP from RARL to RARA, and was used to assess iASPP: PP1c binding (figure 4.5)[82].

Binding experiments directly comparing mutations in these three sites have not been previously performed within the same experiment. Therefore, pull-down experiments using Ni^{2+} NTA and MC-S were used to assess the effect on binding of PP1cα (T320D), PP1cα (1-300), $iASPP_{608-828}$ (D633R), and the previously generated $iASPP_{608-828}$ (L625A) under the buffer conditions used within the functional dephosphorylation experiments that follow in section 4.3.2[82].

Our results differ for the iASPP$_{608-828}$ (L625A) mutation from what has been found previously[82]. Prior studies found that this mutation almost completely disrupted binding, however in our experiments there was only a 20% decrease in binding. This could be due to a difference in NaCl concentration, as previously 500mM NaCl was used whereas our experiments use an overall 125 mM salt concentration. However, in an experiment using 500 mM salt (data not shown) binding was still only decreased to 60% compared to iASPP (WT). The difference may also be due to length of incubation as the previous study used 1-18 hours incubation at 4°C of iASPP with PP1c, whereas our study uses 2 hours at 4°C. Regardless, there is a marginal but significant effect to mutating the RVXF-like motif from RARL to RARA. This effect is in line with the notion that the 4th amino acid is important for RVXF-like binding to PP1cα, however also supports the fact that there are multiple points of contact that are important for the iASPP:PP1c interaction as this single mutation does not obliterate binding[77].

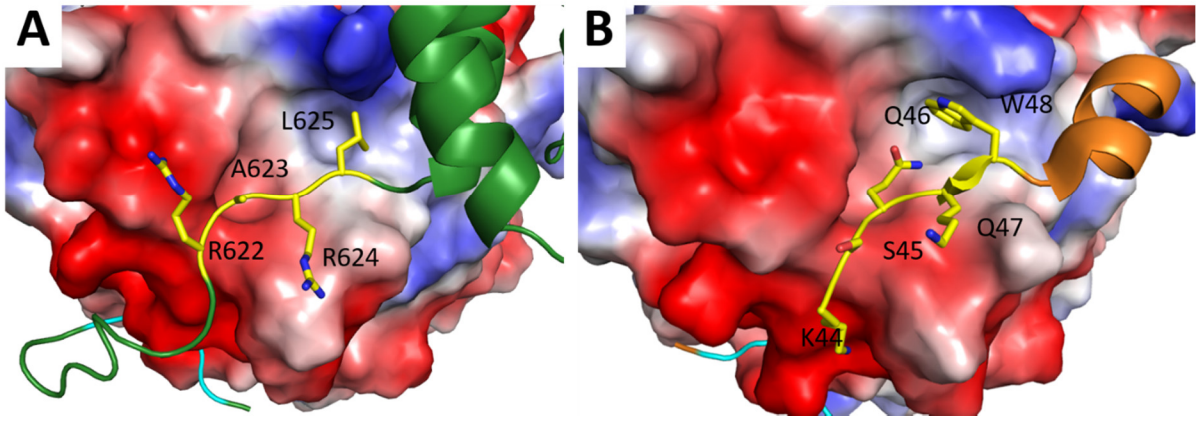

Figure 4.5 iASPP:PP1cα interaction is dependent on the RVXF-like motif.
The figure depicts the RVXF-like motif (yellow) of A) the unpublished iASPP (green):PP1cα (electrostatic surface) structure, and B) that of Inhibitor-2 (orange):PP1cα (electrostatic surface) (PDB:2O8A)[78]. The 4th amino acid is known to be important for binding to a hydrophobic clef of PP1c. Mutation of the amino acid in the 4th position to an alanine (L625A for iASPP) has been used previously to obliterate the RVXF interaction[82].

Our results also identify that D633 does indeed affect the binding of iASPP$_{608-828}$ to PP1cα, albeit by only approximately 20%, roughly the same degree as the mutation to the RVXF-like motif [iASPP$_{608-828}$ (L625A)] (Figure 4.1). The mutation of the PP1cα R261S previously showed a 70% decrease in binding relative to iASPP (WT): PP1cα (WT). It may be that there are other residues within the acidic/ basic patches that are interacting, however it is difficult to directly compare as again previous experiments used 500 mM

NaCl compared to 125 mM salt used in our experiments. The presence of an electrostatic interaction between PP1cα-261 or K260 is proposed to be important for the binding of several regulators, such as Inhibitor-2 (figure 4.6)[82].

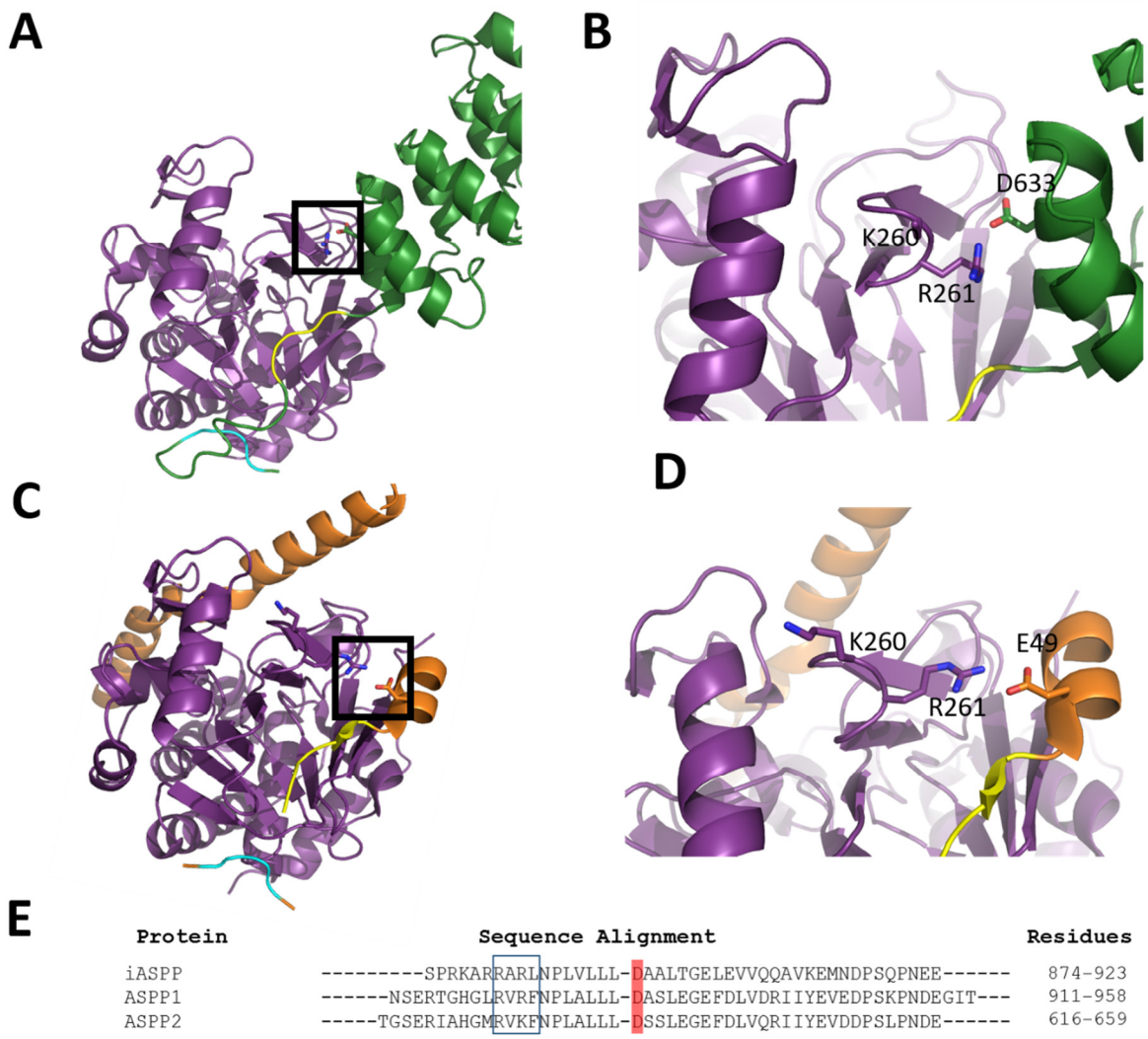

Figure 4.6 PP1cα R261 is important for electrostatic interactions with regulatory subunits. The figure depicts A,B) the unpublished iASPP (green):PP1cα (purple) structure, C,D) Inhibitor-2 (orange):PP1c (purple) structure (PDB:2O8A), and E) a sequence alignment of the ASPP proteins based on RVXF-like motif. A,B) PP1c-R261 interacts with D633 of iASPP. C,D) PP1c-R261 interacts with E49 of Inhibitor-2[82]. E) A sequence alignment based on the RVXF-like motif highlights that the D633 residue is conserved among ASPP family members[78].

In addition, our study replicates the finding that the PP1cα tail is absolutely critical for binding, as the T320D mutant impairs binding by approximately 90%, while the PP1cα (1-300) completely abolishes

binding (figure 4.1). This has been shown previously in similar mutants in the closely related PP1cγ[82]. The crystal structure of iASPP:PP1cα shows the C-terminal tail PXXPXR motif (PITPPR, residues 318-323) bound within the SH3 domain of iASPP, which is similar to the binding of HIV-1 negative regulatory factor (V-1Nef) to the SH3 domain of Fyn (figure 4.7). The PP1cα R323 residue binds on the acidic SH3 "specificity pocket" made up of the evolutionarily conserved residues of iASPP; D775, E776, E795, W798, and Y809. The two PP1cα proline residues, P318 and P321, bind within two shallow grooves called "xP" pockets that contain the SH3 conserved residues of iASPP; W798, P811, Y814, and W767. As shown in figure 4.6, the Thr320 residue resides within an acidic surface patch where phosphorylation of this residue could be predicted to be electrostatically unfavourable.

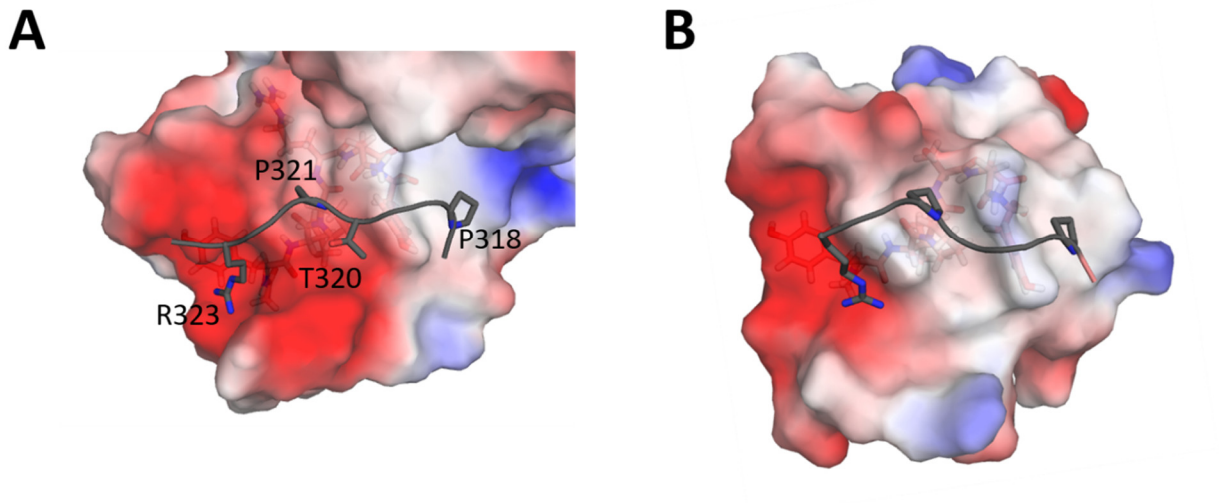

Figure 4.7 PP1cα C-terminal tail binds to iASPP using a PXXPXR:SH3 domain interaction
The figure depicts A) the PP1cα C-terminal tail residues PITPPR (grey) binding to the iASPP-SH3 domain (electrostatic surface), and B) the residues 71-77 of the HIV-1 negative regulatory factor (V-1 Nef) (grey) bound to the SH3 domain of protein-tyrosine kinase, Fyn (surface electrostatic) (PDB: 1AVZ). Both structures show an Arg residue binding within an acidic region called a "specificity pocket" thought to be crucial for the interaction, followed by two prolines binding within shallow grooves called xP pockets[134].

4.2.2 iASPP-mediated dephosphorylation of p53Ser15 relies upon the RVXF-like, D633:R261 electrostatic, and PP1cα C-terminal tail interactions.

As shown in section 3.2.4, iASPP (WT) mediates the dephosphorylation of p53Ser15 by PP1cα. As discussed in Chapter three, how iASPP and PP1cα form a complex with p53 is currently unknown. However, an overlay of the 53BP2:p53 structure (PDB:1YCS) and the iASPP:PP1cα structure with the

PP1cα tail bound shows that both p53 and PP1cα would have to utilize the same charged specificity pocket on iASPP to bind using their respective Arg residues (p53 R248 and PP1cα R323) (figure 4.8). An R248W mutation shows that this residue is critical for p53 binding to 53BP2[10]. Therefore, it is likely that the PP1cα PXXPXR and p53 binding to the iASPP SH3 domain are mutually exclusive.

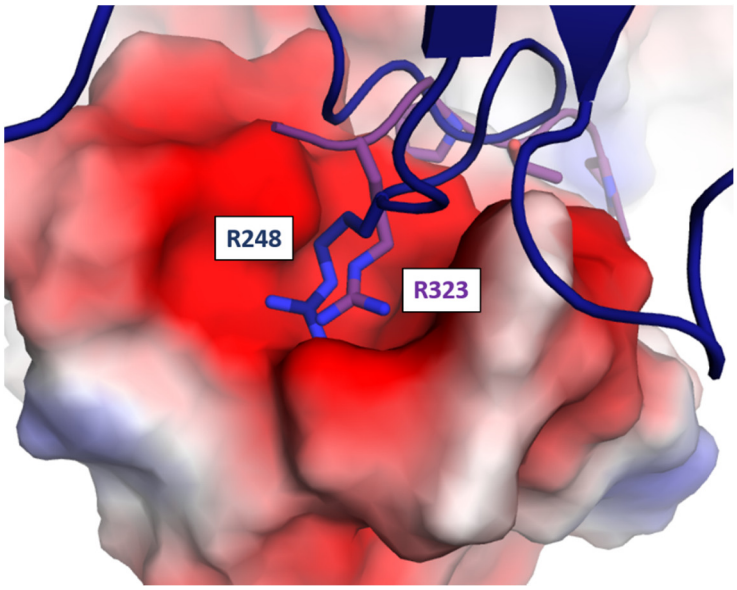

Figure 4.8 Both PP1cα and p53 likely bind to the same SH3 specificity pocket.
The figure depicts an overlay of the SH3 domain of the unpublished iASPP (electrostatic surface):PP1cα (purple) structure and the 53BP2 (not shown):p53 (blue) structure (PDB:1YCS). iASPP was aligned with 53BP2, only iASPP is shown in the figure for clarity. Both p53-R248 (blue) and PP1cα-R323 (purple) bind within the same "specificity pocket" of iASPP, therefore are likely mutually exclusive[10].

The PP1cα (T320D) and PP1cα (1-300) mutations both corroborate this hypothesis. Although binding experiments point to the fact that they are both critical for iASPP:PP1cα heterodimer formation, their importance in the functional dephosphorylation of p53Ser15 is less pronounced. The PP1cα (T320D) mutation had no significant effect compared to PP1cα (WT), while the PP1cα (1-300) did not obliterate iASPP-mediated dephosphorylation of p53 as predicted based on binding. The PP1cα tail likely has multiple points of contact with iASPP and does not solely rely on the PXXPXR: SH3 interaction. The tail may interact with the Ankyrin repeats in a similar manner to that observed in the MYPT1 ankyrin repeats[71]. In the case of the PP1c (T320D) mutant, the Asp residue may not cause complete dissociation of the entire tail from the Ank motifs. However, this mutation does suggest that the PP1cα PXXPXR:SH3 interaction is not critical for iASPP-mediated dephosphorylation, which may be partially explained by the necessity of p53 to bind to the same site on the SH3 domain. SPR experiments showed that PP1cα (WT) bound to $iASPP_{608-828}$ with a

K_D= 26 +/- 0.4 nM, while the PP1cα C-terminal tail (301-330) bound to iASPP iASPP$_{608-828}$ with a K_D= 53 +/- 7 nM[110]. This highlights that although the C-terminal tail is a large factor in heterodimer binding, there are still other determinants that are key to the interaction of iASPP:PP1cα.

The RVXF-like mutant-iASPP (L625A), and the electrostatic D633:R261 mutant- iASPP (D633R), both mediated dephosphorylation in a manner that mirrored their effect in the pull-down binding experiments. The RVXF-like motif is not thought to be a particularly strong interaction, but rather an important anchor to allow for binding of other motifs[66]. Thus, the lack of RVXF-like motif is likely compensated by the other points of interaction. The SILK motif interaction resides only 10 amino acids N-terminal to the RVXF-like interaction, and is present in one of the two crystal structures (figure 1.11). It could be suggested that the SILK compensates for the lack of RVXF-like motif. However, pulldown experiments showed that the binding to PP1cα (WT) was the same for iASPP (L625A) as it was for a truncation, iASPP$_{626-828}$, which removed both the RVXF-like and SILK motifs[82]. This would imply that at least for the strength of interaction needed for a pull-down, the RVXF-like motif is what contributes the most to binding. Unlike the well characterized RVXF-like motif function, the importance of a regulatory protein binding to the R261 of PP1cα is still not fully characterized as it is a relatively newly found interaction motif[82]. In our binding and dephosphorylation experiments the D633R mutation is as detrimental as mutating the RVXF-like motif. As with the RVXF-like motif, the effect on binding and dephosphorylation of the iASPP (D633R) interaction is likely compensated by the presence of other interaction points, including but not limited to the C-terminal tail interaction, the RVXF-like motif, and the SILK motif.

“Double” mutations were also tested to further deduce which sites may be most important functionally. The C-terminal tail truncation (PP1cα (1-300)) combined with the RVXF-like (iASPP (L625A)) or electrostatic mutation (iASPP (D633R)) substantially impaired iASPP-mediated dephosphorylation, however did not return to the levels of phosphorylation seen with PP1cα alone. The PP1cα (T320D) mutation had a general trend of no effect compared to PP1cα (WT) except when combined with iASPP (L625A). Given that the RVXF-like motif is thought to anchor and properly position other interaction sites, its removal in combination with PP1cα tail mutations might indicate that the electrostatic D633:R261 interaction and SILK interactions are not entirely adequate to position iASPP and PP1cα in the correct orientation to mediate dephosphorylation of p53. That said, none of iASPP mutations paired with the PP1cα

(T320D) were able to completely abolish the effect of iASPP dephosphorylation of p53 by PP1cα. These "double mutations" show that there are at least three interaction sites responsible for mediating dephosphorylation, as no combination of two mutations is capable of completely abolishing the effect of iASPP on PP1cα dephosphorylation of p53Ser15.

As with PP1cα (WT), the levels of PP1cα (T320D) were consistently approximately 20% higher in ASPP lanes versus PP1cα (T320D) alone as determined by the Pierce™ Reversible Protein Stain and ImageJ. The levels of PP1cα (1-300) on the other hand, were approximately equal across all lanes. This could be due to the ASPP proteins stabilizing PP1cα (WT) and (T320D) in solution but not PP1cα (1-300), however a stability test of PP1cα (WT) in the presence or absence of iASPP and ASPP2 was performed and showed PP1cα was stable on its own in the buffer conditions used (appendix section B.1). It's unknown why there consistently appears to be more PP1cα (WT) and (T320D) in the ASPP lanes. PP1cα is in relative excess for an enzyme at a 1:1 ratio to p53 substrate for measuring p53Ser15, and the rate of p53Ser15 dephosphorylation is relatively slow, therefore I would predict that this does not substantially affect the results. Regardless, a titration curve of PP1cα levels to relative phosphorylation amount could be used to normalize our data to PP1cα levels and assure that the 20% difference between the PP1cα alone lane and the ASPP lanes does not substantially affect the results.

Overall, these results show that the RVXF-like, the D633:R261 electrostatic interaction, and the PP1cα C-terminal tail interactions are important for iASPP-mediated dephosphorylation of p53Ser15, and thus provide a functional validation of the iASPP:PP1cα structure. This finding is similar to those of other PP1cα regulatory subunits which have multiple sites of interaction[71]. In addition, the PP1cα (T320D) mutation highlights that in contrast to what might be predicted based on pull-down experiments, the PXXPXR motif may not be important for iASPP-mediated dephosphorylation of p53Ser15. This suggests that the PP1cα tail may be able to move to allow binding of p53 to the iASPP SH3 domain and facilitate p53Ser15 dephosphorylation[82].

CHAPTER 5

Conclusions and Future Perspectives

CHAPTER FIVE: CONCLUSIONS AND FUTURE PERSPECTIVES

The multi-site phosphorylation of p53 greatly impacts its interactions with its regulatory proteins, and in turn, has drastic effects on overall cell signaling and the fate of the cell by either affecting; p53 levels within the cell, it's localization within the cell, or its affinity towards transactivation of specific genes over others.

In this thesis, I showed that PP1cα can dephosphorylate not only p53Ser15 and Ser37 *in vitro* as demonstrated previously, but also p53Thr18 and DYRK2-phosphorylated p53. This implicates PP1cα in the inactivation, destabilization, and localization of p53. I went on to show that dephosphorylation of p53Ser15, p53Thr18, and DYRK2-phosphorylation p53 is mediated by iASPP, and as a result at last providing a proposed mechanism by which iASPP negatively regulates p53-mediated apoptosis. Unexpectedly, ASPP2 also mediated the dephosphorylation of p53Ser15. These findings do not clearly provide a mechanism for how full-length ASPP2 positively regulates p53-mediated apoptosis, however may explain why N-terminal truncations ASPP2 have anti-apoptotic functions. I then used site-directed mutagenesis to provide functional validation of the iASPP:PP1cα structure by showing that the RVXF-like motif, the D633:R261 electrostatic interaction, and the PP1cα C-terminal tail interactions were all important for iASPP-mediated dephosphorylation of p53Ser15. Lastly, I provided evidence that the PXXPXR- SH3 interaction may not be essential for iASPP-mediated dephosphorylation of p53 which in turn allows us to speculate that the PP1cα tail could dissociate from the iASPP SH3 domain to allow binding of p53 to iASPP.

These findings provide insight into some questions in the field of ASPP regulation of p53, for example how iASPP could negatively modulate p53 function. Yet, this work poses several more; Do these dephosphorylations occur within the cell? Why would ASPP2 mediate dephosphorylation of p53Ser15? Where are these ASPP-mediated dephosphorylations occurring within the cell? Do they affect p53 localization? Could post-translational modifications of the ASPP proteins affect their interactions with either PP1c or p53? Could the interaction of PP1c with the ASPP proteins mediate ASPP dephosphorylation?

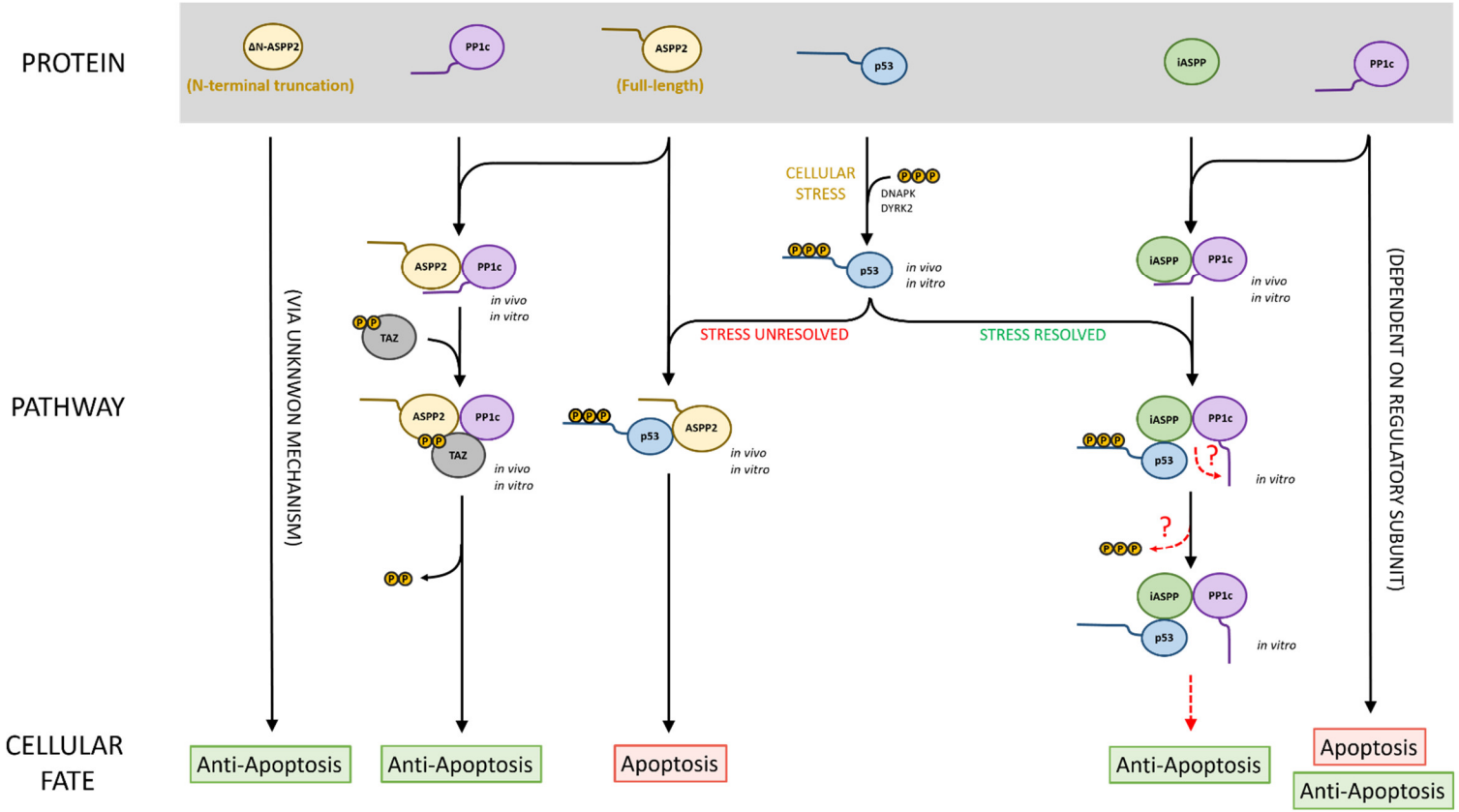

Figure 5.1 A Revised Summary of the ASPP Protein Pathways and Cellular Fates.
The Apoptotic Stimulating Protein of p53-2 (ASPP2) is known to promote p53-dependent apoptosis, however the newly found ΔN-terminal truncated version of ASPP2 appears to have the opposite effect through an unknown mechanism. In this thesis PP1cα was shown to form a complex with p53 and $ASPP2_{905-1128}$ (1), and mediate dephosphorylation of p53Ser15 (2) which may in part explain the anti-apoptotic effect of the ASPP2 truncation. Whether the full-length ASPP2 is capable of forming a complex with PP1cα and p53 is unknown (5). In some cases, the dephosphorylation of p53Ser15 may in fact be beneficial for apoptosis, and whether the full-length ASPP2 is capable of mediating dephosphorylation *in vitro* and *in vivo* is of interest to further characterize the significance of ASPP2-mediated dephosphorylation (5,6, and 7). In this thesis, I also find that the inhibitory ASPP, iASPP, is capable of forming a complex with PP1cα and p53, and that the PP1cα PXXPXR C-terminal tail motif is not essential for this interaction. As the binding of p53 and PP1c for the iASPP SH3 domain are thought to be mutually exclusive, our data suggests the PP1cα tail may move to allow binding and dephosphorylation of p53 (3). I also show for the first time that iASPP can mediate the dephosphorylation of p53 on multiple sites (4) which may explain its anti-apoptotic mechanism in cells (8).

Cell experiments are an obvious next step to confirm that PP1c can indeed dephosphorylate p53Thr18, and allow for evaluation of iASPP and ASPP2-mediated dephosphorylation of p53Ser15 and Thr18 *in vivo*. These experiments could be done in a similar manner to those showing that B56γ regulates PP2A dephosphorylation of p53Thr55[128]. This would include overexpression (or knockdowns) of the ASPP proteins and assessment of p53 phosphorylation at specific sites in the absence or presence of a PP1c inhibitor (okadaic acid) and under normal or stressed conditions (for example UV irradiation). In addition, use of small molecule compounds that affect the interaction of iASPP and/ or ASPP2 with PP1cα could be used (such as those already in development- personal communication Dr. Charles Holmes) to assess mediated dephosphorylation as well. Subcellular fractionation combined with immunoprecipitation (such as MC-S) to isolate cytosolic, nucleic, and mitochondrial fractions, in conjunction with cell imaging, could be used to assess where these proteins are interacting, and the respective phosphorylation status of p53 in those locations. This could be performed in healthy replicating cells compared to those treated with apoptosis inducing agents such as etoposide. One temptation might be to use mutagenesis of the ASPP RVXF motifs, however the *in vitro* dephosphorylation presented in this thesis suggest this may not have a sufficiently large change on mediated-dephosphorylation to see an effect *in vivo*, as the iASPP (L625A) mutation still mediated dephosphorylation of p53Ser15 by roughly 60% compared to wildtype iASPP which mediated 80% dephosphorylation.

One major drawback to the study of p53 phosphorylation and dephosphorylation is the reliance on phospho-specific antibodies, as highlighted with the results with the p53Ser46 antibody. Creating alanine mutations of phospho-sites is therefore crucial for validating the phospho-specificity shown in this thesis. Unfortunately, the current alternative to phospho-specific antibodies would be radiolabeling, however cellular labelling with ^{32}P induces p53 expression and results in cell cycle arrest, and therefore would make the interpretation of the effect of the ASPPs on p53 dephosphorylation difficult[135].

Ideally, when looking at the ASPP-mediated dephosphorylation of p53, one would be able to compare the phosphorylation status of all sites on p53. As recently analogized, the phosphorylation of p53 can be thought of like a barcode where each bar represents a phosphorylation site[136,137]. A particular barcode (or series of barcodes assuming redundancy) is likely responsible for a specific set of actions within

the cell. Hence looking at only the presence or absence of one bar from a barcode of 30 bars may lead to mis-attribution of significance to one site, when really it is the combination of multiple phospho-sites that is dictating function. This is supported by the p53S18A mouse model (Ser15 in humans) which shows a relatively mild phenotype compared to what would be predicted based on *in vitro* models, with no significant effects in p53 stability, cell-cycle, or tumour suppression[137]. However, when two sites were mutated, p53S18A and S23A (Ser15 and Ser20 in humans), mice still had mild effects in p53 stability and transactivation, yet apoptosis was compromised and tumours developed later in life. In addition, if the phosphorylation of only one site, for example Ser15, was key to all of p53 tumour suppressing functions, one might expect this residue to be one of the hotspots of p53 found within cancer. This is not the case, with the majority of mutation hotspots localized within the DNA binding domain[137]. Thus, it is the combination of phosphorylation sites on p53 which dictate its function, not necessarily the absolute presence or absence of only one site. Some advancements in looking at specific phospho-p53 forms have been made on this front using mass-spectrometry[138].

As outlined in Chapter 3, *in vivo* experiments are needed to confirm ASPP-mediated dephosphorylation of p53. However, if the iASPP-mediated dephosphorylation of p53 occurs *in vivo* and thus impairs p53 through dephosphorylation by PP1c, this may be an intriguing avenue for cancer therapy. Explicitly targeting the iASPP:PP1cα interaction (versus the ASPP2:PP1cα interaction) through small-molecule inhibitors (such as those currently under development within the Holmes lab) may prevent iASPP-mediated dephosphorylation of p53 and reactivate a previously iASPP-subdued p53. In contrast to nutlins (which inhibit the Mdm2:p53 interaction with varying success), this line of attack would not only affect a single interaction, but a multitude of phospho-dependent interactions with p53.

Bibliography

BIBLIOGRAPHY

1. Kandoth, C. *et al.* Mutational landscape and significance across 12 major cancer types. *Nature* **502,** 333–339 (2013).
2. Donehower, L. A. The p53-deficient mouse: a model for basic and applied cancer studies. *Semin. Cancer Biol.* **7,** 269–278 (1996).
3. Collavin, L., Lunardi, A. & Del Sal, G. p53-family proteins and their regulators: hubs and spokes in tumor suppression. *Cell Death Differ.* **17,** 901–911 (2010).
4. Anne-Sophie Huart & Ted R. Hupp. Evolution of Conformational Disorder & Diversity of the P53 Interactome. *BioDiscovery* **8,** (2013).
5. Riley, T., Sontag, E., Chen, P. & Levine, A. Transcriptional control of human p53-regulated genes. *Nat. Rev. Mol. Cell Biol.* **9,** 402–412 (2008).
6. Chen, Y., Dey, R. & Chen, L. Crystal structure of the p53 core domain bound to a full consensus site as a self-assembled tetramer. *Struct. Lond. Engl. 1993* **18,** 246–256 (2010).
7. Brázda, V. & Coufal, J. Recognition of Local DNA Structures by p53 Protein. *Int. J. Mol. Sci.* **18,** (2017).
8. Bieging, K. T., Mello, S. S. & Attardi, L. D. Unravelling mechanisms of p53-mediated tumour suppression. *Nat. Rev. Cancer* **14,** 359–370 (2014).
9. Joerger, A. C. & Fersht, A. R. The Tumor Suppressor p53: From Structures to Drug Discovery. *Cold Spring Harb. Perspect. Biol.* **2,** a000919 (2010).
10. Gorina, S. & Pavletich, N. P. Structure of the p53 tumor suppressor bound to the ankyrin and SH3 domains of 53BP2. *Science* **274,** 1001–1005 (1996).

11. Toledo, F. *et al.* Mouse mutants reveal that putative protein interaction sites in the p53 proline-rich domain are dispensable for tumor suppression. *Mol. Cell. Biol.* **27,** 1425–1432 (2007).

12. Berger, M., Stahl, N., Del Sal, G. & Haupt, Y. Mutations in Proline 82 of p53 Impair Its Activation by Pin1 and Chk2 in Response to DNA Damage. *Mol. Cell. Biol.* **25,** 5380–5388 (2005).

13. McGraw, K. L. *et al.* The relationship of TP53 R72P polymorphism to disease outcome and TP53 mutation in myelodysplastic syndromes. *Blood Cancer J.* **5,** e291 (2015).

14. Bergamaschi, D. *et al.* iASPP preferentially binds p53 proline-rich region and modulates apoptotic function of codon 72-polymorphic p53. *Nat. Genet.* **38,** 1133–1141 (2006).

15. Ganguly, D. & Chen, J. Modulation of the Disordered Conformational Ensembles of the p53 Transactivation Domain by Cancer-Associated Mutations. *PLoS Comput. Biol.* **11,** (2015).

16. Uversky, V. N. p53 Proteoforms and Intrinsic Disorder: An Illustration of the Protein Structure-Function Continuum Concept. *Int. J. Mol. Sci.* **17,** (2016).

17. Okuda, M. & Nishimura, Y. Real-time and simultaneous monitoring of the phosphorylation and enhanced interaction of p53 and XPC acidic domains with the TFIIH p62 subunit. *Oncogenesis* **4,** e150 (2015).

18. Jenkins, L. M. M., Durell, S. R., Mazur, S. J. & Appella, E. p53 N-terminal phosphorylation: a defining layer of complex regulation. *Carcinogenesis* **33,** 1441–1449 (2012).

19. van Leeuwen, I. M. M. *et al.* Mechanism-specific signatures for small-molecule p53 activators. *Cell Cycle Georget. Tex* **10,** 1590–1598 (2011).

20. Kussie, P. H. *et al.* Structure of the MDM2 oncoprotein bound to the p53 tumor suppressor transactivation domain. *Science* **274,** 948–953 (1996).

21. Krois, A. S., Ferreon, J. C., Martinez-Yamout, M. A., Dyson, H. J. & Wright, P. E. Recognition of the disordered p53 transactivation domain by the transcriptional adapter zinc finger domains of CREB-binding protein. *Proc. Natl. Acad. Sci. U. S. A.* **113,** E1853–E1862 (2016).

22. Varedi K, S. M., Ventura, A. C., Merajver, S. D. & Lin, X. N. Multisite phosphorylation provides an effective and flexible mechanism for switch-like protein degradation. *PloS One* **5,** e14029 (2010).

23. Loughery, J., Cox, M., Smith, L. M. & Meek, D. W. Critical role for p53-serine 15 phosphorylation in stimulating transactivation at p53-responsive promoters. *Nucleic Acids Res.* **42,** 7666–7680 (2014).

24. Anderson CW, Appella E. Signaling to the p53 tumor suppresor through pathways activated by genotoxic and non gentoxic sress. in *Handbook of Cell Signaling* (ed. R.A. Bradshaw and E. Dennis) 237–247 (Academic Press, 2004).

25. Jones, R. G. *et al.* AMP-activated protein kinase induces a p53-dependent metabolic checkpoint. *Mol. Cell* **18,** 283–293 (2005).

26. Lees-Miller, S. P., Sakaguchi, K., Ullrich, S. J., Appella, E. & Anderson, C. W. Human DNA-activated protein kinase phosphorylates serines 15 and 37 in the amino-terminal transactivation domain of human p53. *Mol. Cell. Biol.* **12,** 5041–5049 (1992).

27. Saito, S. 'ichi *et al.* ATM mediates phosphorylation at multiple p53 sites, including Ser(46), in response to ionizing radiation. *J. Biol. Chem.* **277,** 12491–12494 (2002).

28. Tibbetts, R. S. *et al.* A role for ATR in the DNA damage-induced phosphorylation of p53. *Genes Dev.* **13,** 152–157 (1999).

29. Saito, S. 'ichi *et al.* Phosphorylation Site Interdependence of Human p53 Post-translational Modifications in Response to Stress. *J. Biol. Chem.* **278,** 37536–37544 (2003).

30. Dumaz, N., Milne, D. M. & Meek, D. W. Protein kinase CK1 is a p53-threonine 18 kinase which requires prior phosphorylation of serine 15. *FEBS Lett.* **463,** 312–316 (1999).

31. Lee, C. W., Ferreon, J. C., Ferreon, A. C. M., Arai, M. & Wright, P. E. Graded enhancement of p53 binding to CREB-binding protein (CBP) by multisite phosphorylation. *Proc. Natl. Acad. Sci. U. S. A.* **107,** 19290–19295 (2010).

32. Ferreon, J. C. *et al.* Cooperative regulation of p53 by modulation of ternary complex formation with CBP/p300 and HDM2. *Proc. Natl. Acad. Sci. U. S. A.* **106,** 6591–6596 (2009).

33. Dornan, D. & Hupp, T. R. Inhibition of p53-dependent transcription by BOX-I phospho-peptide mimetics that bind to p300. *EMBO Rep.* **2,** 139–144 (2001).

34. Zhang, Y. & Xiong, Y. A p53 amino-terminal nuclear export signal inhibited by DNA damage-induced phosphorylation. *Science* **292,** 1910–1915 (2001).

35. Park, B. S. *et al.* Phospho-ser 15-p53 translocates into mitochondria and interacts with Bcl-2 and Bcl-xL in eugenol-induced apoptosis. *Apoptosis Int. J. Program. Cell Death* **10,** 193–200 (2005).

36. Cai, X. & Liu, X. Inhibition of Thr-55 phosphorylation restores p53 nuclear localization and sensitizes cancer cells to DNA damage. *Proc. Natl. Acad. Sci. U. S. A.* **105,** 16958–16963 (2008).

37. Horn, H. F. & Vousden, K. H. Coping with stress: multiple ways to activate p53. *Oncogene* **26,** 1306–1316 (2007).

38. Blanco, S., Klimcakova, L., Vega, F. M. & Lazo, P. A. The subcellular localization of vaccinia-related kinase-2 (VRK2) isoforms determines their different effect on p53 stability in tumour cell lines. *FEBS J.* **273,** 2487–2504 (2006).

39. Lopez-Borges, S. & Lazo, P. A. The human vaccinia-related kinase 1 (VRK1) phosphorylates threonine-18 within the mdm-2 binding site of the p53 tumour suppressor protein. *Oncogene* **19,** 3656–3664 (2000).

40. Soubeyrand, S., Schild-Poulter, C. & Haché, R. J. G. Structured DNA promotes phosphorylation of p53 by DNA-dependent protein kinase at serine 9 and threonine 18. *Eur. J. Biochem.* **271,** 3776–3784 (2004).

41. Craig, A. L. *et al.* The MDM2 ubiquitination signal in the DNA-binding domain of p53 forms a docking site for calcium calmodulin kinase superfamily members. *Mol. Cell. Biol.* **27,** 3542–3555 (2007).

42. Teufel, D. P., Bycroft, M. & Fersht, A. R. Regulation by phosphorylation of the relative affinities of the N-terminal transactivation domains of p53 for p300 domains and Mdm2. *Oncogene* **28,** 2112–2118 (2009).

43. ElSawy, K. M., Sim, A., Lane, D. P., Verma, C. S. & Caves, L. S. A spatiotemporal characterization of the effect of p53 phosphorylation on its interaction with MDM2. *Cell Cycle* **14,** 179–188 (2015).

44. Nakamizo, A. *et al.* Phosphorylation of Thr18 and Ser20 of p53 in Ad-p53 – induced apoptosis. *Neuro-Oncol.* **10,** 275–291 (2008).

45. Reuven, N. *et al.* The Tyrosine Kinase c-Abl Promotes Homeodomain-interacting Protein Kinase 2 (HIPK2) Accumulation and Activation in Response to DNA Damage. *J. Biol. Chem.* **290,** 16478–16488 (2015).

46. Pérez, M. *et al.* Mutual regulation between SIAH2 and DYRK2 controls hypoxic and genotoxic signaling pathways. *J. Mol. Cell Biol.* **4,** 316–330 (2012).

47. Okoshi, R. *et al.* Activation of AMP-activated protein kinase induces p53-dependent apoptotic cell death in response to energetic stress. *J. Biol. Chem.* **283,** 3979–3987 (2008).

48. Kodama, M. *et al.* Requirement of ATM for rapid p53 phosphorylation at Ser46 without Ser/Thr-Gln sequences. *Mol. Cell. Biol.* **30,** 1620–1633 (2010).

49. D'Orazi, G. *et al.* Homeodomain-interacting protein kinase-2 phosphorylates p53 at Ser 46 and mediates apoptosis. *Nat. Cell Biol.* **4,** 11–19 (2002).

50. Taira, N., Nihira, K., Yamaguchi, T., Miki, Y. & Yoshida, K. DYRK2 is targeted to the nucleus and controls p53 via Ser46 phosphorylation in the apoptotic response to DNA damage. *Mol. Cell* **25,** 725–738 (2007).

51. Mayo, L. D. *et al.* Phosphorylation of human p53 at serine 46 determines promoter selection and whether apoptosis is attenuated or amplified. *J. Biol. Chem.* **280,** 25953–25959 (2005).

52. Smeenk, L. *et al.* Role of p53 serine 46 in p53 target gene regulation. *PloS One* **6,** e17574 (2011).

53. Polonio-Vallon, T., Krüger, D. & Hofmann, T. G. ShaPINg Cell Fate Upon DNA Damage: Role of Pin1 Isomerase in DNA Damage-Induced Cell Death and Repair. *Front. Oncol.* **4,** (2014).

54. Wosik, K. *et al.* Oligodendrocyte injury in multiple sclerosis: a role for p53. *J. Neurochem.* **85,** 635–644 (2003).

55. Tyner, S. D. *et al.* p53 mutant mice that display early ageing-associated phenotypes. *Nature* **415,** 45–53 (2002).

56. Chang, J. R. *et al.* Role of p53 in Neurodegenerative Diseases. *Neurodegener. Dis.* **9,** 68–80 (2012).

57. Proctor, C. J. & Gray, D. A. GSK3 and p53 - is there a link in Alzheimer's disease? *Mol. Neurodegener.* **5,** 7 (2010).

58. Hientz, K., Mohr, A., Bhakta-Guha, D. & Efferth, T. The role of p53 in cancer drug resistance and targeted chemotherapy. *Oncotarget* **8,** 8921–8946 (2016).

59. Lu, X., Nannenga, B. & Donehower, L. A. PPM1D dephosphorylates Chk1 and p53 and abrogates cell cycle checkpoints. *Genes Dev.* **19,** 1162–1174 (2005).

60. Shang, X. *et al.* Dual-specificity phosphatase 26 is a novel p53 phosphatase and inhibits p53 tumor suppressor functions in human neuroblastoma. *Oncogene* **29,** 4938–4946 (2010).

61. Li, D. W.-C. *et al.* Protein serine/threonine phosphatase-1 dephosphorylates p53 at Ser-15 and Ser-37 to modulate its transcriptional and apoptotic activities. *Oncogene* **25,** 3006–3022 (2006).

62. Olsen, J. V. *et al.* Global, in vivo, and site-specific phosphorylation dynamics in signaling networks. *Cell* **127,** 635–648 (2006).

63. Olsen, J. V. *et al.* Quantitative phosphoproteomics reveals widespread full phosphorylation site occupancy during mitosis. *Sci. Signal.* **3,** ra3 (2010).

64. Li, X., Wilmanns, M., Thornton, J. & Köhn, M. Elucidating human phosphatase-substrate networks. *Sci. Signal.* **6,** rs10 (2013).

65. Virshup, D. M. & Shenolikar, S. From promiscuity to precision: protein phosphatases get a makeover. *Mol. Cell* **33,** 537–545 (2009).

66. Bollen, M., Peti, W., Ragusa, M. J. & Beullens, M. The extended PP1 toolkit: designed to create specificity. *Trends Biochem. Sci.* **35,** 450–458 (2010).

67. Jayapalan, N. Comprehensive Study of Plato. *Atl. Publ. Dist* 10 (2002).

68. Ceulemans, H. & Bollen, M. Functional diversity of protein phosphatase-1, a cellular economizer and reset button. *Physiol. Rev.* **84,** 1–39 (2004).

69. Korrodi-Gregório, L., Esteves, S. L. C. & Fardilha, M. Protein phosphatase 1 catalytic isoforms: specificity toward interacting proteins. *Transl. Res. J. Lab. Clin. Med.* **164,** 366–391 (2014).

70. Gibbons, J. A., Kozubowski, L., Tatchell, K. & Shenolikar, S. Expression of human protein phosphatase-1 in Saccharomyces cerevisiae highlights the role of phosphatase isoforms in regulating eukaryotic functions. *J. Biol. Chem.* **282,** 21838–21847 (2007).

71. Terrak, M., Kerff, F., Langsetmo, K., Tao, T. & Dominguez, R. Structural basis of protein phosphatase 1 regulation. *Nature* **429,** 780–784 (2004).

72. Oberoi, J. *et al.* Structural and functional basis of protein phosphatase 5 substrate specificity. *Proc. Natl. Acad. Sci. U. S. A.* **113,** 9009–9014 (2016).

73. Verbinnen, I., Ferreira, M. & Bollen, M. Biogenesis and activity regulation of protein phosphatase 1. *Biochem. Soc. Trans.* **45,** 89–99 (2017).

74. Hou, H. *et al.* Synaptic NMDA receptor stimulation activates PP1 by inhibiting its phosphorylation by Cdk5. *J. Cell Biol.* **203,** 521–535 (2013).

75. Manser, C., Vagnoni, A., Guillot, F., Davies, J. & Miller, C. C. J. Cdk5/p35 phosphorylates lemur tyrosine kinase-2 to regulate protein phosphatase-1C phosphorylation and activity. *J. Neurochem.* **121,** 343–348 (2012).

76. Choy, M. S. *et al.* Understanding the antagonism of retinoblastoma protein dephosphorylation by PNUTS provides insights into the PP1 regulatory code. *Proc. Natl. Acad. Sci. U. S. A.* **111,** 4097–4102 (2014).

77. Heroes, E. *et al.* The PP1 binding code: a molecular-lego strategy that governs specificity. *FEBS J.* **280,** 584–595 (2013).

78. Hurley, T. D. *et al.* Structural basis for regulation of protein phosphatase 1 by inhibitor-2. *J. Biol. Chem.* **282,** 28874–28883 (2007).

79. Rebelo, S., Santos, M., Martins, F., da Cruz e Silva, E. F. & da Cruz e Silva, O. A. B. Protein phosphatase 1 is a key player in nuclear events. *Cell. Signal.* **27,** 2589–2598 (2015).

80. Wakula, P., Beullens, M., Ceulemans, H., Stalmans, W. & Bollen, M. Degeneracy and function of the ubiquitous RVXF motif that mediates binding to protein phosphatase-1. *J. Biol. Chem.* **278,** 18817–18823 (2003).

81. Chatterjee, J. *et al.* Development of a Peptide that Selectively Activates Protein Phosphatase-1 in Living Cells. *Angew. Chem. Int. Ed Engl.* **51,** 10054–10059 (2012).

82. Skene-Arnold, T. D. *et al.* Molecular mechanisms underlying the interaction of protein phosphatase-1c with ASPP proteins. *Biochem. J.* **449,** 649–659 (2013).

83. Moorhead, G., MacKintosh, R. W., Morrice, N., Gallagher, T. & MacKintosh, C. Purification of type 1 protein (serine/threonine) phosphatases by microcystin-Sepharose affinity chromatography. *FEBS Lett.* **356,** 46–50 (1994).

84. Goldberg, J. *et al.* Three-dimensional structure of the catalytic subunit of protein serine/threonine phosphatase-1. *Nature* **376,** 745–753 (1995).

85. Liu, C. W. Y., Wang, R.-H. & Berndt, N. Protein phosphatase 1alpha activity prevents oncogenic transformation. *Mol. Carcinog.* **45,** 648–656 (2006).

86. Liu, C. W. *et al.* Inhibitory phosphorylation of PP1alpha catalytic subunit during the G(1)/S transition. *J. Biol. Chem.* **274,** 29470–29475 (1999).

87. Li, T., Chalifour, L. E. & Paudel, H. K. Phosphorylation of protein phosphatase 1 by cyclin-dependent protein kinase 5 during nerve growth factor-induced PC12 cell differentiation. *J. Biol. Chem.* **282,** 6619–6628 (2007).

88. Bergamaschi, D. *et al.* iASPP oncoprotein is a key inhibitor of p53 conserved from worm to human. *Nat. Genet.* **33,** 162–167 (2003).

89. Samuels-Lev, Y. *et al.* ASPP proteins specifically stimulate the apoptotic function of p53. *Mol. Cell* **8,** 781–794 (2001).

90. Iwabuchi, K., Bartel, P. L., Li, B., Marraccino, R. & Fields, S. Two cellular proteins that bind to wild-type but not mutant p53. *Proc. Natl. Acad. Sci. U. S. A.* **91,** 6098–6102 (1994).

91. Rotem, S., Katz, C. & Friedler, A. Insights into the structure and protein-protein interactions of the pro-apoptotic protein ASPP2. *Biochem. Soc. Trans.* **35,** 966–969 (2007).

92. Van Hook, K. *et al.* ΔN-ASPP2, a novel isoform of the ASPP2 tumor suppressor, promotes cellular survival. *Biochem. Biophys. Res. Commun.* **482,** 1271–1277 (2017).

93. Naumovski, L. & Cleary, M. L. The p53-binding protein 53BP2 also interacts with Bc12 and impedes cell cycle progression at G2/M. *Mol. Cell. Biol.* **16,** 3884–3892 (1996).

94. Tidow, H., Andreeva, A., Rutherford, T. J. & Fersht, A. R. Solution structure of ASPP2 N-terminal domain (N-ASPP2) reveals a ubiquitin-like fold. *J. Mol. Biol.* **371,** 948–958 (2007).

95. Wang, Y. *et al.* ASPP1 and ASPP2 bind active RAS, potentiate RAS signalling and enhance p53 activity in cancer cells. *Cell Death Differ.* **20,** 525–534 (2013).

96. Ahn, J., Byeon, I.-J. L., Byeon, C.-H. & Gronenborn, A. M. Insight into the structural basis of pro- and antiapoptotic p53 modulation by ASPP proteins. *J. Biol. Chem.* **284,** 13812–13822 (2009).

97. Vives, V. *et al.* ASPP2 is a haploinsufficient tumor suppressor that cooperates with p53 to suppress tumor growth. *Genes Dev.* **20,** 1262–1267 (2006).

98. Liu, Z.-J., Zhang, Y., Zhang, X.-B. & Yang, X. Abnormal mRNA expression of ASPP members in leukemia cell lines. *Leukemia* **18,** 880 (2004).

99. Lossos, I. S., Natkunam, Y., Levy, R. & Lopez, C. D. Apoptosis stimulating protein of p53 (ASPP2) expression differs in diffuse large B-cell and follicular center lymphoma: correlation with clinical outcome. *Leuk. Lymphoma* **43,** 2309–2317 (2002).

100. Schittenhelm, M. M. *et al.* Attenuated expression of apoptosis stimulating protein of p53-2 (ASPP2) in human acute leukemia is associated with therapy failure. *PloS One* **8,** e80193 (2013).

101. Helps, N. R., Barker, H. M., Elledge, S. J. & Cohen, P. T. Protein phosphatase 1 interacts with p53BP2, a protein which binds to the tumour suppressor p53. *FEBS Lett.* **377,** 295–300 (1995).

102. Takahashi, N. *et al.* Inhibition of the 53BP2S-mediated apoptosis by nuclear factor kappaB and Bcl-2 family proteins. *Genes Cells Devoted Mol. Cell. Mech.* **10,** 803–811 (2005).

103. Liu, C.-Y. *et al.* PP1 cooperates with ASPP2 to dephosphorylate and activate TAZ. *J. Biol. Chem.* **286,** 5558–5566 (2011).

104. Zhang, P. *et al.* ASPP1/2-PP1 complexes are required for chromosome segregation and kinetochore-microtubule attachments. *Oncotarget* **6,** 41550–41565 (2015).

105. Sullivan, A. & Lu, X. ASPP: a new family of oncogenes and tumour suppressor genes. *Br. J. Cancer* **96,** 196 (2007).

106. Robinson, R. A., Lu, X., Jones, E. Y. & Siebold, C. Biochemical and structural studies of ASPP proteins reveal differential binding to p53, p63, and p73. *Struct. Lond. Engl. 1993* **16,** 259–268 (2008).

107. Dong, P. *et al.* Reactivating p53 functions by suppressing its novel inhibitor iASPP: a potential therapeutic opportunity in p53 wild-type tumors. *Oncotarget* **6,** 19968–19975 (2015).

108. Qiu, S., Cai, Y., Gao, X., Gu, S.-Z. & Liu, Z.-J. A small peptide derived from p53 linker region can resume the apoptotic activity of p53 by sequestering iASPP with p53. *Cancer Lett.* **356,** 910–917 (2015).

109. Notari, M. *et al.* iASPP, a previously unidentified regulator of desmosomes, prevents arrhythmogenic right ventricular cardiomyopathy (ARVC)-induced sudden death. *Proc. Natl. Acad. Sci. U. S. A.* **112,** E973 (2015).

110. Arnold, T. D. Molecular Mechanisms Underlying the Regulation of Protein Phosphatase-1c by the Apoptotic Stimulating Proteins of p53. (University of Alberta (Canada), 2013).

111. Boland, M. P., Smillie, M. A., Chen, D. Z. & Holmes, C. F. A unified bioscreen for the detection of diarrhetic shellfish toxins and microcystins in marine and freshwater environments. *Toxicon Off. J. Int. Soc. Toxinology* **31,** 1393–1405 (1993).

112. Kok, B. P. C. *et al.* Conserved Residues in the N Terminus of Lipin-1 Are Required for Binding to Protein Phosphatase-1c, Nuclear Translocation, and Phosphatidate Phosphatase Activity. *J. Biol. Chem.* **289,** 10876–10886 (2014).

113. Shieh, S. Y., Ikeda, M., Taya, Y. & Prives, C. DNA damage-induced phosphorylation of p53 alleviates inhibition by MDM2. *Cell* **91,** 325–334 (1997).

114. Shouse, G. P., Cai, X. & Liu, X. Serine 15 Phosphorylation of p53 Directs Its Interaction with B56γ and the Tumor Suppressor Activity of B56γ-Specific Protein Phosphatase 2A. *Mol. Cell. Biol.* **28,** 448 (2008).

115. Dashzeveg, N., Taira, N., Lu, Z.-G., Kimura, J. & Yoshida, K. Palmdelphin, a novel target of p53 with Ser46 phosphorylation, controls cell death in response to DNA damage. *Cell Death Dis.* **5,** e1221 (2014).

116. Okuda, M. & Nishimura, Y. Extended string binding mode of the phosphorylated transactivation domain of tumor suppressor p53. *J. Am. Chem. Soc.* **136,** 14143–14152 (2014).

117. Mavinahalli, J. N., Madhumalar, A., Beuerman, R. W., Lane, D. P. & Verma, C. Differences in the transactivation domains of p53 family members: a computational study. *BMC Genomics* **11,** S5 (2010).

118. Lee, Chang-Ro; Park, Young-Ha; Kim, Yeon-Ran; Peterkofsky, Alan; Seok, Yeong-Jae; Phosphorylation-Dependent Mobility Shift of Proteins on SDS-PAGE is Due to Decreased Binding of SDS. *Bulletin of the Korean Chemical Society* **34,** 2063–2066 (2013).

119. Long, X., Wu, G., Gaa, S. T. & Rogers, T. B. Inhibition of protein phosphatase-1 is linked to phosphorylation of p53 and apoptosis. *Apoptosis Int. J. Program. Cell Death* **7,** 31–39 (2002).

120. Dong, P. *et al.* Suppression of iASPP-dependent aggressiveness in cervical cancer through reversal of methylation silencing of microRNA-124. *Sci. Rep.* **6,** 35480 (2016).

121. Wilson, A. M. *et al.* Inhibitor of apoptosis-stimulating protein of p53 (iASPP) is required for neuronal survival after axonal injury. *PloS One* **9,** e94175 (2014).

122. Laska, M. J. *et al.* Enforced expression of PPP1R13L increases tumorigenesis and invasion through p53-dependent and p53-independent mechanisms. *Mol. Carcinog.* **48,** 832–842 (2009).

123. Chikh, A. *et al.* iASPP/p63 autoregulatory feedback loop is required for the homeostasis of stratified epithelia. *EMBO J.* **30,** 4261–4273 (2011).

124. Lu, M. *et al.* A Code for RanGDP Binding in Ankyrin Repeats Defines a Nuclear Import Pathway. *Cell* **157,** 1130–1145 (2014).

125. Lu, M. *et al.* Restoring p53 Function in Human Melanoma Cells by Inhibiting MDM2 and Cyclin B1/CDK1-Phosphorylated Nuclear iASPP. *Cancer Cell* **30,** 822–823 (2016).

126. Hu, Y. *et al.* Caspase cleavage of iASPP potentiates its ability to inhibit p53 and NF-κB. *Oncotarget* **6,** 42478–42490 (2015).

127. Chikh, A. *et al.* iASPP is a novel autophagy inhibitor in keratinocytes. *J. Cell Sci.* **127,** 3079–3093 (2014).

128. Li, H.-H., Cai, X., Shouse, G. P., Piluso, L. G. & Liu, X. A specific PP2A regulatory subunit, B56γ, mediates DNA damage-induced dephosphorylation of p53 at Thr55. *EMBO J.* **26,** 402–411 (2007).

129. Benyamini, H. & Friedler, A. The ASPP interaction network: electrostatic differentiation between pro- and anti-apoptotic proteins. *J. Mol. Recognit. JMR* **24,** 266–274 (2011).

130. Trigiante, G. & Lu, X. ASPP [corrected] and cancer. *Nat. Rev. Cancer* **6,** 217–226 (2006).

131. Vassilev, L. T. *et al.* In vivo activation of the p53 pathway by small-molecule antagonists of MDM2. *Science* **303,** 844–848 (2004).

132. Shi, D. *et al.* CBP and p300 are cytoplasmic E4 polyubiquitin ligases for p53. *Proc. Natl. Acad. Sci. U. S. A.* **106,** 16275–16280 (2009).

133. Pavithra, L. *et al.* SMAR1 forms a ternary complex with p53-MDM2 and negatively regulates p53-mediated transcription. *J. Mol. Biol.* **388,** 691–702 (2009).

134. Arold, S. *et al.* The crystal structure of HIV-1 Nef protein bound to the Fyn kinase SH3 domain suggests a role for this complex in altered T cell receptor signaling. *Struct. Lond. Engl. 1993* **5,** 1361–1372 (1997).

135. Bond, J. A. *et al.* p53-Dependent growth arrest and altered p53-immunoreactivity following metabolic labelling with 32P ortho-phosphate in human fibroblasts. *Oncogene* **18,** 3788–3792 (1999).

136. Murray-Zmijewski, F., Slee, E. A. & Lu, X. A complex barcode underlies the heterogeneous response of p53 to stress. *Nat. Rev. Mol. Cell Biol.* **9,** 702–712 (2008).

137. Toledo, F. & Wahl, G. M. Regulating the p53 pathway: in vitro hypotheses, in vivo veritas. *Nat. Rev. Cancer* **6,** 909–923 (2006).

138. Merrick, B. A. *et al.* Site-specific phosphorylation of human p53 protein determined by mass spectrometry. *Biochemistry (Mosc.)* **40,** 4053–4066 (2001).

Appendix

APPENDIX

A) Site-Directed Mutagenesis and Cloning in this Study

The following are the list of primers used for generating the PP1cα and iASPP mutations for this study, followed by a figure depicting the vector maps of the newly generated clones.

Table S1 List of primers used for site-directed mutagenesis and cloning of iASPP$_{608-828}$ (D633R), PP1cα (T320D), and PP1cα (1-300).

Primer Name	Primer Sequence	Cut sites and mutations introduced
iASPP (D633R) forward primer	5' ggtgctcctcctg**cgc**gcggcgctgaccgggg<u>agctc</u>gaggtgg 3'	• D633R, GAC→**CGC** • Introduction of a SacI cut site (mutated to <u>gagctc</u> from gagctg) 18 residues 3' of mutation
iASPP (D633R) reverse primer	5' ccacctcgagctccccggtcagcgccgcgcgcaggaggagcacc 3'	
PP1cα (T320D) forward primer	5' ccctggaggccgaccc<u>atc**gat**</u>ccaccccgcaattccgcc 3'	• T320D, ACC→**GAT** • Introduction of a ClaI/Bsu12I site (<u>ATCGAT</u>) at the site of mutation
PP1cα (T320D) reverse primer	5' ggcggaattgcggggtgg<u>atcgat</u>gggtcggcc 3'	
PP1cα (1-300) forward primer	5' cacacaggaaaca<u>gaattc</u>atgtccg 3'	• For isolation of [5' Plasmid DNA-<u>EcoRI</u>-Start- PP1cα (1-300) 3']
PP1cα (1-300) reverse primer	5' ctttttaa<u>gcttc</u>tagtcggcgggc 3'	• For isolation of [5' scrambled DNA-<u>HindIII</u>-STOP-PP1c (300-1)]

B) Setting up dephosphorylation reaction conditions

B.1) ASPP-mediated Dephosphorylation Buffer Conditions

As mentioned in the materials and methods and chapter three, the initial method for measuring in vitro dephosphorylation was designed by Dr. Tamara Skene-Arnold. After initial experiments, it was found that the kinase buffer used for the phosphorylation and dephosphorylation time courses (section 3.2.1 and 3.2.2) did not fully support PP1cα stability. This became apparent when the samples containing ASPP proteins reproducibly had more PP1cα present. The hypothesis for this was that the ASPP proteins were capable of binding and maintaining PP1cα in solution, while on its own, PP1cα became unstable and fell out of solution. To test this hypothesis, PP1cα alone or with iASPP (L625A) was incubated for 20 minutes at 30°C, then spun down for 5 mins at 13k rpm. The supernatant was removed and any remaining pellet was solubilized using 2 x SB. The pellet and supernatant were run on a coomassie gel and it was apparent that in the absence of ASPP protein, PP1cα fell out of solution to a great extent than when the ASPP protein was present. In addition, some of the ASPP protein also fell out of solution. A series of buffers were tested with the same method to test which would best support the stability of both proteins (data not shown). The final buffer conditions used in the dephosphorylation experiments conducted in this thesis were chosen based on figure B1. B, showing very minimal to no PP1cα in the pellet, and minimal ASPP protein in the pellet.

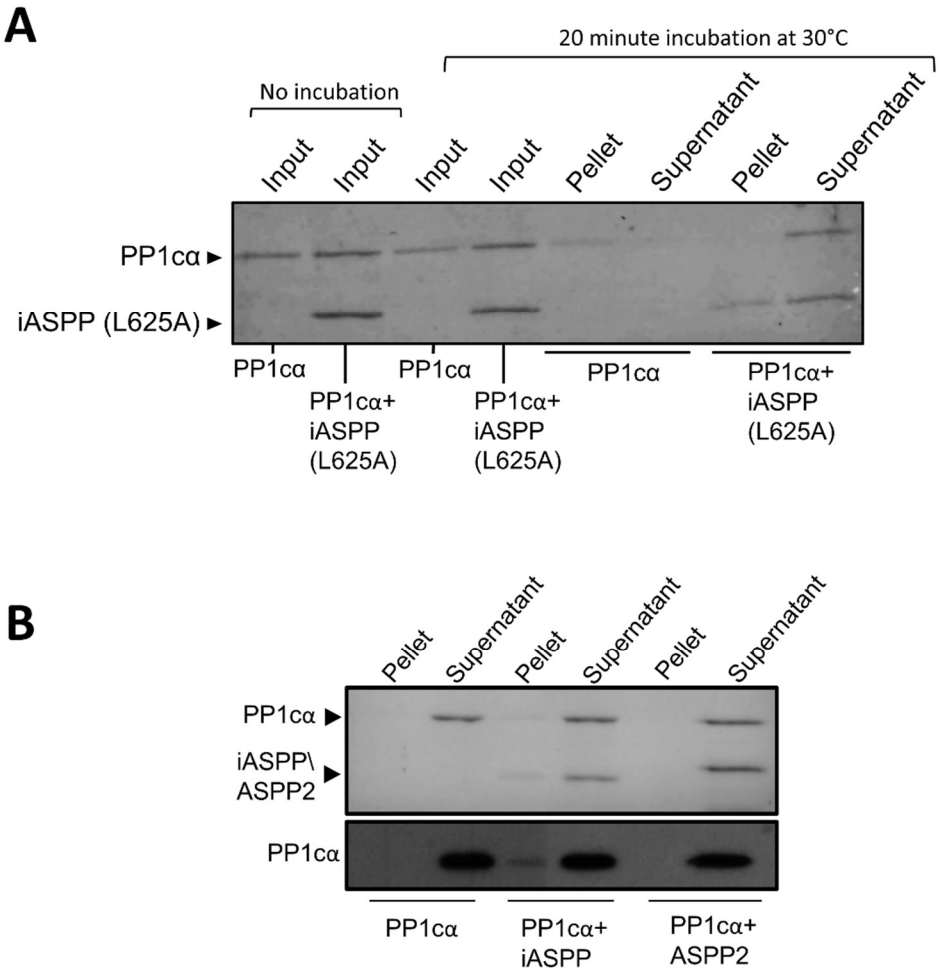

Figure B1. PP1cα and ASPP proteins are stable in the dephosphorylation experiments conducted in this thesis.

A) Under the intial buffer conditions, the same amount of PP1 or ASPP were incubated alone or together at 20 minutes at 30C. Protein was spun down for 5 minutes at 13k rpm, and the supernatant and pellet were run on a coomassie gel. B) Using the buffer used for all experiments containing ASPP proteins in this thesis, the same amount of PP1 or ASPP were incubated alone or together for 20 minutes at 30C. Protein was spun down for 5 minutes at 13k rpm, and the supernatant and pellet were run on a coomassie gel (upper panel), while a duplicate was transferred to nitrocellulose for detection of PP1cα by western blot (bottom panel)

B.2) p53Ser46 subsequent antibody tests

Given that p53Ser46 phosphorylation seemed to increase over time, the Ser46 antibody was further tested for its ability to detect Ser46 *in vitro*. An experiment with DNAPK phosphorylated p53 vs. DYRK2 phosphorylated p53 showed that p53Ser46 did not detect p53 that had been phosphorylated by DNAPK (data not shown). Therefore the antibody is specific to detecting phosphorylation sites phosphorylated by DYRK2.

In a separate experiment PP1cα was incubated alone or in the presence of ASPP proteins that were phosphorylated by DYRK2. In these experiments it's clear that the addition of PP1cα increases the apparent p53Ser46 signal.

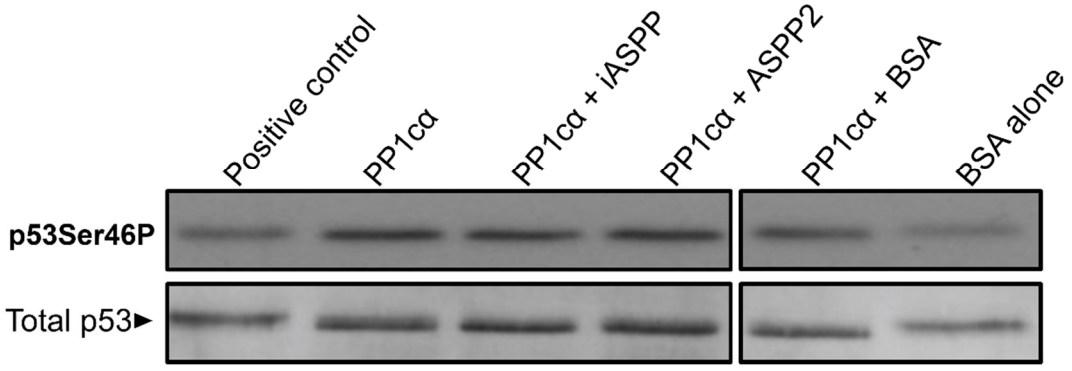

Figure B2. Addition of PP1cα increases p53Ser46 signal.
The figure depicts a dephosphorylation experiment in the presence of ASPP proteins similar to those performed with Ser15 and DYRK2 phosphorylated p53 conducted in the thesis.

B.3) BSA does not interact with PP1cα or p53

The control for the ASPP mediated dephospphroylation experiments was BSA. This was determined to be a sufficient control after binding experiments showed that BSA did not interact with either PP1cα or p53, as shown in figure B3.

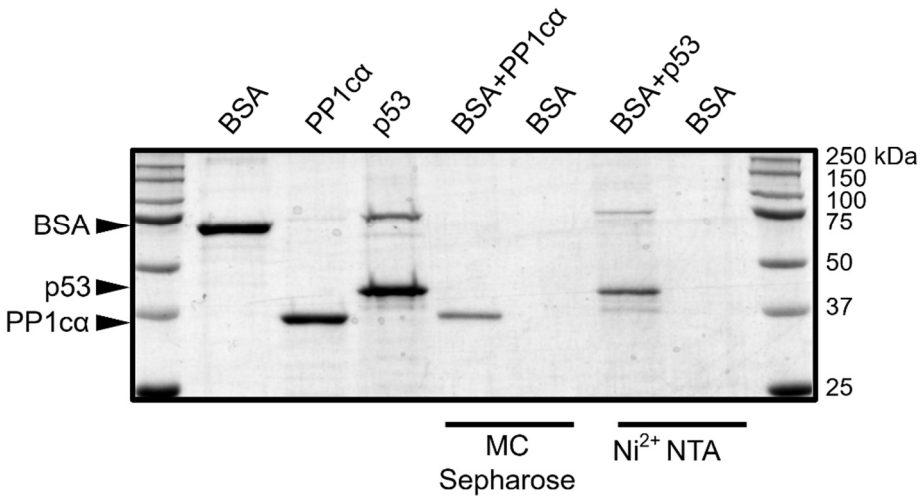

Figure B3. BSA does not interact with p53 or PP1cα.
The figure depicts the results of a MC-S binding experiment between PP1cα and BSA, and a Ni^{2+} NTA experiment between p53 and BSA. 5 µg of PP1cα was incubated with microcystin Sepharose in MC Binding Buffer, and 5 µg of p53 was incubated with Ni^{2+} NTA beads in Ni^{2+} NTA Binding Buffer, for 2 hours at 4°C. Beads were washed and subsequently incubated with 5 µg of BSA in their respective buffers with 150 mM added NaCl, and 0.1% added Tween-20, overnight at 4°C. The beads were then washed and the bound protein was eluted using 2 x Laemmli sample buffer and heat at 100°C. Samples were loaded onto a 12% SDS-PAGE gel, in addition to 1 µg of BSA, PP1cα, and p53 for reference.

B.4) PP1cα titration for p53Thr18 experiments

Given that Thr18 was dephosphorylated at a much quicker rate than Ser15, a dephosphorylation titration was conducted to find which concentration of PP1cα would result in 50% dephosphorylation at 30 minutes incubation. The results in B4 identify 0.0156 µg and the amount of PP1cα which achieved 50% dephosphorylation relative to no PP1cα.

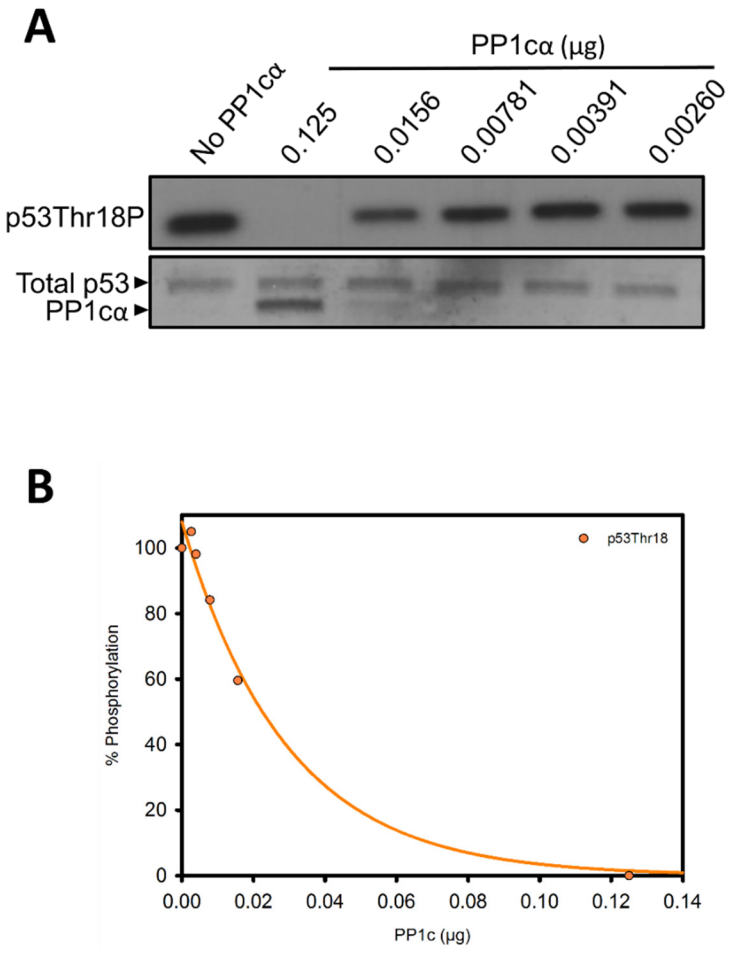

Figure B4. PP1cα titration used to find the amount of PP1cα necessary for p53Thr18 ASPP experiments.
The figure depicts the titration of PP1cα and resulting phosphorylation status of p53Thr18 measured at 30 minutes incubation at 30°C. p53 was phosphorylated by DNAPK as outlined in the thesis for 90 minutes, DNAPK was inhibited by LY294002, and a range of PP1cα concentrations were incubated for an additional 30 minutes. Phosphorylation was assessed as outlined in the thesis for Thr18.

C) Statistical Analysis of Variance

The following are the results of a one-way ANOVA test, followed by a multiple comparisons test for the ASPP-mediated dephosphorylation of p53 Ser15, Thr18, and DYRK2 phosphorylated p53, by PP1cα (WT), PP1cα (T320D),or PP1cα (1-300).

PP1cα (WT) p53Ser15 One Way Analysis of Variance

Number of families	1					
Number of comparisons per family	3					
Alpha	0.05					
Tukey's multiple comparisons test	Mean Diff.	95.00% CI of diff.	Significant?	Summary	Adjusted P Value	
iASPP vs. ASPP2	-0.02698	-0.2466 to 0.1927	No	ns	0.9349	
iASPP vs. BSA	-0.867	-1.104 to -0.6298	Yes	****	<0.0001	
ASPP2 vs. BSA	-0.84	-1.077 to -0.6028	Yes	****	<0.0001	
Test details	Mean 1	Mean 2	Mean Diff.	SE of diff.	n1	DF
iASPP vs. ASPP2	0.1889	0.2159	-0.02698	0.07687	4	8
iASPP vs. BSA	0.1889	1.056	-0.867	0.08303	4	8
ASPP2 vs. BSA	0.2159	1.056	-0.84	0.08303	4	8

PP1cα (WT) p53Thr18 One Way Analysis of Variance

Number of families	1					
Number of comparisons per family	3					
Alpha	0.05					
Tukey's multiple comparisons test	Mean Diff.	95.00% CI of diff.	Significant?	Summary	Adjusted P Value	
iASPP vs. ASPP2	-0.2784	-0.6397 to 0.08282	No	ns	0.1213	
iASPP vs. BSA	-0.5401	-0.9013 to -0.1788	Yes	**	0.0089	
ASPP2 vs. BSA	-0.2616	-0.6229 to 0.09961	No	ns	0.1455	
Test details	Mean 1	Mean 2	Mean Diff.	SE of diff.	n1	DF
iASPP vs. ASPP2	0.6609	0.9393	-0.2784	0.1177	3	6
iASPP vs. BSA	0.6609	1.201	-0.5401	0.1177	3	6
ASPP2 vs. BSA	0.9393	1.201	-0.2616	0.1177	3	6

DYRK2-phosphorylated p53 One Way Analysis of Variance

Number of families	1						
Number of comparisons per family	3						
Alpha	0.05						
Tukey's multiple comparisons test	Mean Diff.	95.00% CI of diff.	Significant?	Summary	Adjusted P Value		
iASPP vs. ASPP2	-19.47	-39.86 to 0.9094	No	ns	0.0592		
iASPP vs. BSA	-28.37	-48.76 to -7.99	Yes	*	0.0124		
ASPP2 vs. BSA	-8.899	-29.28 to 11.48	No	ns	0.4264		
Test details	Mean 1	Mean 2	Mean Diff.	SE of diff.	n1	q	DF
iASPP vs. ASPP2	68.11	87.59	-19.47	6.643	3	4.146	6
iASPP vs. BSA	68.11	96.48	-28.37	6.643	3	6.044	6
ASPP2 vs. BSA	87.59	96.48	-8.899	6.643	3	1.894	6

One Way Analysis of Variance- PP1c WT, T320D, 1-300 Timecourse

Number of families	1
Number of comparisons per family	91
Alpha	0.05

Tukey's multiple comparisons test	Mean Diff.	95.00% CI of diff.	Significant?	Summary	Adjusted P Value
PP1 WT, 2min vs. PP1 T320D, 2min	-0.08496	-0.3915 to 0.2216	No	ns	0.9987
PP1 WT, 2min vs. PP1 1-300, 2min	0.04397	-0.2626 to 0.3506	No	ns	>0.9999
PP1 T320D, 2min vs. PP1 1-300, 2min	0.1289	-0.1988 to 0.4567	No	ns	0.9698
PP1 WT, 10min vs. PP1 T320D, 10min	-0.3015	-0.6081 to 0.005081	No	ns	0.0574
PP1 WT, 10min vs. PP1 1-300, 10min	-0.148	-0.4546 to 0.1586	No	ns	0.8779
PP1 T320D, 10min vs. PP1 1-300, 10min	0.1535	-0.1743 to 0.4813	No	ns	0.8985
PP1 WT, 30min vs. PP1 T320D, 30min	-0.1819	-0.4885 to 0.1247	No	ns	0.6581
PP1 WT, 30min vs. PP1 1-300, 30min	-0.1633	-0.4699 to 0.1433	No	ns	0.7905
PP1 T320D, 30min vs. PP1 1-300, 30min	0.01862	-0.3091 to 0.3464	No	ns	>0.9999
PP1 WT, 45min vs. PP1 T320D, 45min	-0.1563	-0.504 to 0.1913	No	ns	0.9216
PP1 WT, 45min vs. PP1 1-300, 45min	0.01416	-0.3335 to 0.3618	No	ns	>0.9999
PP1 T320D, 45min vs. PP1 1-300, 45min	0.1705	-0.2309 to 0.5719	No	ns	0.9469
PP1 T320D, 60min vs. PP1 1-300, 60min	0.00989	-0.3179 to 0.3376	No	ns	>0.9999

PP1cα: iASPP Single Mutation p53Ser15 One Way Analysis of Variance

Number of families	1
Number of comparisons per family	10
Alpha	0.05

Tukey's multiple comparisons test	Mean Diff.	95.00% CI of diff.	Significant?	Summary	Adjusted P Value
iASPP WT vs. iASPP L625A	-0.2172	-0.4126 to -0.02174	Yes	*	0.0264
iASPP WT vs. iASPP D633R	-0.2566	-0.4521 to -0.06123	Yes	**	0.0082
iASPP WT vs. PP1 T320D	0.00277	-0.1926 to 0.1982	No	ns	>0.9999
iASPP WT vs. PP1 1-300	-0.2333	-0.4444 to -0.02221	Yes	*	0.0274
iASPP L625A vs. iASPP D633R	-0.03949	-0.2349 to 0.1559	No	ns	0.9677
iASPP L625A vs. PP1 T320D	0.2199	0.02452 to 0.4154	Yes	*	0.0244
iASPP L625A vs. PP1 1-300	-0.01613	-0.2272 to 0.1949	No	ns	0.9992
iASPP D633R vs. PP1 T320D	0.2594	0.06401 to 0.4548	Yes	**	0.0075
iASPP D633R vs. PP1 1-300	0.02336	-0.1877 to 0.2344	No	ns	0.9966
PP1 T320D vs. PP1 1-300	-0.2361	-0.4471 to -0.02499	Yes	*	0.0254